

Fault Detection in Trajectory Tracking of Wheeled Mobile Robots

Hani Khoshdel Nikkhoo

A Thesis
in
The Department
of
Electrical and Computer Engineering

Presented in Partial Fulfillment of the Requirements
for the Degree of Master of Applied Science (Electrical & Computer Engineering) at
Concordia University
Montréal, Québec, Canada

March 2008

©Hani Khoshdel Nikkhoo, 2008



Library and
Archives Canada

Published Heritage
Branch

395 Wellington Street
Ottawa ON K1A 0N4
Canada

Bibliothèque et
Archives Canada

Direction du
Patrimoine de l'édition

395, rue Wellington
Ottawa ON K1A 0N4
Canada

Your file Votre référence
ISBN: 978-0-494-40886-5
Our file Notre référence
ISBN: 978-0-494-40886-5

NOTICE:

The author has granted a non-exclusive license allowing Library and Archives Canada to reproduce, publish, archive, preserve, conserve, communicate to the public by telecommunication or on the Internet, loan, distribute and sell theses worldwide, for commercial or non-commercial purposes, in microform, paper, electronic and/or any other formats.

The author retains copyright ownership and moral rights in this thesis. Neither the thesis nor substantial extracts from it may be printed or otherwise reproduced without the author's permission.

AVIS:

L'auteur a accordé une licence non exclusive permettant à la Bibliothèque et Archives Canada de reproduire, publier, archiver, sauvegarder, conserver, transmettre au public par télécommunication ou par l'Internet, prêter, distribuer et vendre des thèses partout dans le monde, à des fins commerciales ou autres, sur support microforme, papier, électronique et/ou autres formats.

L'auteur conserve la propriété du droit d'auteur et des droits moraux qui protègent cette thèse. Ni la thèse ni des extraits substantiels de celle-ci ne doivent être imprimés ou autrement reproduits sans son autorisation.

In compliance with the Canadian Privacy Act some supporting forms may have been removed from this thesis.

Conformément à la loi canadienne sur la protection de la vie privée, quelques formulaires secondaires ont été enlevés de cette thèse.

While these forms may be included in the document page count, their removal does not represent any loss of content from the thesis.

Bien que ces formulaires aient inclus dans la pagination, il n'y aura aucun contenu manquant.


Canada

ABSTRACT

Fault Detection in Trajectory Tracking of Wheeled Mobile Robots

Hani Khoshdel Nikkhoo

The problem of fault detection in nonlinear systems with application to trajectory tracking of nonholonomic wheeled mobile robots (WMRs) is addressed in this thesis. For the considered application, a nonholonomic wheeled mobile robot -having nonlinear kinematics- is required to follow a predefined smooth trajectory (in the absence of obstacles in the environment). This goal has to be accomplished despite the presence of faults that may occur in two of its major subsystems which are vital for navigation, namely the driving subsystem and the steering subsystem. These faults are assumed to be caused by actuator faults in either of these two subsystems. The problem addressed here is to detect the presence of faults and to determine the subsystem which has been affected by these faults. Toward this end, two different fault detection approaches are proposed and investigated. The first approach is based on system identification through Extended Kalman Filters (EKF) whereas the second one is based on system identification via artificial neural networks. In the former approach a novel method for residual generation is proposed while in the latter by utilizing the neural network's formal stability properties the desired performance can be guaranteed. Each of the proposed fault detection methods is studied subject to two different kinds of controllers (namely a dynamic linear controller and a dynamic feedback linearization based controller) and two different types of actuator faults (namely the Loss-of-Effectiveness fault and Locked-In-Place fault). In this way, the impact of the controller strategy on the fault detection approach is also investigated and evaluated.

“The only true wisdom is in knowing you know nothing.”

-Socrates

*With my deepest gratitude,
I thank and dedicate this dissertation to my Mom and Dad:
Mina & Masoud*

Acknowledgements

I do thank and acknowledge my supervisor Prof. K. Khorasani for his continuing supervision and support of my work . I thank him for his vision.

I thank my parents, Mina & Masoud, for believing in me and sacrificing while I studied. Both of them showed nothing but enthusiasm and excitement for my work, never once complaining or resenting. My parents lift me up and love me without condition. I thank them both and continue to count on them as my soft place to fall.

Lastly, but certainly not least, I thank all of those who have supported me during my stay at The Electrical and Computer Engineering Department of Concordia University.

Contents

List of Figures	xi
List of Tables	xv
1 Introduction	1
1.1 Motivation & Justification of the Research	1
1.2 Statement of the Problem	3
1.3 Accomplished Tasks and Contributions	4
1.4 Brief Outline of the Thesis	5
2 Backgrounds and Preliminaries	7
2.1 Introduction	7
2.2 Nomenclature in Fault Diagnosis	9
2.3 Model-Free Methods For FDIR	13
2.4 Model Consistency Based Diagnosis	14
2.5 Computational Intelligence Methodologies in FDI	18
2.5.1 Neural Network Applications	19
2.5.2 Fuzzy Logic Applications	19
2.5.3 Neuro-Fuzzy Systems Applications	20
2.5.4 Genetic Algorithms	21

2.6	Active Fault Diagnosis vs. Passive Fault Diagnosis	21
2.7	Modeling of Faulty Systems	24
2.8	Properties of Fault Diagnosis Techniques	25
2.9	Implementation Issues	26
2.10	Summary	28
3	Trajectory Planning for Wheeled Mobile Robots (WMR)	30
3.1	Introduction	30
3.2	Basic Motion Tasks	31
3.3	Modeling & Control Properties of WMRs	32
3.3.1	Controllability about a Trajectory	33
3.3.2	Chained Canonical Forms	34
3.4	Trajectory Tracking	35
3.4.1	Generation of the Feedforward Command	35
3.4.2	Linear Control Design	38
3.4.3	Dynamic Feedback Linearization	39
3.5	Simulation Results	43
3.6	Summary and Conclusions	46
4	Fault Detection Design for the WMR	48
4.1	Introduction	48
4.2	Major Subsystems of WMRs Subject to Faults	49
4.3	Kalman Filtering	51
4.3.1	What is a Kalman Filter?	51
4.3.2	Mathematical Foundation of Optimum Estimates	53
4.3.3	Derivation of the Kalman Filter	54
4.3.4	Derivation of the Extended Kalman Filter	61

CONTENTS	ix
4.3.5 Fault Detection	65
4.4 Neural Network Model Based Fault Detection Approach	67
4.4.1 The Neural Network Based Identifier	69
4.4.2 Fault Detection	72
4.5 Summary and Conclusions	73
5 Comparative Study and Simulation Results	75
5.1 Introduction	75
5.2 Controller Performance Under Faulty Conditions	76
5.2.1 Locked In Place Fault	76
5.2.2 Loss of Effectiveness Fault	79
5.3 Convergence Properties of EKF	80
5.4 Permanent-Fault Detection Through EKF Approach	82
5.4.1 Locked In Place Fault in the Driving Subsystem (v)	83
5.4.2 Loss of Effectiveness Fault in the Driving Subsystem (v)	85
5.5 Permanent-Fault Detection Through Neural Network Approach	91
5.5.1 Locked In Place Fault in the Driving Subsystem (v)	92
5.5.2 Loss of Effectiveness Fault in the Driving Subsystem (v)	95
5.6 Intermittent-Fault Detection Through EKF Approach	101
5.6.1 Locked In Place Fault in the Driving Subsystem (v)	102
5.6.2 Loss Of Effectiveness Fault in the Driving Subsystem (v)	104
5.7 Intermittent-Fault Detection Through Neural Network Approach	106
5.7.1 Locked In Place Fault in Driving Subsystem (v)	107
5.7.2 Loss Of Effectiveness Fault in Driving Subsystem (v)	109
5.8 Summary and Conclusions	111

<i>CONTENTS</i>	x
6 Concluding Remarks	114
6.1 Conclusions	114
6.2 Future Research Directions	116
Bibliography	118

List of Figures

2.1	Model consistency based diagnosis	15
2.2	Consistency based diagnosis principle	16
2.3	Model consistency based fault diagnosis	17
2.4	Active Fault Diagnosis	23
2.5	Active Fault Diagnosis Operations	23
2.6	Modeling of Faulty Systems	25
2.7	Development Scheme for Fault Diagnosis Systems	29
3.1	The desired eight-shaped reference trajectory which the WMR wants to follow	44
3.2	Trajectory tracking with dynamic linear feedback design	45
3.3	Trajectory tracking with dynamic feedback linearization	46
4.1	Schematic of the exploited model consistency based fault diagnosis approach	49
4.2	Signal flow graph of a linear discrete time dynamic system	51
4.3	Schematic of the Proposed Fault Detection Approach Based on Ex- tended Kalman Filter (EKF)	66
4.4	Schematic of the Neural Network Identifier	70

4.5	Schematic of the Proposed Fault Detection Approach Based on Neural Networks	72
5.1	Dynamic Linear controller performance in the presence of a locked in place fault which has occurred at $t = 15s$	78
5.2	Dynamic feedback linearization controller performance in the presence of a locked in place fault which has occurred at $t = 15s$	79
5.3	Dynamic linear controller performance in the presence of a 50% loss of effectiveness fault which has occurred at $t = 15s$	81
5.4	Dynamic feedback linearization controller performance in the presence of a 50% loss of effectiveness fault which has occurred at $t = 15s$	82
5.5	Performance of the EKF State Estimator	83
5.6	EKF Fault Detection Approach for System Subject to Locked In Place Fault under Dynamic Linear Control	85
5.7	EKF Fault Detection Approach for System Subject to Locked In Place Fault under Feedback Linearization Based Control	86
5.8	EKF Fault Detection Approach for System Subject to 80% Loss of Effectiveness Fault under Dynamic Linear Control	87
5.9	EKF Fault Detection Approach for System Subject to 50% Loss Of Effectiveness Fault under Dynamic Linear Control	88
5.10	EKF Fault Detection Approach for System Subject to 20% Loss Of Effectiveness Fault under Dynamic Linear Control	89
5.11	EKF Fault Detection Approach for System Subject to 80% Loss Of Effectiveness Fault under Feedback Linearization Based Control	91
5.12	EKF Fault Detection Approach for System Subject to 50% Loss of Effectiveness Fault under Feedback Linearization Based Control	92

5.13 EKF Fault Detection Approach for System Subject to 20% Loss of Effectiveness Fault under Feedback Linearization Based Control . . .	93
5.14 Neural Network-based Fault Detection Approach Subject to Permanent Locked In Place Fault under Dynamic Linear Control	94
5.15 Neural Network-based Fault Detection Approach Subject to Permanent Locked In Place Fault under Feedback Linearization Based Control	95
5.16 Neural Network-based Fault Detection Approach Subject to 80% Permanent Loss Of Effectiveness Fault under Dynamic Linear Control . .	96
5.17 Neural Network-based Fault Detection Approach Subject to 50% Permanent Loss Of Effectiveness Fault under Dynamic Linear Control . .	97
5.18 Neural Network-based Fault Detection Approach Subject to 20% Permanent Loss Of Effectiveness Fault under Dynamic Linear Control . .	98
5.19 Neural Network-based Fault Detection Approach Subject to 80% Permanent Loss Of Effectiveness Fault under Feedback Linearization Based Control	99
5.20 Neural Network-based Fault Detection Approach Subject to 50% Permanent Loss Of Effectiveness Fault under Feedback Linearization Based Control	101
5.21 Neural Network-based Fault Detection Approach Subject to 20% Permanent Loss Of Effectiveness Fault under Feedback Linearization Based Control	102
5.22 EKF Fault Detection Approach Subject to Intermittent Locked In Place Fault under Dynamic Linear Control	103
5.23 EKF Fault Detection Approach Subject to Intermittent Locked In Place Fault under Feedback Linearization Based Controller	104

5.24 EKF Fault Detection Approach Subject to 80% Intermittent(between 15s and 25s) Loss Of Effectiveness Fault under Dynamic Linear Control 105

5.25 EKF Fault Detection Approach Subject to 80% Intermittent(between 15s and 25s) Loss Of Effectiveness Fault under Feedback Linearization Based Controller 106

5.26 NN Fault Detection Approach Subject to Intermittent Locked In Place Fault under Dynamic Linear Control 108

5.27 NN Fault Detection Approach Subject to Intermittent Locked In Place Fault under Feedback Linearization Based Control 109

5.28 NN Fault Detection Approach Subject to 80% Intermittent(between 15s and 25s) Loss Of Effectiveness Fault under Dynamic Linear Control 110

5.29 NN Fault Detection Approach Subject to 80% Intermittent (between 15s and 25s) Loss Of Effectiveness Fault under Feedback Linearization Based Controller 111

List of Tables

1.1	Typical failure rates of mechanical and electromechanical elements [RAC 95]	3
5.1	Permanent-Fault detection time & delay for the EKF approach	90
5.2	Permanent-Fault detection time & delay for the neural network model consistency based approach	100
5.3	Intermittent-Fault detection time & delay for the EKF approach . . .	107
5.4	Intermittent-Fault detection time & delay for the neural network model consistency based approach	112

List of Symbols and Abbreviations

λ	rate of failure
w_k, v_k	independent, zero-mean, Gaussian noise processes
Q_k, R_k	covariance matrices
G_k	Kalman gain matrix
A	availability
<i>EKF</i>	extended Kalman filter
<i>FDD</i>	fault detection and diagnosis
<i>FDI</i>	fault detection and isolation
<i>HiL</i>	hardware-in-the-loop
<i>MTTF</i>	meantime to failure
<i>MTTR</i>	meantime to repair
<i>SiL</i>	software-in-the-loop
<i>WMR</i>	wheeled mobile robot

Chapter 1

Introduction

1.1 Motivation & Justification of the Research

With today's broad areas of applications for wheeled mobile robots – ranging from industrial manufacturing, logistics, medical and healthcare to space and military deployments – the demands for higher safety, reliability and autonomy have increased significantly. In the advent of novel advanced unmanned ground vehicles based on the design of classical mobile robots, one of the crucial issues which needs to be dealt with is autonomy. Autonomy will be extremely helpful for increasing the overall efficiency of modern and sophisticated multi-agent systems by decreasing the amount of human support and resources required for mobile robot operations.

For instance, when mobile robots are used for planet explorations in space missions, they should be able to operate for a rather long period of time without intervention from the central command and control station based on earth [Anderson 83]. In other words, communication with a central station is limited to a short period of time even during fault free and healthy conditions. Furthermore, due to the long round trip

communication delays ¹, the capability of a central station to respond to emergencies and stimuli which do not fit into the class of expected perceptions is very limited and real-time monitoring is impossible. Consequently, the major subsystems ² of a mobile robot, such as the power subsystem, the driving subsystem, the steering subsystem, communication and sensors should be as autonomous as possible. As a matter of fact, in such applications, autonomy will play a vital role in the accomplishment of the mobile robot mission.

One of the major characteristics which autonomous systems, in general, and mobile robots in particular, should possess is the capability of fault diagnosis. In other words, these complex systems need to be equipped with intelligent mechanisms designed for fast detection and isolation of faults and early detection of performance degradations for cost effective and timely maintenance. As a matter of fact, fault diagnosis procedures not only contribute to the autonomy these of systems but also change the maintenance philosophy which has been used for a long time. With the development of advanced fault diagnosis systems maintenance can be done:

- on condition
- opportunistic
- and not “per failure” nor “per schedule”

In recent years there has been intensive research work on fault diagnosis on a variety of components and subcomponents of wheeled mobile robots, such as motors [Zanardelli 05], gears [Zheng 02], tires [Roumeliotis 98a], suspension [Luo 05], sensors [Carlson 03], etc. But according to a field study reflected in Table 1.1 ³, one of the ma-

¹For example, the round trip communication delay between Earth and Mars ranges from about 6.5 minutes at closest approach to 44 minutes at superior conjunction

²These subsystems have been extensively explained in Section 4.2

³The failure rates in Table 1.1 are *per hour*. For more details see Equation (2.1)

Table 1.1: Typical failure rates of mechanical and electromechanical elements [RAC 95]

Mechanical Elements	$\lambda[\mathbf{h}^{-1}]$	Electromechanical Elements	$\lambda[\mathbf{h}^{-1}]$
ball bearing	1.64×10^{-6}	actuator, general	26×10^{-6}
sleeve bearing	2.38×10^{-6}	brush, general	9×10^{-6}
belt	19.72×10^{-6}	cable, general	1×10^{-6}
coupling	5.54×10^{-6}	electric motor, general	9×10^{-6}
gear	4.69×10^{-6}	generator, general	73×10^{-6}
pump	43.65×10^{-6}	regulator, general	13×10^{-6}
seal	5.47×10^{-6}		
valve, hydraulic	8.83×10^{-6}		

major sources of faults is the actuator. This thesis emphasizes mainly on actuator fault which might cause degradation of performance in driving and steering subsystems of the Wheeled Mobile Robots (WMRs).

1.2 Statement of the Problem

The problem of fault detection and isolation in trajectory tracking of a nonholonomic wheeled mobile robot is addressed in this thesis.

As the name states, the main characteristic of wheeled mobile robots is their mobility. Therefore, it is very important to monitor and detect faults and degradation of performance in their main components and subsystems which play a key role in providing mobility.

The case scenario investigated here may be stated as follows:

“A nonholonomic wheeled mobile robot with nonlinear kinematics is required to follow a predefined smooth trajectory in the absence of obstacles in an environment. Furthermore, faults may occur in two of its major subsystems which are vital for its navigation namely the driving subsystem and the steering subsystem. These faults are assumed to be caused by actuator faults in either of these two subsystems. The problem is to detect and identify the appearance of faults and to determine the subsystem which has been affected by these faults”

The solution should be capable of coping with multiple faults in noisy environments where external disturbances may exist.

1.3 Accomplished Tasks and Contributions

In order to propose a solution for the stated problem, first two different controllers are designed which allow the nonholonomic wheeled mobile robot to follow its desired predefined trajectory. One of the controllers is based on the tangent linearization approach along the reference trajectory, while the other one is based on the dynamic feedback linearization method. The designed control commands are of nonlinear time-varying nature in both cases. The rationale behind designing two different types of controllers instead of one is the desire of investigating the impact of the controller design and controller robustness on the fault diagnosis behavior and performance.

With a nonholonomic wheeled mobile robot capable of tracking the desired smooth trajectory at our disposal a fault diagnosis module based on residual generation scheme with Extended Kalman Filter (EKF) is designed. As a matter of fact, the Extended Kalman Filter has been used for state estimation of the nonlinear kinematics

equations of the system and a novel residual generation method based on the state prediction is then proposed.

Subsequently, an alternative neural network model-based approach is also discussed and a comprehensive comparative study between the two methodologies is conducted.

1.4 Brief Outline of the Thesis

This thesis is organized as follows:

Chapter 2 discusses the major tasks of supervision, monitoring, fault detection and fault diagnosis in general. Since the subject of fault diagnosis is distributed over a variety of technological fields, the exploited terminology is not unique. Therefore, an attempt is made to provide definitions of frequently used terms in this dissertation. Also, other background and preliminary results have been discussed and a literature survey has also been accomplished.

Chapter 3 presents the motion control problem of wheeled mobile robots (WMRs). With respect to the kinematics of the considered mobile robot, two different control strategies for trajectory tracking problem in an obstacle free environment have been proposed. The simulation results which approbate the controller designs are also given.

Chapter 4 mainly tries to characterize the proposed Fault Diagnosis Scheme for mobile robots. Toward this end, it describes the mathematical foundations of the Extended Kalman Filter used for generating the residuals and the required analytical

redundancy. It also introduces the injected faults and the way they should be handled.

Chapter 5 introduces an alternative neural network model-based fault diagnosis approach for comparison of results with the formerly proposed Extended Kalman Filter approach. Comprehensive simulation and comparison results are also provided.

Chapter 6 includes a summary of the main topics and contributions presented in this dissertation. Furthermore, some of the major needs and suggestions for the future of fault detection and isolation (FDI) research on wheeled mobile robot platforms are also discussed.

Chapter 2

Backgrounds and Preliminaries

2.1 Introduction

Throughout history and until a few decades ago, the term *diagnosis* was monotonously associated with medicine and its various branches concerning the ways of recognition of a medical condition or disease by its signs and symptoms.

Encyclopedia Britannica describes diagnosis as follows:

“The process of determining the nature of a disease or disorder and distinguishing it from other possible conditions. The term comes from the Greek *gnosis*, meaning knowledge.

The diagnosis process is the method by which health professionals select one disease over another, identifying one as the most likely cause of the person’s symptoms. Symptoms that appear early in the course of a disease are often more vague and undifferentiated than those that arise as the disease progresses, making this the most difficult time to make an accurate diagnosis. Reaching an accurate conclusion depends on the timing and sequence of the symptoms, past medical history and risk factors for certain

diseases, and a recent exposure to disease. From the large number of facts obtained, a list of possible diagnosis can be determined, which are referred to as the differential diagnosis. The physician organizes the list with the most likely diagnosis given first. Additional information is identified, and appropriate tests are selected that will narrow the list to confirm one of the possible diseases.”

The advent of *technical diagnosis* goes back to the early 1970's when various researchers in different locations began the development of fault diagnosis mechanisms for systems. For instance, Beard [Beard 71] and Jones [Jones 73] reported the well-known “*failure detection filter*” for linear systems. Early developments in this field are well summarized by Willsky [Willsky 76]. The application of diagnosis methods for fault detection of jet engines was first introduced by Rault et al. [Rault 71]. Leak detection in a chemical process by correlation methods was done by Siebert and Isermann in 1976 [Siebert 76].

The first book on the model based fault diagnosis with applications to chemical and petrochemical processes was published by Himmelblau [Himmelblau 78]. Analytical redundancy of multiple observers is the approach used by Clark [Clark 78] to detect instrument and sensor failures.

Parameter estimation techniques were also applied for fault detection of dynamical systems by Hohmann [Hohmann 77], Bakiotis [Bakiotis 79], Geiger [Geiger 82], Filbert and Metzger [Filbert 82]. In 1984, Isermann [Isermann 84] summarized process fault detection methods based on modeling, parameter and state estimation. He has revised that summary twice since then in 1997 and 2005 [Isermann 97a; Isermann 05].

Chow and Willsky [Chow 84] were the people who first brought the idea of parity equation based method to the literature. Later, this approach was developed further due to the efforts of Patton and Chen [Patton 94], Gertler [Gertler 91], Höfling and

Pfeufer [Höfling 94].

Generally, when the impacts of faults and disturbances have frequency characteristics which are unlike each other, frequency domain methods can be used for fault diagnosis as in such cases the frequency spectra serve as criterion to distinguish the faults. Massoumnia et al. [Masoumnia 89], Frank et al. [Frank 00] and Ding et al. [Ding 00] were among the first researchers who worked on this idea.

2.2 Nomenclature in Fault Diagnosis

A review of the literature will show that the terminology in this field is not consistent. As a result, it will be arduous to apprehend the goals of the contributions and to compare the various approaches that have been developed in the field. This inconsistency, to some extent, is due to the fast and multidirectional development of diagnosis methods and the different variety of their applications. In order to tackle this problem, a number of influential scientists in this field began a unified movement in 1997 at IFAC to create a common lexicon for all those that are involved with this field. Of course, the development of this lexicon is considered to be ongoing; in the sense that new definitions, expressions and updates are being appended to it as time goes by.

The following Definitions are based on the proposed terminology by the *IFAC Technical Committee SAFEPROCESS* published in a variety of references [Isermann 97b; Gustafsson 00; Simani 03; Isermann 05]. These adopted definitions have been widely accepted and used by experts of this field.

States and Signals:

- ***Fault:*** Unpermitted deviation of at least one characteristic property

or parameter of the system from the acceptable, usual or standard condition.

- **Failure:** A permanent interruption of a system's ability to perform a required function under specified operating conditions.
- **Malfunction:** An intermittent irregularity in the fulfilment of a system's desired function.
- **Error:** A deviation between a measured or computed value of an output variable and its true or theoretically correct one.
- **Disturbance:** An *unknown* (and uncontrolled) *input*.
- **Residual:** A fault indicator, based on the deviation between measurements and model equation based computations.
- **Symptom:** A change of an observable quantity from normal behavior.

Functions:

- **Fault detection:** Determination of faults present in a system and time of detection.
- **Fault isolation:** Determination of kind, location and time of detection of a fault. Follows fault detection.
- **Fault identification:** Determination of the size and time-variant behavior of fault. Follows fault isolation.
- **Fault diagnosis:** Determination of kind, size, location and time of a fault. Follows fault detection. Includes fault isolation and identification.

- **Monitoring:** A continuous real-time task of determining the conditions of a physical system and recognizing and indicating anomalies of its behavior.
- **Supervision:** Monitoring a physical system and taking appropriate actions to maintain the operation in case of faults.
- **Protection:** Means by which a potentially dangerous behavior of the system is suppressed if possible, or means by which the consequences of a dangerous behavior are avoided.

Models:

- **Quantitative Model:** Use of static and dynamic relations among system variables and parameters in order to describe the behavior of the system in quantitative mathematical terms.
- **Qualitative Model:** Use of static and dynamic relations among system variables and parameters in order to describe the behavior of the system in qualitative terms such as causalities or if-then rules.
- **Analytical redundancy:** Use of two, but not necessarily identical ways to determine a quantity where one way uses a mathematical process model in analytical form.

System Properties:

- **Reliability:** Ability of a system to perform a required function under stated conditions, within a given scope, during a given period of time.

Measures: $MTTF = \text{Mean Time To Failure}$

$$MTTF = \frac{1}{\lambda} \quad (2.1)$$

where λ is the rate of failure, e.g. failures per hour.

- **Safety:** Availability of a system not to cause a danger for persons, equipment or environment.
- **Availability:** Probability that a system or equipment will operate satisfactorily and effectively at any point of time measure:

$$A = \frac{MTTF}{MTTF + MTTR} \quad (2.2)$$

MTTR: Mean Time To Repair

$$MTTF = \frac{1}{\mu} \quad (2.3)$$

where μ is the rate of repair.

Time dependency of faults:

- **Abrupt fault:** Faults modeled by a stepwise function. It represents bias in the monitored signal.
- **Incipient fault:** Faults modeled by ramp signals. It represents drift of the monitored signal.
- **Intermittent fault:** Faults modeled by a combination of impulses with different amplitudes.

Fault affixation:

- **Additive fault:** Influences a variable by addition of the fault itself. They may represent, e.g. offsets of sensors.
- **Multiplicative fault:** Is represented by the product of a variable with the fault itself. It can appear as parameter changes within a process.

It is noteworthy to mention that in this thesis, FDIR is used as an abbreviation for *Fault Detection, Isolation and Recovery*. With respect to the definition of the concepts introduced, the next sections will try to depict the big picture in FDIR by surveying the methodologies used in this area.

2.3 Model-Free Methods For FDIR

Typically fault diagnosis methods can be categorized into two major classes: those which do not use the mathematical model of the system and those which do. The methods which do not use mathematical models of the plants are called model-free and are defined as follows:

- **Physical Redundancy:** Multiple sensors can be utilized to evaluate and measure the same physical quantity. In this case, any major discrepancy between the measured values can be considered as a fault. By utilizing only two parallel sensors, fault isolation would not be possible but with three sensors or more, a voting scheme can be formed which isolates the faulty sensor.

Physical redundancy imposes extra hardware cost and extra space and weight. while in some applications like aerospace applications, the latter might be a serious problem.

- **Special Sensors:** In this approach, special sensors might be use exclusively for diagnosis. For instance, special sensors might be utilized to measure some fault-indicating physical quantities, such as sound, vibration, elongation, etc in some mechanical systems, specific sensors might be used for limit checking in hardware.
- **Limit Checking:** In this approach, plant measurements are compared by a

computer to preset limits and exceeding the threshold indicates a faulty situation. In most cases, there are at least two levels of limits. The first level plays a pre-warning role, while the second triggers an emergency reaction. Although, this is an unvarnished approach, it is impaired by two serious shortcomings.

Firstly, a single component fault may propagate to miscellaneous plant variables, causing multiple alarms and making isolation extremely arduous.

Secondly, due to the normal input variations, the plant variables may alter broadly. So, the test thresholds need to be defined conservatively and cautiously.

- **Spectrum Analysis:** Since most plant variables display a typical frequency spectrum under typical operating conditions, any deviation from this nominal spectrum can be interpreted as an indication of faulty conditions. Particular faults may have their own exclusive signature in the frequency spectrum which makes the fault isolation straightforward.
- **Logical Reasoning:** This approach is based on evaluating the symptoms obtained by detection hardware and software. The simplest techniques consist of tree of logical rules of the “IF-symptom-AND-symptom-THEN-conclusion” type. In this way, each conclusion would be able to serve as a symptom in the next rule, until the final conclusion is reached.

2.4 Model Consistency Based Diagnosis

Model-based fault diagnosis is based on the comparison of the system’s available measurements, with a priori information represented by mathematical model of the system. To be capable of detecting a fault, the measurement information $(U(t), Y(t))$ -where $U(t)$ and $Y(t)$ are the input and output vectors of the plant at time t - alone

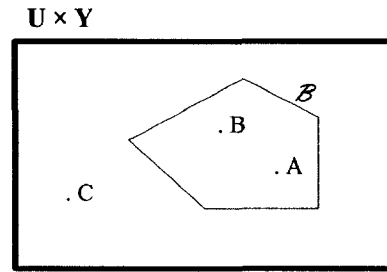


Figure 2.1: Model consistency based diagnosis

is not sufficient; but a reference which describes the nominal plant behavior is necessary. This reference can be provided by the mathematical model of the plant which describes the relation between possible input sequences and output sequences. This model is considered to be a representation of the plant behavior \mathbb{B} .

As illustrated in Figure 2.1, assume that the current input-output pair is represented by point A . If the system is healthy and faultless (and the model is correct) then A lies in the set \mathbb{B} . But if the system is faulty, it generates a different output $\hat{Y}(t)$ for the given input $U(t)$. If the new input-output pair $(U(t), \hat{Y}(t))$ is represented by point C , which is outside of \mathbb{B} then the fault is detectable. If the faulty system generates the input-output pair represented by point B , no inconsistency occurs in spite of the existence of the fault. So, the fault is not detectable in this case.

The consistency-based diagnosis principle is to check whether or not the measurement $(U(t), Y(t))$ is consistent with the system behavior. If the input-output pair is checked with respect to the nominal system behavior, a fault is detected if $(U(t), Y(t)) \notin \mathbb{B}$ holds. If the input-output pair is consistent with the behavior B_f of the system subject to the fault, the fault f may have occurred. In this case, f is called a fault candidate. To elaborate further, assume that the system behavior is known for faults f_0, f_1, f_2 . Although, the corresponding behaviors $\mathbb{B}_0, \mathbb{B}_1, \mathbb{B}_2$ are usually different, there are some overlaps most of the time. In other words, there

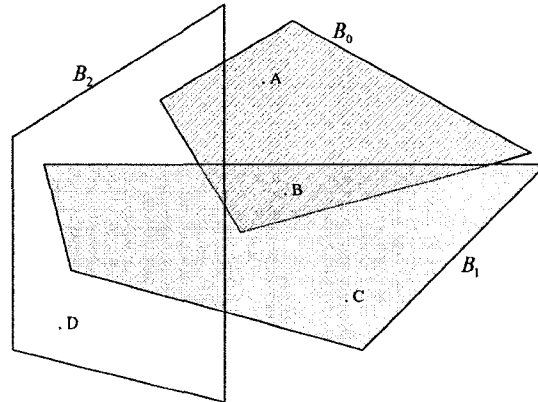


Figure 2.2: Consistency based diagnosis principle

are input-output pairs that might occur for more than one fault. If the input-output pair is shown by the points A,C and D the faults found are f_0, f_1 and f_2 respectively. However, if the measurement sequence is a point like point B, the system might be subject to either fault f_0 or fault f_1 . In this case, the diagnosis algorithm cannot make a distinction between these faults because of the fact that the measured input-output pair may occur for both faults. As a matter of fact, the ambiguity of the diagnosis is because of the nature of the system which generates the same information for both faults, and is not caused by the diagnoser. There exists no diagnosis method capable of removing this ambiguity by means of given measurement information $(U(t), Y(t))$.

As a conclusion, it can only be said that $F_c = \{f_0, f_1\}$ is the set of all fault candidates. The important question of whether or not a fault can be detected, itself has been broadly investigated by a number of researchers and is beyond the scope of this chapter. The consistency based diagnosis principle can be summarized as follows:

Model-consistency-based diagnosis: Check if the input-output pair $(U(t), Y(t))$ satisfies the relation $(U(t), Y(t)) \in \mathbb{B}_f$ where \mathbb{B}_f is the behavior of the system subject to the faults $f \in F$.

- **Fault detection:** If the input-output pair is not consistent with the faultless

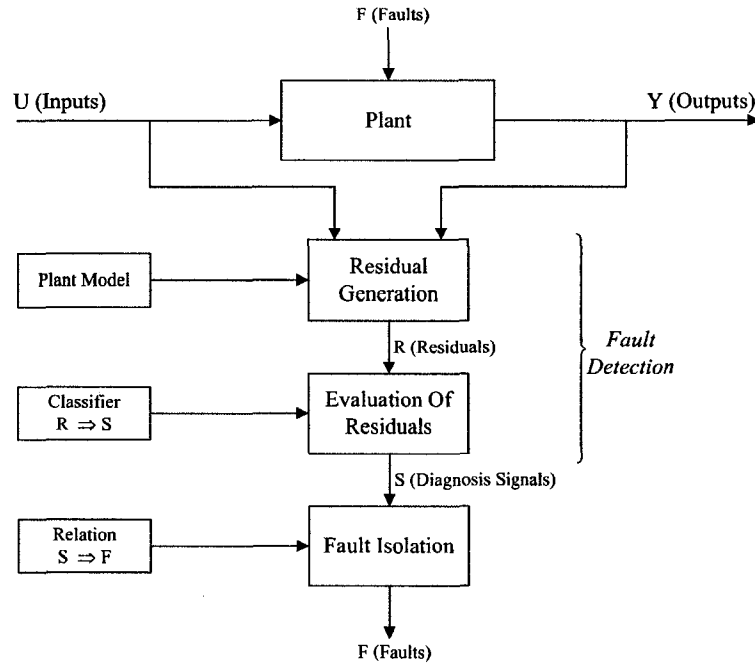


Figure 2.3: Model consistency based fault diagnosis

behavior of the system \mathbb{B}_0 ; in other words if $(U(t), Y(t)) \notin \mathbb{B}_0$ then a fault has occurred.

- **Fault isolation and identification:** If the input-output pair is consistent with the behavior \mathbb{B}_f ; in other words if $(U(t), Y(t)) \in \mathbb{B}_f$ then the fault f may have occurred; f is a fault candidate in this case.

Based on the preceding mathematical reasoning, usually a more feasible approach which is illustrated in Figure 2.3 is used. In this figure, the residual generation block generates the residual signals using available inputs and outputs from the monitored system. The fault symptom which is usually named residual should indicate the occurrence of a fault. Typically, the value of the residual should be very close to zero under healthy (faultless) conditions and distinguishably different from the value under faulty conditions. The block which performs the evaluation of residuals is basically responsible for checking the decision rule which determines the occurrence

of a fault. It may perform a simple threshold test on the instantaneous values or moving averages of the residuals. It may consist of statistical methods, generalized likelihood ratio (GLR) test, sequential probability ratio testing or a variety of other methods for change detection [Basseville 93].

Since the decision making process can be rather unequivocal and palpable if the residuals are well generated, most of the contributions in the field of quantitative model-based fault diagnosis and isolation focus on the residual generation problem.

2.5 Computational Intelligence Methodologies in FDI

The performance of analytical approaches to FDI systems depend on the accuracy of the mathematical model of the monitored system. Therefore, modeling errors will affect the performance of the FDI systems. The exploitation of computational intelligence approaches, i.e. neural networks, fuzzy logic-based systems, neuro-fuzzy hybrid systems, or evolutionary computing techniques such as genetic algorithms might be a good counterbalance for modeling errors and uncertainties.

Patton et al. [Patton 99] in their survey on fault diagnosis recommend that “a robust FDI system should combine both numerical (quantitative) and symbolic (qualitative) information.” The category of hybrid systems called neuro-fuzzy systems represents an example of such robust systems. Another category of robust FDI systems can be created by combining classical approaches, i.e. observer-based or parameter estimation, used for residual generation phase, on the one hand, and neural networks, fuzzy logic or evolutionary computing techniques, used for decision making phase, on the other hand. The computational intelligence approaches to fault

detection and isolation can be summarized in the following major classes [Palade 06]:

- Neural Network Applications
- Fuzzy Logic Applications
- Neuro-Fuzzy Systems Applications
- Genetic Algorithms

2.5.1 Neural Network Applications

Neural networks are information processing units made of interconnecting processing units which are called *neurons*. Neurons are independent processing units that transform their inputs via a function called *activation function*. The relationships among neurons are featured by *weight* values that act as the memory of the neural network. The most significant features of neural networks which makes them a merited apparatus for modeling the behavior of a system are:

- Generalization ability
- Noise tolerance
- Fast response once trained

Neural networks can be utilized for both detection and isolation in FDI systems. In the detection phase, the typical behavior of the monitored system can be *modeled* by a neural network. Then by a comparison between the output of the neural network with the output of the system, residual signals can be generated. In the isolation phase, neural networks can be utilized to fulfil the classification of the residuals into the matching categories of faults. There exist some FDI systems that utilize neural

networks for both detection and isolation, while there are also hybrid FDI systems which employ neural networks for either detection or isolation phase only.

2.5.2 Fuzzy Logic Applications

Fuzzy logic can be utilized for both fault detection (via modeling), and fault isolation (via classification). In order to construct the fuzzy model of the system, Mamdani [Mamdani 76] introduced a *linguistic* tool. Later, Takagi and Sugeno [Takagi 85] introduced a *mathematical* tool to build the fuzzy model of the system. These sorts of models are more accurate in comparison to Mamdani models for modeling. The price for this gain is the transparency offered by the usage of linguistic terms to human subjects which is rather lost.

Fuzzy logic is also very popular for fault isolation. Because the relationship between residual signals and the faulty status of the system can be easily expressed by a set of *If-Then* rules. Unlike in fault detection, in fault isolation Mamdani models are preferred to Takagi-Sugeno models because of the fact that they offer more transparency by utilizing linguistic terms.

2.5.3 Neuro-Fuzzy Systems Applications

Two notable classes of combinations between neural networks and fuzzy systems are mainly utilized in this field. First, there are neuro-fuzzy systems where each framework retains its identity. In other words, in such cases the neuro-fuzzy system consists of neural networks and fuzzy systems which operate independently while their input and outputs are interconnected to gain an added value due to each other's capabilities. These neuro-fuzzy systems are categorized under the class of *combination hybrid intelligent systems* [Palade 02].

The second notable class are neuro-fuzzy systems where one of the two frameworks is integrated into the other. This sort of systems belong to the *fusion hybrid intelligent system* class. Generally, neuro-fuzzy systems can be utilized for both fault detection (modeling)[Babuska 02; Palade 02; Uppal 02]and fault isolation (classification) [Calado 01].

2.5.4 Genetic Algorithms

Genetic algorithms in the domain of fault diagnosis are usually utilized as a support framework for other computational intelligence techniques, especially for parameter tuning purposes. Nevertheless, there also exist methods that exploit genetic algorithms as an autonomous technique for fault diagnosis.

A review of the literature shows that genetic algorithms can be used for fault diagnosis either *directly* or *indirectly*. Indirectly, genetic algorithms can be used mainly for tuning the parameters of computational intelligence based fault diagnosis systems like neural networks [Marcu 03] or fuzzy-logic based classifiers [Bocaniala 04; Bocaniala 05]. Nevertheless, a genetic algorithm can be utilized directly for fault diagnosis. For instance, Yangping et al. [Yangping 00] articulate the fault diagnosis problem as a function inversion problem, where $\mathcal{S} = g(\mathcal{F})$ is the function that is desired to be inverted. \mathcal{S} is the available signals from the plant and \mathcal{F} is the set of faults associated different parts of the plant. The elements in \mathcal{F} represent binary values denoting whether the corresponding fault occurred or not. Genetic algorithms are utilized to calculate g^{-1} in order to determine which faults took place.

2.6 Active Fault Diagnosis vs. Passive Fault Diagnosis

Most of the contributions in fault diagnosis are based on *passive fault detection*. In this approach, the fault detection module has no authority to act upon the system. In other words, the fault diagnosis module is only capable of monitoring the inputs and outputs of the system and then to decide if a fault has occurred and if possible of what kind. A significant drawback of the passive approach is that faults can be masked by the operation of the system. This can be particularly the case for controlled systems as the goal of controllers is usually to maintain some equilibrium point even if the behavior of the system changes. This robustness which is felicitous in control systems, might mask abnormal behaviors of the system. This issue makes tackling fault diagnosis challenging, especially if it is desired to detect faults that degrade performance. By the time the controller is no longer capable of maintaining the equilibrium point and compensating for the fault, the situation might become more severe, with much more severe aftermaths. A good example of this effect is the known fact that it is harder for someone who is driving a car which is equipped with power steering to distinguish a under inflated or flat front tire, in comparison to someone who is driving a car without power steering equipment. This trade-off between fault diagnosis performance and controller robustness has been noticed in the literature and has induced the investigation of integrated design of controller and fault diagnosis module [Tyler 94; Niemann 97; Blanke 06].

A more serious situation occurred in 1987 when a pilot flying an F-117 Nighthawk, which is a twin-tailed aircraft known as the stealth fighter, encountered bad weather during a training mission. One of the tail assemblies was lost but the pilot managed to return the fighter to its base and land without ever knowing that there was any missing

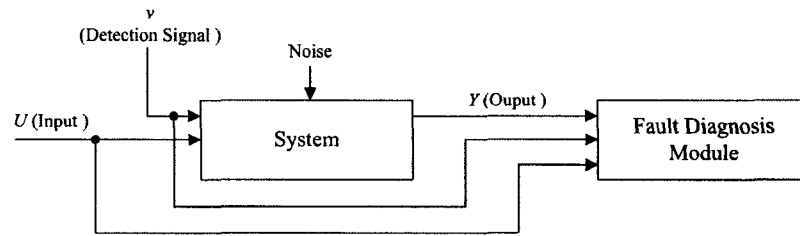


Figure 2.4: Active Fault Diagnosis

part of the tail. In this case, the robustness of the control system had the advantage of enabling the pilot to return to the base safely; but, it also had the disadvantage that the pilot had not realized that the aircraft had reduced capability and that the plane was no longer capable of high-speed maneuvers if required [Campbell 04].

A substitute for passive detection, which could overcome the problem of faults being masked by system operation is *active detection*. This method acts upon the system at critical times or on a periodic basis using a test signal - usually called “*auxiliary signal*” - in order to detect faults which would be left undetected during normal plant operations. The structure of this approach is illustrated in Figure 2.4. In order to explain the general idea, suppose that there is only one possible type of fault.

In Figure 2.5 set $\mathcal{A}_0(v)$ is the set of input-output $(U(t), Y(t))$ associated with normal behavior and $\mathcal{A}_1(v)$ is the set of input-output associated with faulty behavior. The problem of auxiliary signal design for guaranteed failure detection is to find a *reasonable* v such that $\mathcal{A}_0(v) \cap \mathcal{A}_1(v) = \emptyset$.

By “*reasonable* v ” it is meant that it should not perturb the normal operation of the system. Campbell and Nikoukhah [Campbell 04] have comprehensively addressed this issue.

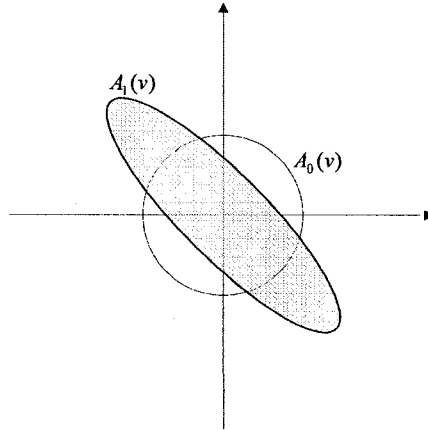


Figure 2.5: Active Fault Diagnosis Operations

2.7 Modeling of Faulty Systems

In order to utilize model-based FDI methodologies, in the first step one should provide a mathematical description of the system through which all possible fault cases can be shown. The major components which might be faulty are the *plant* itself, the *actuators*, *input and output sensors* and finally the *controller*.

Fig. 2.6 depicts the fault topology. In this figure the mentioned signals can be described as follows:

- $u_r(t)$ is the reference input signal
- $u_c(t)$ is the actuator command signal issued by the controller
- $u^*(t)$ is the actual process input (usually not available)
- $y^*(t)$ is the actual process output (usually not available)
- $u(t)$ is the measured input signal
- $y(t)$ is the measured output signal
- $f_c(t)$ represents controller fault

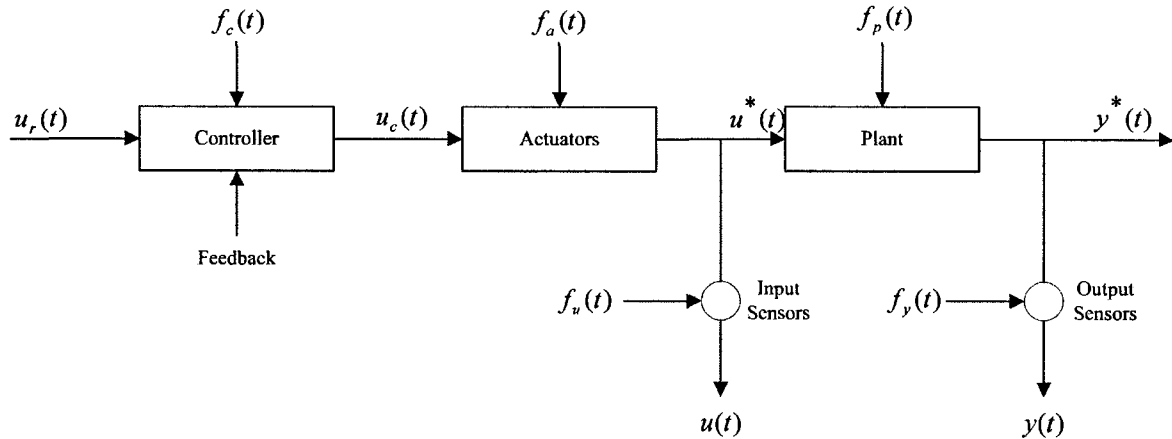


Figure 2.6: Modeling of Faulty Systems

- $f_a(t)$ represents actuator fault
- $f_p(t)$ represents plant components fault
- $f_u(t)$ represents the input sensor fault
- $f_y(t)$ represents the output sensor fault

2.8 Properties of Fault Diagnosis Techniques

A typical fault diagnosis technique should be able to accomplish the following major tasks:

- Detect and isolate faults in sensors, actuators and components, and
- Detect and isolate incipient faults as well as abrupt faults

As a matter of fact in the design of fault diagnosis systems the following questions should be considered and answered:

- How to deal with noise in the system?

- How to cope with disturbances (additive uncertainty)?
- How to handle multiple faults?
- How to deal with nonlinearity?
- How to create robustness in the face of modeling errors?
- How to cope with detection delay?
- How to overcome complication in the FDI algorithm design?
- How to reduce the complexity in implementation (or execution) of the FDI algorithm?
- What are the requirements for *a priori* modeling information?
- How good are self learning and adaptive capabilities?

2.9 Implementation Issues

The development and implementation of the fault diagnosis systems can be summarized in Figure 2.7. This framework is a combination of what is proposed by [Guide 89; VDI2206 03; Isermann 05] and the functionality of steps proposed in it can be described as follows:

Clearly, the statement of the *requirements* is the first step. This includes summarizing the desired functions of the fault detection and diagnosis (FDD) system such as the faults to be diagnosed (a fault list), determination of the units that can be replaced if they contain a fault and the allowable cost for both the final product and the different stages of the design.

In the next step, *specifications* are formulated based on the requirements. Here, It should be noted how the requirements are can be fulfilled, by partitioning the functions, the available sensors and actuators, the available computing power, use of further knowledge and definition of milestones.

It is common to start the fault diagnosis system design with mathematical *modeling* of the process, its signals and expected faults. This accommodates the *simulation* of the behavior without and with faults.

Design of the methods for fault diagnosis (FD), fault isolation and fault-tolerance (if required) is performed based on the considerations of the previous steps.

The *development* of the fault diagnosis methods with software-in-the-loop simulators (SiL) is the next step. Here, common software systems are used for simulation of the process, the faults and the FDI functions. Moreover, a powerful real-time prototype computer together with the real process can be applied (*prototyping*).

The FDI system is then mature enough for *implementation* of the final software for the series product microcomputer. As the next step, *testing and tuning procedures* for the FDD-microcomputer hardware and software begins. First tests are made by *hardware-in-the-loop simulation*(HiL). Here the microcomputer operates together with other real parts, like actuators and real-time simulation of the process and another powerful computer. This requires a special sensor-simulation-interface. HiL is performed if expensive tests with the system can be saved or experiments with faults are to be made which are not permitted with the real process. Otherwise, tests can be conducted with the real process directly.

Usually the fault diagnosis system is implemented together with other functions, e.g. automatic control. *System integration* needs to be performed considering the functional dependencies of all control levels, from lower level control to top level process management.

The next tests are *system tests*, including verification and validation. *Verification* examines if the system meets its specifications, i.e. fulfills the functions of the specifications correctly. *Validation* considers the system as whole in terms of satisfying the requirements, i.e. examines if the system is appropriate for its intended purpose. Hence, it includes consideration of correctness of the specification. For critical systems external regulating authorities have to be convinced to achieve *certification*. In this step, standards and guidelines are checked and tests have to show, e.g. the fault coverage for given operating conditions. *Field tests* are usually undertaken to test the system under many different operating conditions, production tolerances of the processes and hard environmental conditions. This is a necessary stop before the system is given to series production.

2.10 Summary

The development of fault diagnosis mechanisms began in early 1970's. But due to the fast and multidirectional development of diagnosis methods and the different variety of their applications, the terminology used by researchers in this field is still not completely consistent. This makes the comprehension of goals, contributions and comparison in this field arduous. Therefore, a common nomenclature for fault diagnosis is introduced in this chapter.

In addition, this chapter provides a quick glance at the problem of fault diagnosis in general. Fault detection methods based on the knowledge about the model of the system, as well as those that do not require a model, have been discussed. Although, the description of particular problems is brief but reference to main stream authorities has been provided.

Since this thesis uses a model based approach for fault detection, modeling of

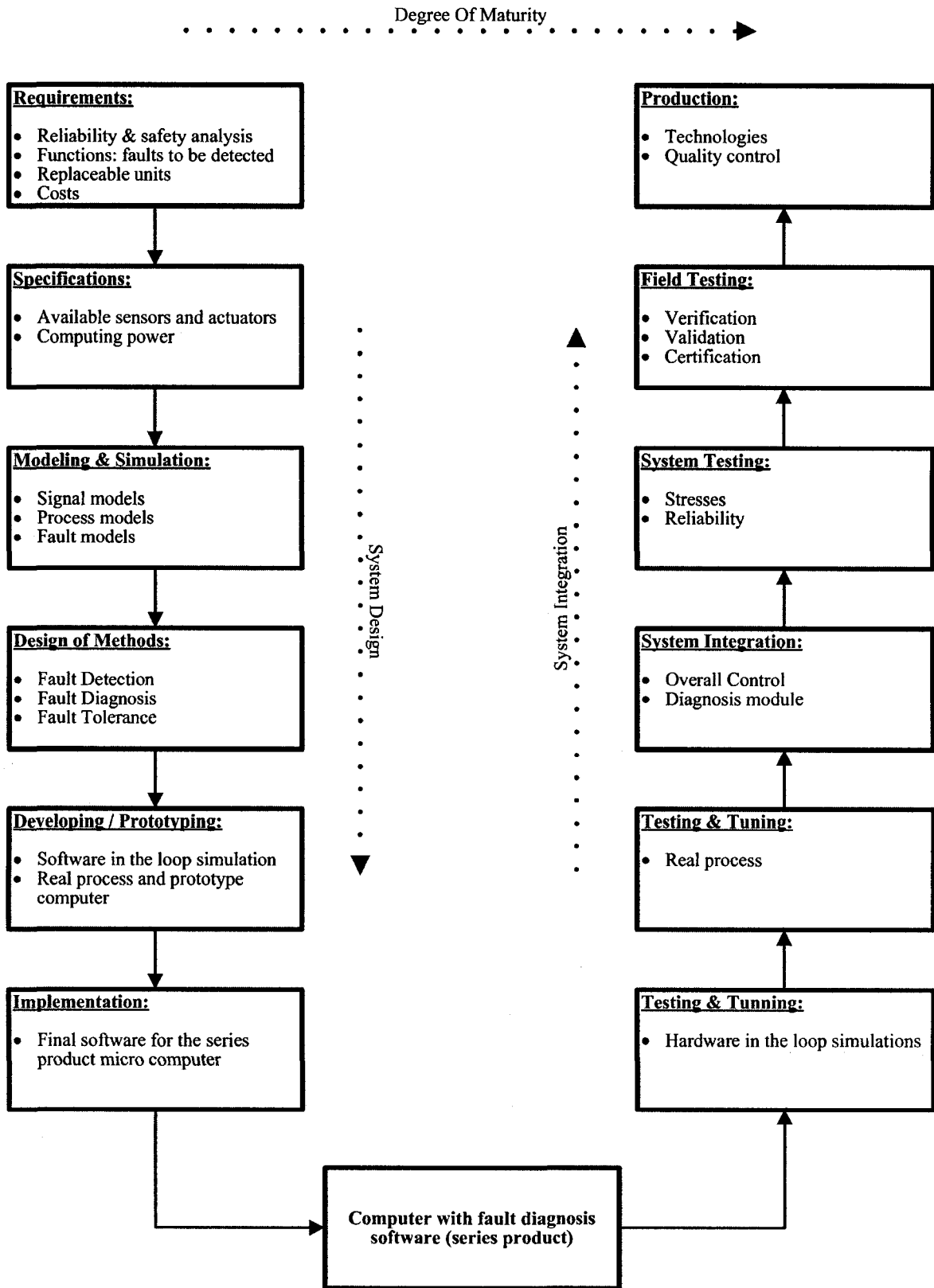


Figure 2.7: Development Scheme for Fault Diagnosis Systems

faulty system and properties of fault detection techniques is described as well. In the end, the development scheme for fault diagnosis systems in the real world is addressed.

Of course, not all of the methods and problems could have been taken into account in this chapter. Nevertheless, this chapter addresses all the fundamental concepts which have been used throughout this thesis.

Chapter 3

Trajectory Planning for Wheeled Mobile Robots (WMR)

3.1 Introduction

With the highly increased demand for autonomous motion capabilities in a variety of applications from routine industrial jobs to network-centric operations, wheeled mobile robots (WMRs) are playing an important role in providing those capabilities on reasonably smooth grounds and surfaces. Due to the heterogeneous applications of these robots, their mobility configurations as represented by wheel number, wheel type, wheel location and actuation, vehicle structure (single-body or multi-body) can be quite different. A rather comprehensive study of kinematics of WMRs can be found in [Alexander 89].

Another reason which has inspired researchers to investigate the problem of autonomous motion planning and control of WMRs is its theoretical challenges. Specifically, these systems belong to a class of nonholonomic mechanisms because of the

pure rolling constraint on the motion of their wheels (rolling without slipping)¹. This issue has been addressed in [Neimark 72].

Basically, in the absence of obstacles in the workspace of WMRs, their major motion task will be either moving between two robot postures or following a desired trajectory. It has been acknowledged by researchers that feedback stabilization at a given posture cannot be achieved with smooth time-invariant control [Campion 91]. This articulates that the problem is nonlinear and hence linear control is not suitable, even locally, and alternative approaches should be used. Therefore, after a few attempts to design local controllers, the trajectory tracking problem was finally solved through utilizing a nonlinear feedback in [Samson 91] and by using a dynamic feedback linearization in [De Luca 93; d'Andrea-Novel 95]. Moreover, recursive methods through backstepping techniques has also been used in [Jiang 99] to solve the tracking problem of nonholonomic chained form. In order to solve the posture stabilization problem a variety of time-varying [Samson 93; Samson 95] and discontinuous (often time-varying) feedback controllers [Canudas de Wit 92; Aicardi 95; Sørдалen 95; M'Closkey 97; Morin 97] have been suggested.

3.2 Basic Motion Tasks

Usually, the main tasks that we consider for WMRs in the absence of obstacles in an environment are *trajectory tracking* and *point-to-point motion*.

- ***Trajectory tracking*** is the case where a reference point of WMR should follow a trajectory in the cartesian space starting from a given initial configuration.

Here, a trajectory is defined as a geometric path with an associated timing law.

¹For mathematical definition see Equation (3.3)

- ***Point-to-point motion*** is the case where the WMR should reach a given goal configuration starting from a given initial configuration.

3.3 Modeling & Control Properties of WMRs

Suppose $q^{n \times 1} \in \mathcal{Q}$ is the vector of the generalized coordinates of WMR. *Pfaffian nonholonomic systems*² are distinguishable by the existence of m non-integrable differentiated constraints on the generalized velocities of the form:

$$\mathcal{A}(\mathbf{q})\dot{\mathbf{q}} = 0 \quad (3.1)$$

In the case of WMRs, this condition arises from the rolling without slipping constraint for the wheels. That is, all attainable motions at each instance of time can be expressed as:

$$\dot{\mathbf{q}} = G(\mathbf{q})\mathbf{w} \quad (3.2)$$

where $\mathbf{w} \in R^m$. This equation represents a driftless³ nonlinear system and is called the (first-order) *kinematic model*. If we assume the generalized coordinates as $\mathbf{q} = (x, y, \theta) \in R^3$ ($n = 3$) and *rolling without slipping constraint* as:

$$\dot{x} \sin \theta - \dot{y} \cos \theta = 0 \quad (3.3)$$

²The term “nonholonomic” refers to differential constraints that cannot be completely integrated. This means they cannot be converted into constraints that involve no derivatives.

³Problems defined using phase spaces typically have an interesting property known as *drift*. This means that for some $x \in X$, there does *not* exist any $u \in U$ such that $f(x, u) = 0$. If such u does always exist they are called *driftless*. For instance, in a dynamical system it is impossible to instantaneously stop due to momentum, which is a form of drift. For example, a car will drift into a brick wall if it is 3 meters away and traveling at 100 km/hr in the direction of the wall. There exists no action (e.g., stepping firmly on the brakes) that could instantaneously stop the car. In general, there is no way to instantaneously stop in the phase space.

then the kinematic model of the robot can be considered as:

$$\begin{bmatrix} \dot{x} \\ \dot{y} \\ \dot{\theta} \end{bmatrix} = g_1(\mathbf{q})v + g_2(\mathbf{q})\omega = \begin{bmatrix} \cos \theta \\ \sin \theta \\ 0 \end{bmatrix} v + \begin{bmatrix} 0 \\ 0 \\ 1 \end{bmatrix} \omega \quad (3.4)$$

where v and w are linear velocity and angular velocity of the center of mass of the robot. These two variables are assumed as available control inputs ($m = 2$).

3.3.1 Controllability about a Trajectory

Assume that there is a desired cartesian trajectory which the wheeled mobile robot (WMR) wants to follow; it might be convenient to find a corresponding state trajectory $q_d(t) = (x_d(t), y_d(t), \theta_d(t))$ but we should keep in mind that this trajectory should satisfy the nonholonomic constraint on the motion of the vehicle; in other words, it must be consistent with equation (3.3). The way for generating $q_d(t)$, $v_d(t)$ and $w_d(t)$ will be discussed later in Section 3.4. Here, the issue of interest is the controllability about such a trajectory. By defining input variations as $\tilde{v} = v - v_d$ and $\tilde{\omega} = \omega - \omega_d$ and the state tracking error as $\tilde{\mathbf{q}} = \mathbf{q} - \mathbf{q}_d$, the tangent linearization of equation (3.4) will be:

$$\dot{\tilde{\mathbf{q}}} = \begin{bmatrix} 0 & 0 & -v_d \sin \theta_d \\ 0 & 0 & v_d \cos \theta_d \\ 0 & 0 & 0 \end{bmatrix} \tilde{\mathbf{q}} + \begin{bmatrix} \cos \theta_d & 0 \\ \sin \theta_d & 0 \\ 0 & 1 \end{bmatrix} \begin{bmatrix} \tilde{v} \\ \tilde{\omega} \end{bmatrix} = A(t)\tilde{\mathbf{q}} + B(t) \begin{bmatrix} \tilde{v} \\ \tilde{\omega} \end{bmatrix} \quad (3.5)$$

As witnessed in Equation (3.5), the linearized system is time-varying. Therefore, a necessary and sufficient condition is that the controllability Gramian is nonsingular. An easier analysis can be done by defining the state tracking error through a rotation

matrix as:

$$\tilde{\mathbf{q}}_R = \begin{bmatrix} \cos \theta_d & \sin \theta_d & 0 \\ -\sin \theta_d & \cos \theta_d & 0 \\ 0 & 0 & 1 \end{bmatrix} \tilde{\mathbf{q}} \quad (3.6)$$

and using (3.5), we will have:

$$\dot{\tilde{\mathbf{q}}}_R = \begin{bmatrix} 0 & w_d & 0 \\ -w_d & 0 & v_d \\ 0 & 0 & 0 \end{bmatrix} \tilde{\mathbf{q}}_R + \begin{bmatrix} 1 & 0 \\ 0 & 0 \\ 0 & 1 \end{bmatrix} \begin{bmatrix} \tilde{v} \\ \tilde{\omega} \end{bmatrix} \quad (3.7)$$

When v_d and w_d are constant, the linear system (3.7) becomes time-invariant and controllable, since the following controllability matrix has rank 3 if either v_d or w_d is nonzero.

$$C = [B \quad AB \quad A^2B] = \begin{bmatrix} 1 & 0 & 0 & 0 & -\omega_d^2 & v_d \omega_d \\ 0 & 0 & -\omega_d & v_d & 0 & 0 \\ 0 & 1 & 0 & 0 & 0 & 0 \end{bmatrix} \quad (3.8)$$

Hence, we deduce that linear feedback can locally stabilize the kinematic system (3.4) about trajectories which consist of linear or circular paths which are desired to be traveled with a constant velocity. Later in Section 3.4, it is shown that local stabilization for arbitrary trajectories is feasible if they do not come to a stop.

3.3.2 Chained Canonical Forms

For nonholonomic mobile robots, the existence of canonical forms for kinematic models leads to a systematic and standardized approach of design for both open-loop and closed-loop control procedures. *Chained form* is the most popular canonical structure. For a system with two inputs and n generalized coordinates the chained form

would be as follows:

$$\begin{aligned}
 \dot{z}_1 &= u_1 \\
 \dot{z}_2 &= u_2 \\
 \dot{z}_3 &= z_2 u_1 \\
 &\vdots \\
 \dot{z}_n &= z_{n-1} u_1
 \end{aligned} \tag{3.9}$$

A two input driftless nonholonomic system with up to four generalized coordinates can always be converted to chained form by static feedback transformation [De Luca 98]. In practice, most WMRs can be transformed into chained form. For the kinematic model given in Equation (3.4), one can define the following coordinate transformation:

$$\begin{aligned}
 z_1 &= \theta \\
 z_2 &= x \cos \theta + y \sin \theta \\
 z_3 &= x \sin \theta - y \cos \theta
 \end{aligned} \tag{3.10}$$

and the static state feedback:

$$\begin{aligned}
 v &= u_2 + z_3 u_1 \\
 w &= u_1
 \end{aligned} \tag{3.11}$$

to result in:

$$\begin{aligned}
 \dot{z}_1 &= u_1 \\
 \dot{z}_2 &= u_2 \\
 \dot{z}_3 &= z_2 u_1
 \end{aligned} \tag{3.12}$$

It is noteworthy that the transformation in chained form is not unique [Canudas de Wit 93].

3.4 Trajectory Tracking

In order to acquire asymptotic trajectory tracking of a given path, a combination of a nominal feedforward with a feedback action on error is required. This error can

be defined with respect to either the reference output trajectory (output error) or an associated reference state trajectory (state error).

3.4.1 Generation of the Feedforward Command

Assume that the representative point (x, y) of the WMR must follow the cartesian trajectory $(x_d(t), y_d(t))$, with $t \in [0, T]$. From the kinematic model Equation (3.4) one has:

$$\theta = ATAN2(\dot{y}, \dot{x}) + k\pi \quad k = 0, 1 \quad (3.13)$$

where $ATAN2$ is the four-quadrant inverse tangent function (undefined only if both arguments are zero). Therefore, the nominal feedforward commands are:

$$v_d = \pm \sqrt{\dot{x}_d^2(t) + \dot{y}_d^2(t)} \quad (3.14)$$

$$\omega_d = \frac{\ddot{y}_d(t)\dot{x}_d(t) - \ddot{x}_d(t)\dot{y}_d(t)}{\dot{x}_d^2(t) + \dot{y}_d^2(t)} \quad (3.15)$$

where $w_d(t)$ has been derived from (3.13) through differentiation. The sign of $v_d(t)$ will determine forward or backward motion of the vehicle. Obviously, in order to generate $(w_d(t), v_d(t))$ the desired cartesian motion $(x_d(t), y_d(t))$ should be twice differentiable in $[0, T]$. A noticeable property of the WMR is that given an initial posture, a *consistent* desired output trajectory $(x_d(t), y_d(t))$ and its derivative, there would exist a unique associated state trajectory $q_d(t) = (x_d(t), y_d(t), \theta_d(t))$ which can be computed in an entirely algebraic way, since

$$\theta_d(t) = ATAN2(\dot{y}_d(t), \dot{x}_d(t)) + k\pi \quad k = 0, 1 \quad (3.16)$$

where the value of k is chosen such that $\theta_d(0) = \theta(0)$. If $k = 1$, a backward motion will result. As a result, the nominal orientation $\theta_d(t)$ may be computed off-line and used for defining a state trajectory error.

There are a number of facts regarding the implementation of this command which should be taken into account:

Firstly, when the desired linear velocity $v_d(t)$ is zero for some \bar{t} , neither the nominal angular velocity ($\omega_d(t)$) (Equation (3.15)) nor the nominal orientation ($\theta_d(t)$) (Equation (3.16)) would be valid. Such a situation may occur at the beginning of the motion, or at a cusp⁴ along the geometric path underlying the cartesian trajectory $(x_d(t), y_d(t))$. For the first case, higher order differential information about $(x_d(t), y_d(t))$ at $t = 0$ (if available) can be used to determine the consistent initial orientation and the initial angular velocity command. For the second case, continuous motion is guaranteed by keeping the same orientation attained at \bar{t}^- ; thus, through the application of the L'Hoptial analysis in Equation (3.15) the value of $\omega_d(\bar{t})$ would be computable.

Secondly, in a more general case, the reference trajectory may be defined by separating the geometric aspects of the path (parameterized by a scalar s) from the timing law $s = s(t)$ used for path execution. Here, the kinematic model (the driftless nature) of the WMR assists in tackling this *zeros velocity problem*. For the unicycle

⁴In singularity theory a *cusp* is a singular point of a curve. *Spinode* is an alternative name, but this is less commonly used today. For a curve defined as the zero set of a function of two variables $f(x, y) = 0$, the cusps on the curve will have the following properties:

1. $f(x, y) = 0$
2. $\frac{\partial f}{\partial x} = \frac{\partial f}{\partial y} = 0$
3. The determinant of the Hessian matrix of second derivatives is zero

A classic example of a curve that has a cusp is the curve defined by $x^3 - y^2 = 0$

WMR, one can paraphrase the purely geometric relationship as:

$$\begin{bmatrix} \frac{dx}{ds} \\ \frac{dy}{ds} \\ \frac{d\theta}{ds} \end{bmatrix} = \begin{bmatrix} \cos \theta \\ \sin \theta \\ 0 \end{bmatrix} v' + \begin{bmatrix} 0 \\ 0 \\ 1 \end{bmatrix} \omega' \quad (3.17)$$

where $v(t) = v'(s)\dot{s}(t)$ and $\omega(t) = \omega'(s)\dot{s}(t)$. Zero velocity points with well defined geometric tangents (e.g. cusps) are then attained for $\dot{s}(t) = 0$. The feedforward pseudo velocity commands $v'_d(s)$ and $w'_d(s)$ are computed by replacing time derivatives with space derivatives in Equations (3.14), (3.15).

3.4.2 Linear Control Design

The easiest trajectory tracking control design is based on tangent linearization along the reference trajectory. It is worth to reconsider the linearization procedure of the unicycle WMR around the trajectory. Define the state tracking error e as:

$$\begin{bmatrix} e_1 \\ e_2 \\ e_3 \end{bmatrix} = \begin{bmatrix} \cos \theta & \sin \theta & 0 \\ -\sin \theta & \cos \theta & 0 \\ 0 & 0 & 1 \end{bmatrix} \begin{bmatrix} x_d - x \\ y_d - y \\ \theta_d - \theta \end{bmatrix} \quad (3.18)$$

where e is very similar to \tilde{q}_R in Equation (3.7) with the only differences being the change of sign in the right hand side and computation at the current location instead of the desired location. Applying the following nonlinear transformation of velocity inputs:

$$\begin{aligned} v &= v_d \cos e_3 - u_1 \\ w &= w_d - u_2 \end{aligned} \quad (3.19)$$

the error dynamics would become:

$$\dot{\mathbf{e}} = \begin{bmatrix} 0 & w_d & 0 \\ -w_d & 0 & 0 \\ 0 & 0 & 0 \end{bmatrix} \mathbf{e} + \begin{bmatrix} 0 \\ \sin e_3 \\ 0 \end{bmatrix} v_d + \begin{bmatrix} 1 & 0 \\ 0 & 0 \\ 0 & 1 \end{bmatrix} \begin{bmatrix} u_1 \\ u_2 \end{bmatrix} \quad (3.20)$$

By linearizing Equation (3.20) around the reference, we obtain the same linear time-varying Equation (3.7) with input (u_1, u_2) and state \mathbf{e} . By defining the linear feedback law as:

$$\begin{aligned} u_1 &= -k_1 e_1 \\ u_2 &= -k_2 \text{sign}(v_d(t)) e_2 - k_3 e_3 \end{aligned} \quad (3.21)$$

and the gains as:

$$k_1 = k_3 = 2\xi a \quad (3.22)$$

$$k_2 = \frac{a^2 - \omega_d^2(t)}{|v_d(t)|} \quad (3.23)$$

a desired closed loop characteristic equation $(\lambda + 2\xi a)(\lambda^2 + 2\xi a\lambda + a^2)$, $\xi, a > 0$ which has constant eigenvalues can be reached. Obviously, the system has one negative real eigenvalue at $-2\xi a$ and a complex pair eigenvalue with natural angular frequency $a > 0$ and damping coefficient $\xi \in (0, 1)$. Nevertheless, k_2 will go to infinity as $v_d \rightarrow 0$; in other words, an infinite control effort would be required for the transient stage. Therefore, a convenient *gain scheduling* is attained by defining $a = a(t) = \sqrt{\omega_d^2(t) + bv_d^2}$ such that $k_1 = k_3 = 2\xi \sqrt{\omega_d^2(t) + bv_d^2}$ and $k_2 = b |v_d(t)|$; where $b > 0$ has been defined as an additional degree of freedom.

In compliance with the controllability analysis in Section 3.3.1, these gains go to zero when local controllability around the trajectory is lost because the latter stops.

This design leads to the following *nonlinear time-varying* controller in term of the nominal control input:

$$v = v_d \cos(\theta_d - \theta) + k_1 [\cos \theta (x_d - x) + \sin \theta (y_d - y)] \quad (3.24)$$

$$w = w_d + k_2 \text{sign}(v_d) [\cos \theta(x_d - x) + \sin \theta(y_d - y)] + k_3(\theta_d - \theta) \quad (3.25)$$

It is noteworthy that although the closed loop eigenvalues are constant with negative real part, this control law does not guarantee the asymptotic stability of the state tracking error \mathbf{e} ; because the system is still time-varying. A complete Lyapunov based stability analysis can be accomplished by a nonlinear modification as addressed in [Nicosia 01; De Luca 03].

3.4.3 Dynamic Feedback Linearization

In this part, following [De Luca 93; d'Andrea-Novel 95; Nicosia 01], a nonlinear controller -based on exact dynamic feedback linearization- has been designed for trajectory tracking. Generally, the dynamic feedback linearization problem for nonholonomic driftless systems [Equation (3.2)] consists of obtaining a dynamic state feedback compensator of the form:

$$\begin{aligned} \dot{\xi} &= a(\mathbf{q}, \xi) + b(\mathbf{q}, \xi)u \\ w &= c(\mathbf{q}, \xi) + d(\mathbf{q}, \xi)u \end{aligned} \quad (3.26)$$

with v -dimensional state ξ and m -dimensional external input, such that under a state transformation $z = T(\mathbf{q}, \xi)$, Equation (3.2) and Equation (3.26) are equivalent to a linear controllable system. Constructive algorithms, which are intrinsically based on input-output decoupling, can be found in [Isidori 95]. First, it is necessary to define an appropriate m -dimensional system output $\eta = h(\mathbf{q})$, to which a desired behavior can be assigned (in this case, tracking a desired trajectory). One then proceeds by successively differentiating the output until the input appears in a nonsingular way. At some phase, the addition of integrators on the subset of the input channels may be necessary in order to avoid subsequent differentiation of the original inputs. This *dynamic extension algorithm* generates the state ξ of the dynamic compensator

(3.26). The algorithm terminates after a finite number of differentiations whenever the system is invertible from the chosen output. If the sum of the output differentiation orders equals the dimension $n + v$ of the extended state space, full input-output linearization will also be attained. The closed loop system would be equivalent to a set of decoupled input-output chains of integrators from u_i to η_i where $i = 1, \dots, m$. To elaborate further, this exact linearization procedure for the unicycle WMR model [Equation (3.4)] will be carried out here. First, define the linearizing output vector as $\eta = (x, y)$. By differentiating η with respect to time we would get:

$$\dot{\eta} = \begin{bmatrix} \dot{x} \\ \dot{y} \end{bmatrix} = \begin{bmatrix} \cos \theta & 0 \\ \sin \theta & 0 \end{bmatrix} \begin{bmatrix} v \\ \omega \end{bmatrix} \quad (3.27)$$

which shows that only v affects $\dot{\eta}$ and the angular velocity w cannot be found from this first-order differential information. Hence, we would require to add an integrator (whose state is denoted by ξ) on the linear velocity input

$$v = \xi, \dot{\xi} = a \Rightarrow \dot{\eta} = \xi \begin{bmatrix} \cos \theta \\ \sin \theta \end{bmatrix} \quad (3.28)$$

This new input a is the *linear acceleration* of the unicycle. Differentiating further yields:

$$\ddot{\eta} = \dot{\xi} \begin{bmatrix} \cos \theta \\ \sin \theta \end{bmatrix} + \xi \dot{\theta} \begin{bmatrix} -\sin \theta \\ \cos \theta \end{bmatrix} = \begin{bmatrix} \cos \theta & -\xi \sin \theta \\ \sin \theta & \xi \cos \theta \end{bmatrix} \begin{bmatrix} a \\ w \end{bmatrix} \quad (3.29)$$

and the matrix $\begin{bmatrix} \cos \theta & -\xi \sin \theta \\ \sin \theta & \xi \cos \theta \end{bmatrix}$ is nonsingular provided that $\xi \neq 0$. Under this assumption, we can define:

$$\begin{bmatrix} a \\ w \end{bmatrix} = \begin{bmatrix} \cos \theta & -\xi \sin \theta \\ \sin \theta & \xi \cos \theta \end{bmatrix}^{-1} \begin{bmatrix} u_1 \\ u_2 \end{bmatrix} \quad (3.30)$$

so,

$$\ddot{\eta} = \begin{bmatrix} \ddot{\eta}_1 \\ \ddot{\eta}_2 \end{bmatrix} = \begin{bmatrix} u_1 \\ u_2 \end{bmatrix} = u \quad (3.31)$$

As a result, the dynamic compensator would be:

$$\begin{aligned} \dot{\xi} &= u_1 \cos \theta + u_2 \sin \theta \\ v &= \xi \\ w &= \frac{u_2 \cos \theta - u_1 \sin \theta}{\xi} \end{aligned} \quad (3.32)$$

Here, the dynamic compensator is *one*-dimensional, so we have $n + v = 3 + 1 = 4$ which is equal to the aggregated number of output differentiations in Equation (3.31). Hence, in the following new coordinates, the extended system would be fully linearized in a control form.

$$\begin{aligned} z_1 &= x \\ z_2 &= y \\ z_3 &= \dot{x} = \xi \cos \theta \\ z_4 &= \dot{y} = \xi \sin \theta \end{aligned} \quad (3.33)$$

This system can be described by the two chains of second-order input-output integrators given by Equation (3.31) rephrased as:

$$\begin{aligned} \ddot{z}_1 &= u_1 \\ \ddot{z}_2 &= u_2 \end{aligned} \quad (3.34)$$

It is noteworthy that the dynamic feedback linearizing controller (3.32) has a potential singularity at $\xi = v = 0$ which occurs when the robot is not rolling. The appearance of such a singularity in the dynamic extension process has been proven to be structural for nonholonomic systems [De Luca 93]. Obviously, this must be taken into account when designing control laws on the equivalent linear model.

Assume that the unicycle must follow a smooth output trajectory $(x_d(t), y_d(t))$ which is persistent, i.e., such that the nominal control input $v_d = \sqrt{\dot{x}_d^2 + \dot{y}_d^2}$ along the trajectory does never go to zero. It is rather routine to design a globally exponentially stabilizing feedback for the desired trajectory on the equivalent linear and decoupled system (3.34). Therefore, the feedback law would be:

$$\begin{aligned} u_1 &= \ddot{x}_d(t) + k_{p1}(x_d(t) - x) + k_{d1}(\dot{x}_d(t) - \dot{x}) \\ u_2 &= \ddot{y}_d(t) + k_{p2}(y_d(t) - y) + k_{d2}(\dot{y}_d(t) - \dot{y}) \end{aligned} \quad (3.35)$$

where $k_{pi} > 0$, $k_{di} > 0$ ($i=1,2$) are chosen PD gains. In practice, velocities \dot{x} and \dot{y} can be computed via the last two expressions in Equation (3.33), as a function of the robot state and of the compensator state ξ . Alternatively, one can use estimates of \dot{x} and \dot{y} obtained from odometric measurements. This approach is more robust with respect to unmodeled dynamics.

There are a number of issues which should be taken into account in applying this dynamic feedback linearization approach to the system:

- The state of the dynamic compensator should be initialized at $\xi(0) = v_d(0)$. This guarantees exact trajectory tracking for a matched initial state of the robot. In this case, the control law [Equations (3.32) and (3.35)] reduces to pure feedforward action.
- Since this approach is purely based on output tracking error definition, it requires neither the explicit computation of $\theta_d(t)$ nor the measurement of the orientation angle.
- Problems may arise if the actual command $v = \xi$ crosses zero during an initial transient. Nevertheless, this situation can be avoided by choosing an appropriate initial state for the dynamic compensator. For instance, an uncomplicated

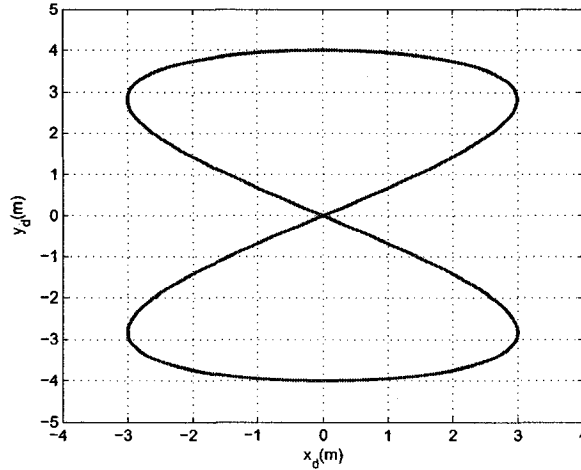


Figure 3.1: The desired eight-shaped reference trajectory which the WMR wants to follow

way to keep the actual command bounded is to reset the state ξ whenever its value falls below a given threshold. This will generate isolated discontinuities with respect to time in the input command v .

3.5 Simulation Results

In this section, some simulation results are provided as substantiation of the potency of the controllers designed in Section 3.4.2 and Section 3.4.3.

The reference trajectory which the WMR wants to follow is assumed to be in the form of Equation (3.36)

$$x_d(t) = A_1 \sin(f_1 t) \quad y_d(t) = A_2 \sin(f_2 t) \quad t \in [0, T] \quad (3.36)$$

The numerical results are given for the eight-shaped reference trajectory where $A_1 = 3$, $A_2 = 4$, $f_1 = 1$ and $f_2 = 0.5$. Figure 3.1 depicts this trajectory. The trajectory starts from the origin with $\theta_d(0) = \frac{\pi}{6}$ rad. A full cycle is completed in $T = \frac{2\pi}{0.5} \simeq$

12.57 s. The reference initial velocities are:

$$v_d(0) \simeq 3.61 \text{ m/s} \quad \omega_d(0) = 0 \text{ rad/s} \quad (3.37)$$

These two values are consistent with Equation (3.14) and Equation (3.15).

In the provided set of simulations, the initial robot configuration is assumed to be matched with the desired reference trajectory; in other words, we have $q(0) = q_d(0)$. Hence, the feedforward commands of Equations (3.14) and (3.15) would acquiesce to precise trajectory tracking in ideal conditions. Nevertheless, if the WMR starts at rest and nonzero high-level commands $v_d(0)$ and $\omega_d(0)$ are given to the robot, there would be some transients before the velocities can be actually achieved; this phenomenon is due to actuator and vehicle dynamics.

Figures 3.2(b), 3.2(c) and 3.2(d) show the results obtained with the dynamic linear controller design (Equations 3.24 and 3.25), using the described gains with $\xi = 3.99$ and $b = 1$. The tracking of the reference trajectory of Figure 3.1 is quite accurate. The small appearing errors are mainly due to quantization and discretization of velocity commands as well as to other nonidealities. This is clearly shown in Figure 3.2(d) which shows the norm of the cartesian error.

Similar performance is obtained with the dynamic feedback linearization controller (3.32), choosing the gains in Equation (3.35) as $k_{p1} = k_{p2} = 0.7$, $k_{d1} = k_{d2} = 1$ and initializing the dynamic compensator at $\xi(0) = v_d(0)$. To recognize the slight improvement in performance, compare the norm of the cartesian tracking error in Figure 3.3(d) with the previous result in Figure 3.2(d).

3.6 Summary and Conclusions

With regard to the statement of the problem in Section 1.2, under the considered scenario the nonholonomic wheeled mobile robot with nonlinear kinematics is required to

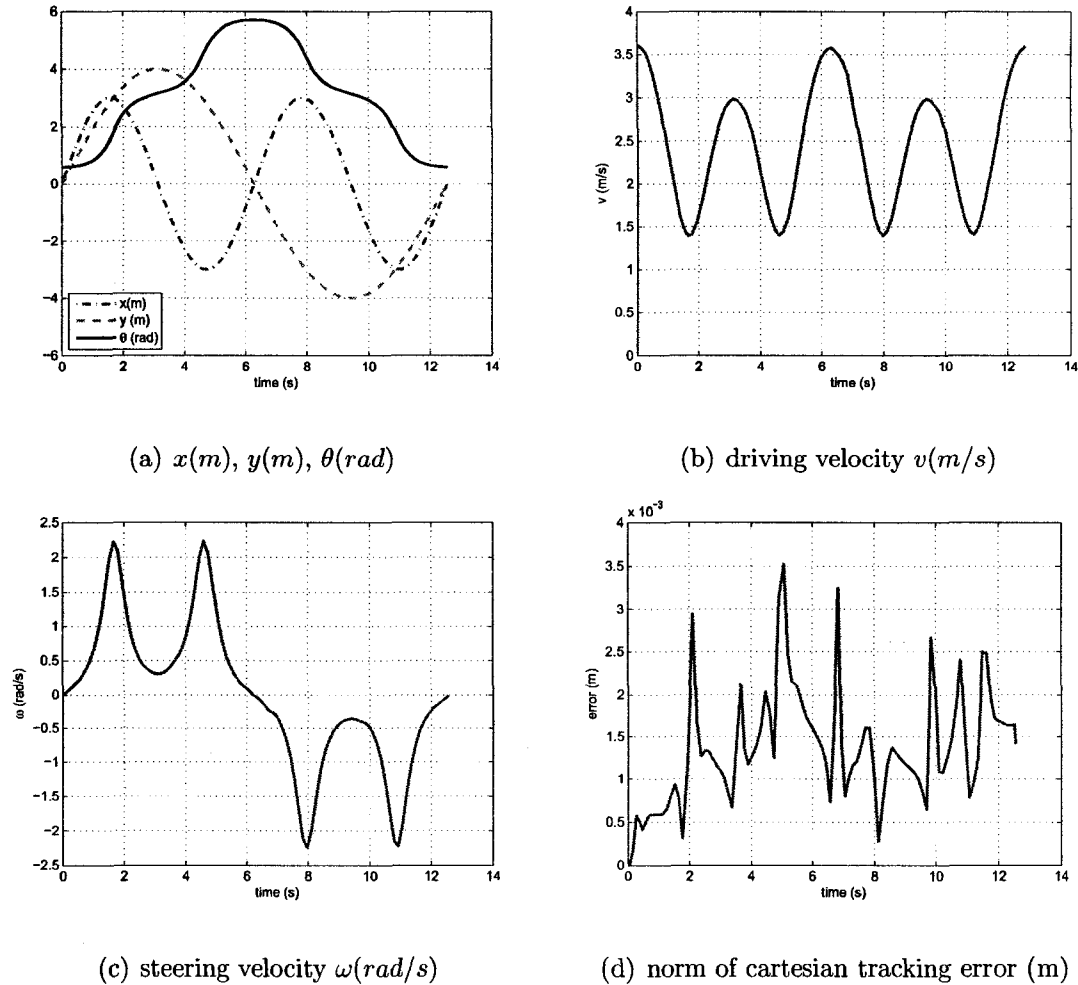


Figure 3.2: Trajectory tracking with dynamic linear feedback design

follow a predefined smooth trajectory in the absence of obstacles in the environment. In order to make the wheeled mobile robot capable of performing this maneuver, designing controllers for trajectory planning are essential. Therefore, two different types of controllers have been designed. The first one is based on dynamic linear control design strategy while the second one is based on dynamic feedback linearization.

By comparing Equations (3.35),(3.24) and (3.25) it is obvious that although the dynamic linear controller requires both the desired orientation angle $\theta_d(t)$ and the measurement of the orientation angle $\theta(t)$, the dynamic feedback linearization ap-

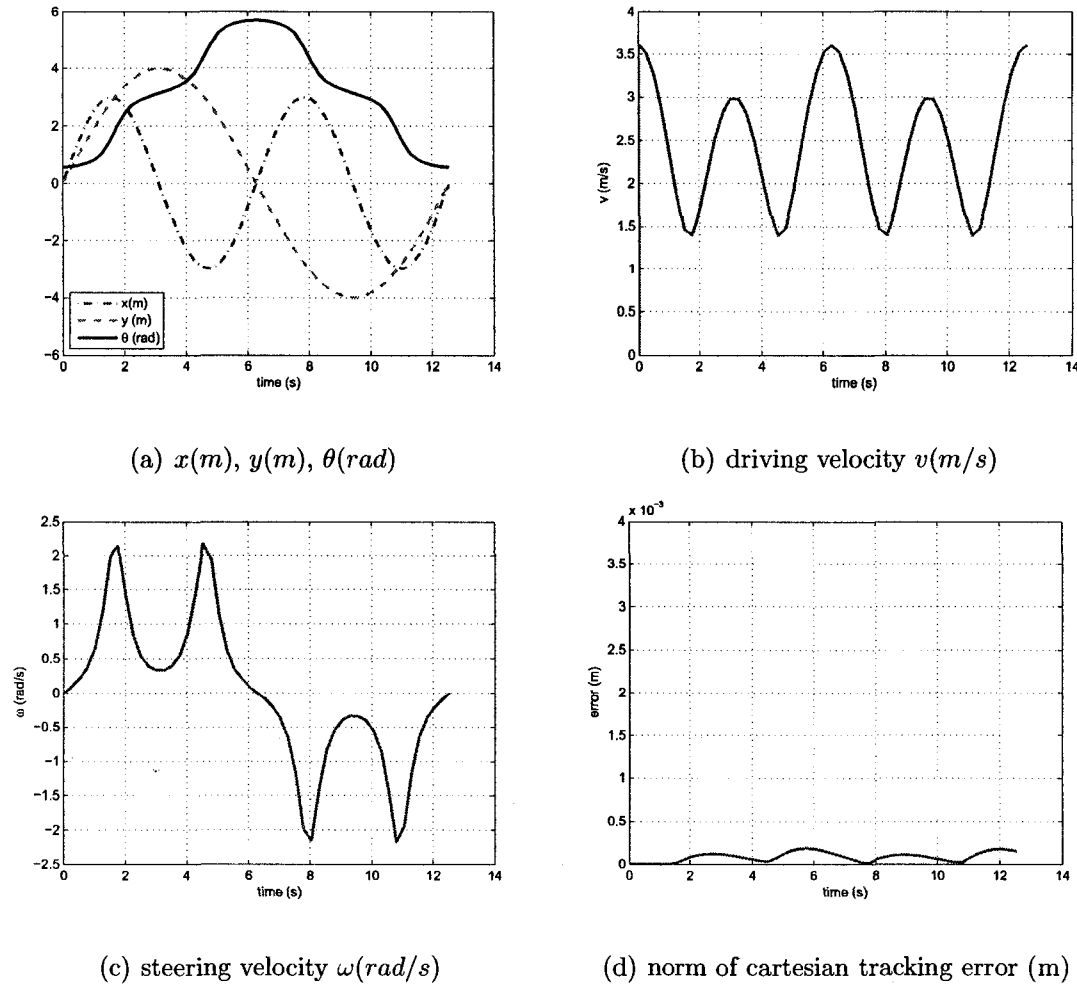


Figure 3.3: Trajectory tracking with dynamic feedback linearization

proach is purely based on the output tracking error definition and requires neither $\theta_d(t)$ nor $\theta(t)$.

With respect to the achieved controller performance, by comparing Figure 3.2(d) and Figure 3.3(d), one can easily recognize that the performance of the dynamic feedback linearization controller is better than the the dynamic linear controller. The impact of the controller type on the performance of the fault detection system will be studied in *Chapter 4*.

Chapter 4

Fault Detection Design for the WMR

4.1 Introduction

The particular objective of this chapter is to design appropriate fault detection systems for the trajectory tracking problem of wheeled mobile robots (WMR). In order to do so, first the principal subsystems of wheeled mobile robots which might be subject to faults have been introduced. Then, two different techniques -which are developed on the ground of the model consistency based scheme as illustrated in Fig. 4.1- are proposed for fault detection in a general class of nonlinear systems. Indeed, the mobile robot trajectory tracking problem would essentially be covered as a subclass of the studied nonlinear systems.

The first proposed technique is based on identification of the system via Extended Kalman Filtering (EKF). In this technique, a novel residual generation method has been introduced.

The second proposed fault detection scheme, is based on system identification

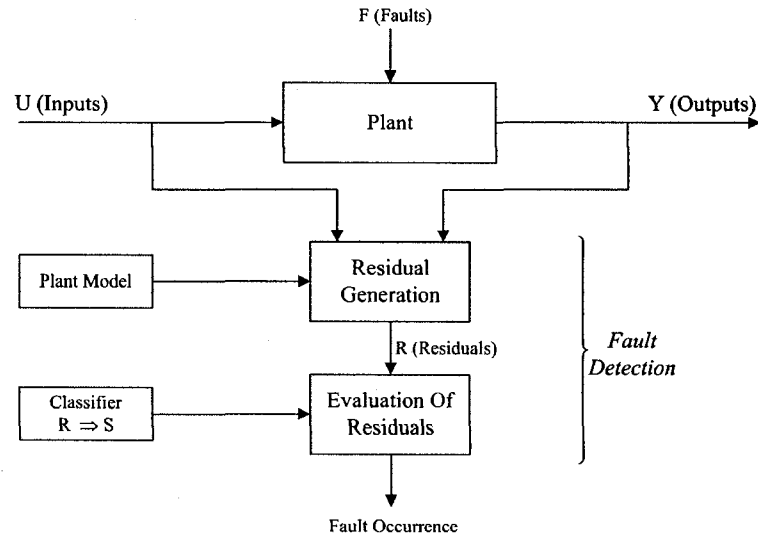


Figure 4.1: Schematic of the exploited model consistency based fault diagnosis approach

through artificial neural networks. In this approach, a modified stable backpropagation algorithm has been used.

Subsequently in Chapter 5, a comparative study of the performance of these two methods is provided.

4.2 Major Subsystems of WMRs Subject to Faults

A WMR needs a variety of subsystems to provide its expected functionalities, i.e., motion on the ground, sensing the surrounding environment, communicating with other mobile or stationary systems. The following are some of the most basic subsystems which are common among a large number of WMR types.

- *Power Subsystem*: This part is in charge of providing energy to all parts of the WMR. It usually consists of a power source (such as battery cells) and a power distribution network (such as wires, switches, safety circuits). Faults in the

power subsystem could cripple the WMR thoroughly or cause complete failure.

- *Driving Subsystem:* This subsystem provides the required force for the WMR to move forward according to the commands issued by the host computer. It typically consists of motors, gearbox, amplifiers, breaks, motion control card and encoders. As a matter of fact, this subsystem plays a major role in the mobility of a WMR.
- *Steering Subsystem:* This subsystem exploits actuators to control the direction of the vehicle and therefore orient its heading angle. It usually includes an actuator (Hydraulic actuator or linear DC motor), a mechanical linkage made up of joints and links and an encoder. Obviously, a fault in the steering subsystem will impair the mobility of the WMR.
- *Suspensions:* This part helps depress vibration during operation and maintains the balance of the WMR. It consists of suspensions and rubber tires. A fault in this subsystem, i.e., suspension hardening or flat tire, may not be critical but may lead to faulty vehicle control because of the improper balance of the robot.
- *Communication:* Usually WMRs need wireless communication to exchange command and data with the control center or other stationary or mobile systems. A serious problem may be posed in case of loss of communication especially during cooperative activities. Communication delay can be the cause of instability in formation manoeuvre control of team of WMRs as well.
- *Sensors:* Sensors are responsible to measure quantities such as position, velocity, steering angle, relative distance to obstacles, etc. Since these sensors play a crucial role in fault diagnosis of WMRs, their measurement reliability needs to be certified and guaranteed before the deployment of fault diagnosis methods.

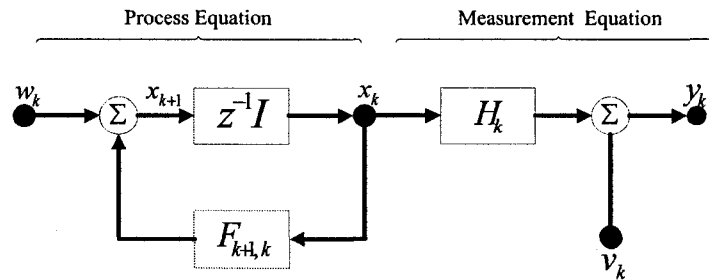


Figure 4.2: Signal flow graph of a linear discrete time dynamic system

4.3 Kalman Filtering

The *Kalman filter*, was first introduced by Rudolf E. Kalman in 1960, when he published his well-known paper describing a recursive solution to the linear optimal filtering problem. This approach can be applied to both stationary and nonstationary environments. In this recursive solution, each updated estimate of the state is derived from the previous estimate and the new input data; as a result, only the previous estimate needs to be stored. Besides eliminating the necessity of storing the entire past data, the Kalman filter is computationally more efficient than computing the estimate directly from the entire past observed data at each step. In this part, an introductory discussion about Kalman filters is made to pave the road for their application in the subsequent parts. I have chosen to follow the original paper by Kalman [Kalman 60] for the derivation. Moreover, I have tried to include the highlights of the works done by [Grewal 01; Haykin 01; Welch 04].

4.3.1 What is a Kalman Filter?

Consider a linear, discrete-time dynamical system described by the block diagram depicted in Figure 4.2. The concept of *state* is very important in the description of a system. The *state* or *state vector* is defined as the minimal set of data that is

sufficient to uniquely describe the unforced dynamical behavior of the system and is denoted by x_k ; the subscript k denotes the discrete time. In other words, the state is the least amount of data on the past behavior of the system that is required to predict the behavior of the system in the future. Usually, the state x_k is unknown and we use a set of observed data denoted by y_k to estimate it.

In terms of mathematics, Figure 4.2 includes the following equations:

- *Process equation:*

$$\mathbf{x}_{k+1} = \mathbf{F}_{k+1,k} \mathbf{x}_k + \mathbf{w}_k \quad (4.1)$$

where $\mathbf{F}_{k+1,k}$ is the *transition matrix* taking the state \mathbf{x}_k from time k to time $k + 1$. The process noise \mathbf{W}_k is assumed to be additive, white and Gaussian, with zero mean and with covariance matrix defined by:

$$E[w_n w_k^T] = \begin{cases} Q_k & \text{for } n = k \\ 0 & \text{for } n \neq k \end{cases} \quad (4.2)$$

where the superscript T denotes matrix transposition. The dimension of the state space is denoted by M .

- *Measurement equation:*

$$\mathbf{y}_k = \mathbf{H}_k \mathbf{x}_k + \mathbf{v}_k \quad (4.3)$$

where y_k is the *observable* at time k and \mathbf{H}_k is the measurement matrix. The measurement noise v_k , as the noise defined in the previous equation, is assumed to be additive, white and Gaussian with zero mean. Its covariance matrix is defined by

$$E[v_n v_k^T] = \begin{cases} R_k & \text{for } n = k \\ 0 & \text{for } n \neq k \end{cases} \quad (4.4)$$

In addition, the measurement noise v_k is assumed to be uncorrelated with the process noise w_k . The dimension of the measurement space is denoted by N .

Now, the general Kalman filtering problem can be addressed as follows:

“Use the entire observed data, consisting of vectors y_1, y_2, \dots, y_k to find for each $k \geq 1$ the minimum mean-square error estimate of the state x_i ”

In other words, the problem is jointly solving the process and measurement equations for the unknown state in an optimum manner. This problem is called *filtering* if $i = k$, *prediction* if $i > k$, and *smoothing* if $1 \leq i < k$.

4.3.2 Mathematical Foundation of Optimum Estimates

Prior to deriving the Kalman filter, it is beneficial to review some of the mathematical foundations of optimum estimates. For simplicity reasons, this review is done in the context of scalar random variables; but the generalization of these concepts to vector random variables is straightforward. Suppose the observable $y_k = x_k + v_k$ is given; where x_k is an unknown signal and v_k is an additive noise component. Let \hat{x}_k denote a posteriori estimate of the signal, given the observations y_1, y_2, \dots, y_k . In practice, the estimate \hat{x}_k is different from the unknown signal x_k . In order to derive this estimate optimally, a *cost function* for incorrect and imprecise estimates is required. This cost function must maintain the following two requirements:

1. must be nonnegative
2. must be a nondecreasing function of the *estimation error* \tilde{x}_k defined by

$$\tilde{x}_k = x_k - \hat{x}_k \quad (4.5)$$

These two requirements are satisfied by the *mean-square error* defined by:

$$J_k = E[(x_k - \hat{x}_k)^2] = E[\tilde{x}_k^2] \quad (4.6)$$

where E is the expectation operator. Here, the dependence of the cost function J_k on time k indicates the nonstationary nature of the recursive estimation process.

The optimum value for the estimate \hat{x}_k , can be derived by invoking the following two theorems from stochastic process theory [Kalman 60; Papoulis 02]:

Theorem 1 (Conditional Mean Estimator). *If the stochastic processes $\{x_k\}$ and $\{y_k\}$ are jointly Gaussian, then the optimum estimate \hat{x}_k that minimizes the mean-square error J_k is the conditional mean estimator:*

$$\hat{x}_k = E[x_k | y_1, y_2, \dots, y_k] \quad (4.7)$$

Theorem 2 (Principle Of Orthogonality). *Let the stochastic processes $\{x_k\}$ and $\{y_k\}$ be of zero means; i.e., $E[x_k] = E[y_k] = 0$ for all k ; then the stochastic process $\{x_k\}$ and $\{y_k\}$ are jointly Gaussian; or if the optimal estimate \hat{x}_k is restricted to be a linear function of the observables and the cost function is the mean-square error; then the optimum estimate \hat{x}_k , given the observables y_1, y_2, \dots, y_k is the orthogonal projection of x_k on the space spanned by these observables.*

Now, with respect to these two theorems, the derivation of Kalman filter follows:

4.3.3 Derivation of the Kalman Filter

Suppose that at time k , a measurement on a linear dynamical system described by (4.1) and (4.3) has been made. The goal is to exploit the information contained in the new measurement \mathbf{y}_k to update the estimate of the the unknown state \mathbf{x}_k .

Let $\hat{\mathbf{x}}_k^-$ denote a *a priori estimate* of the state, which is accessible at time k . Since our objective is a linear estimator, we can articulate the *a posteriori estimate* $\hat{\mathbf{x}}_k$ as a linear combination of the *a priori estimate* and the new measurement:

$$\hat{\mathbf{x}}_k = \mathbf{G}_k^{(1)} \hat{\mathbf{x}}_k^- + \mathbf{G}_k \mathbf{y}_k \quad (4.8)$$

where the matrix coefficients $\mathbf{G}_k^{(1)}$ and \mathbf{G}_k are to be derived. In order to find these matrices, the *Principle of Orthogonality* introduced in Theorem [2] should be invoked.

By defining the *state-error vector* as:

$$\tilde{x}_k = x_k - \hat{x}_k \quad (4.9)$$

we can apply the Principle of Orthogonality as follows:

$$E[\tilde{x}_k y_k^T] = 0 \quad \text{for } i = 1, 2, \dots, k-1 \quad (4.10)$$

So, by using (4.10), (4.9), (4.8), and (4.3), for $i = 1, 2, \dots, k-1$ we have,

$$\begin{aligned} E[\tilde{x}_k y_k^T] &= E[(x_k - \hat{x}_k) y_i^T] \\ &= E[(x_k - (\mathbf{G}_k^{(1)} \hat{x}_k^- + \mathbf{G}_k y_k)) y_i^T] \\ &= E[(x_k - \mathbf{G}_k^{(1)} \hat{x}_k^- - \mathbf{G}_k (\mathbf{H}_k x_k + w_k)) y_i^T] \\ &= E[(x_k - \mathbf{G}_k^{(1)} \hat{x}_k^- - \mathbf{G}_k \mathbf{H}_k x_k - \mathbf{G}_k w_k) y_i^T] \\ &= E[(\mathbf{I} - \mathbf{G}_k \mathbf{H}_k) x_k y_i^T - \mathbf{G}_k^{(1)} x_k y_i^T + \mathbf{G}_k^{(1)} x_k y_i^T - \mathbf{G}_k^{(1)} \hat{x}_k^- y_i^T - \mathbf{G}_k w_k y_i^T] \\ &= E[(\mathbf{I} - \mathbf{G}_k \mathbf{H}_k - \mathbf{G}_k^{(1)}) x_k y_i^T + \mathbf{G}_k^{(1)} (x_k - \hat{x}_k^-) y_i^T - \mathbf{G}_k w_k y_i^T] \\ &= 0 \end{aligned} \quad (4.11)$$

where \mathbf{I} is the identity matrix. Since the process noise w_k and the measurement noise v_k are uncorrelated, it follows that:

$$E[w_k y_i^T] = 0 \quad (4.12)$$

Moreover, the Principle of Orthogonality implies that:

$$E[(x_k - \hat{x}_k^-) y_i^T] = 0 \quad (4.13)$$

Hence, with respect to (4.12) and (4.13), (4.11) can be simplified as:

$$(\mathbf{I} - \mathbf{G}_k \mathbf{H}_k - \mathbf{G}_k^{(1)}) E[x_k y_i^T] = 0 \quad (4.14)$$

For all arbitrary values of x_k and y_i , (4.14) can only be true if the coefficients \mathbf{G}_k and $\mathbf{G}_k^{(1)}$ satisfy the following relation:

$$\mathbf{I} - \mathbf{G}_k \mathbf{H}_k - \mathbf{G}_k^{(1)} = \mathbf{0} \quad (4.15)$$

In other words:

$$\mathbf{I} - \mathbf{G}_k \mathbf{H}_k = \mathbf{G}_k^{(1)} \quad (4.16)$$

Now, by plugging (4.16) into (4.1), the *a posteriori estimate* of the state at time k would be:

$$\hat{\mathbf{x}}_k = \hat{\mathbf{x}}_k^- + \mathbf{G}_k (\mathbf{y}_k - \mathbf{H}_k \hat{\mathbf{x}}_k^-) \quad (4.17)$$

where \mathbf{G}_k is called the *Kalman gain*.

Now the problem which needs to be taken care of is the derivation of an explicit form for \mathbf{G}_k . From the Principle of Orthogonality, we have:

$$E[(\mathbf{x}_k - \hat{\mathbf{x}}_k) \mathbf{y}_k^T] = 0 \quad (4.18)$$

It follows that:

$$E[(\mathbf{x}_k - \hat{\mathbf{x}}_k) \hat{\mathbf{y}}_k^T] = 0 \quad (4.19)$$

where $\hat{\mathbf{y}}_k^T$ is an estimate of \mathbf{y}_k given the previous measurements y_1, y_2, \dots, y_{k-1} .

Now, we define a *new* process:

$$\tilde{\mathbf{y}}_k = \mathbf{y}_k - \hat{\mathbf{y}}_k \quad (4.20)$$

This new process symbolizes a measure of the new information contained in \mathbf{y}_k ; it can also be articulated as follows:

$$\begin{aligned} \tilde{\mathbf{y}}_k &= \mathbf{y}_k - \mathbf{H}_k \hat{\mathbf{x}}_k^- \\ &= \mathbf{H}_k \mathbf{x}_k + \mathbf{v}_k - \mathbf{H}_k \hat{\mathbf{x}}_k^- \\ &= \mathbf{H}_k (\mathbf{x}_k - \hat{\mathbf{x}}_k^-) + \mathbf{v}_k \\ &= \mathbf{H}_k \tilde{\mathbf{x}}_k^- + \mathbf{v}_k \end{aligned} \quad (4.21)$$

Furthermore, by subtracting (4.19) from (4.18) and using the definition of (4.20), it can be concluded that:

$$E[(\mathbf{x}_k - \hat{\mathbf{x}}_k)\tilde{\mathbf{y}}_k^T] = 0 \quad (4.22)$$

(4.17) and (4.3) imply that:

$$\begin{aligned} \mathbf{x}_k - \hat{\mathbf{x}}_k &= \mathbf{x}_k - (\hat{\mathbf{x}}_k^- + \mathbf{G}_k(\mathbf{y}_k - \mathbf{H}_k\hat{\mathbf{x}}_k^-)) \\ &= (\mathbf{x}_k - \hat{\mathbf{x}}_k^-) - \mathbf{G}_k(\mathbf{H}_k\mathbf{x}_k + \mathbf{v}_k - \mathbf{H}_k\hat{\mathbf{x}}_k^-) \\ &= (\mathbf{x}_k - \hat{\mathbf{x}}_k^-) - \mathbf{G}_k(\mathbf{H}_k(\mathbf{x}_k - \hat{\mathbf{x}}_k^-) + \mathbf{v}_k) \\ &= \tilde{\mathbf{x}}_k^- - \mathbf{G}_k\mathbf{H}_k\tilde{\mathbf{x}}_k^- - \mathbf{G}_k\mathbf{v}_k \\ &= (\mathbf{I} - \mathbf{G}_k\mathbf{H}_k)\tilde{\mathbf{x}}_k^- - \mathbf{G}_k\mathbf{v}_k \end{aligned} \quad (4.23)$$

Therefore using (4.21) and (4.23), from (4.22) we can infer the following:

$$E[((\mathbf{I} - \mathbf{G}_k\mathbf{H}_k)\tilde{\mathbf{x}}_k^- - \mathbf{G}_k\mathbf{v}_k)(\mathbf{H}_k\tilde{\mathbf{x}}_k^- + \mathbf{v}_k)] = 0 \quad (4.24)$$

With the knowledge that the measurement noise v_k is independent of the state \mathbf{x}_k and therefore $\tilde{\mathbf{x}}_k^-$; so, (4.24) can be simplified as:

$$(\mathbf{I} - \mathbf{G}_k\mathbf{H}_k)E[\tilde{\mathbf{x}}_k^-\tilde{\mathbf{x}}_k^{T-}]\mathbf{H}_k^T - \mathbf{G}_kE[\mathbf{v}_k\mathbf{v}_k^T] = 0 \quad (4.25)$$

So, we define the *a priori covariance matrix*:

$$\mathbf{P}_k^- = E[(\mathbf{x}_k - \hat{\mathbf{x}}_k^-)(\mathbf{x}_k - \hat{\mathbf{x}}_k^-)^T] = E[\tilde{\mathbf{x}}_k^-\tilde{\mathbf{x}}_k^{T-}] \quad (4.26)$$

By invoking the covariance definitions of (4.4) and (4.26), we can rewrite (4.25) as follows:

$$(\mathbf{I} - \mathbf{G}_k\mathbf{H}_k)\mathbf{P}_k^-\mathbf{H}_k^T - \mathbf{G}_k\mathbf{R}_k = 0 \quad (4.27)$$

By solving (4.27) for \mathbf{G}_k , the desired formula will be derived:

$$\mathbf{G}_k = \mathbf{P}_k^-\mathbf{H}_k^T[\mathbf{H}_k\mathbf{P}_k^-\mathbf{H}_k^T + \mathbf{R}_k]^{-1} \quad (4.28)$$

where $[\cdot]^{-1}$ denotes the inverse of the matrix inside the square brackets. Equation (4.28) is the desired formula for calculating the *Kalman gain* \mathbf{G}_k , which is defined in terms of the a priori covariance matrix \mathbf{P}_k^- .

In order to accomplish the recursive estimation procedure, we consider the *error covariance propagation*, which characterizes the effect of time on the covariance matrices of estimation error. This propagation includes two steps of evolution:

1. The a priori covariance matrix \mathbf{P}_k^- at time k is defined by (4.26). Given \mathbf{P}_k^- , compute the posteriori covariance matrix \mathbf{P}_k , which at time k is defined by:

$$\mathbf{P}_k = E[\tilde{\mathbf{x}}_k \tilde{\mathbf{x}}_k^T] = \mathbf{E}[(\mathbf{x}_k - \hat{\mathbf{x}}_k)(\mathbf{x}_k - \hat{\mathbf{x}}_k)^T] \quad (4.29)$$

2. Given the *old* a posteriori covariance matrix \mathbf{P}_{k-1} , compute the *updated* a priori covariance matrix \mathbf{P}_k^- .

To carry out step 1, we plug (4.23) into (4.29); it is noteworthy that the noise process \mathbf{v}_k is independent of the a priori estimation error $\tilde{\mathbf{x}}_k^-$. So, we would attain:

$$\begin{aligned} \mathbf{P}_k &= (\mathbf{I} - \mathbf{G}_k \mathbf{H}_k) E[\tilde{\mathbf{x}}_k^- \tilde{\mathbf{x}}_k^{-T}] (\mathbf{I} - \mathbf{G}_k \mathbf{H}_k)^T + \mathbf{G}_k E[\mathbf{v}_k \mathbf{v}_k^T] \mathbf{G}_k^T \\ &= (\mathbf{I} - \mathbf{G}_k \mathbf{H}_k) \mathbf{P}_k^- (\mathbf{I} - \mathbf{G}_k \mathbf{H}_k)^T + \mathbf{G}_k \mathbf{R}_k \mathbf{G}_k^T \end{aligned} \quad (4.30)$$

By using (4.27), we would be able to rewrite (4.30) as:

$$\begin{aligned} \mathbf{P}_k &= (\mathbf{I} - \mathbf{G}_k \mathbf{H}_k) \mathbf{P}_k^- - (\mathbf{I} - \mathbf{G}_k \mathbf{H}_k) \mathbf{P}_k^- \mathbf{H}_k^T \mathbf{G}_k^T + \mathbf{G}_k \mathbf{R}_k \mathbf{G}_k^T \\ &= (\mathbf{I} - \mathbf{G}_k \mathbf{H}_k) \mathbf{P}_k^- - \mathbf{G}_k \mathbf{R}_k \mathbf{G}_k^T + \mathbf{G}_k \mathbf{R}_k \mathbf{G}_k^T \\ &= (\mathbf{I} - \mathbf{G}_k \mathbf{H}_k) \mathbf{P}_k^- \end{aligned} \quad (4.31)$$

For the second step of error covariance propagation, we know that the a priori estimate of the state is defined in terms of the *old* a posteriori estimate as:

$$\hat{\mathbf{x}}_k^- = \mathbf{F}_{k,k-1} \hat{\mathbf{x}}_{k-1} \quad (4.32)$$

Hence, by using (3.31) and (4.32), the a priori estimation error can be written in the form of:

$$\begin{aligned}
\tilde{\mathbf{x}}_k^- &= \mathbf{x}_k - \hat{\mathbf{x}}_k^- \\
&= (\mathbf{F}_{k,k-1}\hat{\mathbf{x}}_{k-1}) - (\mathbf{F}_{k,k-1}\hat{\mathbf{x}}_{k-1}) \\
&= \mathbf{F}_{k,k-1}(\mathbf{x}_{k-1} - \hat{\mathbf{x}}_{k-1}) + \mathbf{w}_{k-1} \\
&= \mathbf{F}_{k,k-1}\tilde{\mathbf{x}}_{k-1} + \mathbf{w}_{k-1}
\end{aligned} \tag{4.33}$$

Now, by plugging (4.33) into (4.26) and noting that the process noise \mathbf{w}_k is independent of $\tilde{\mathbf{x}}_{k-1}$, we attain the following conclusion:

$$\begin{aligned}
\mathbf{P}_k^- &= \mathbf{F}_{k,k-1}\mathbf{E}[\tilde{\mathbf{x}}_{k-1}\tilde{\mathbf{x}}_{k-1}^T]\mathbf{F}_{k,k-1}^T + E[\mathbf{w}_{k-1}\mathbf{w}_{k-1}^T] \\
&= \mathbf{F}_{k,k-1}\mathbf{P}_{k-1}\mathbf{F}_{k,k-1}^T + \mathbf{Q}_{k-1}
\end{aligned} \tag{4.34}$$

This formula describes the dependence of the a priori covariance matrix \mathbf{P}_k^- on the *old a posteriori* covariance matrix \mathbf{P}_{k-1} .

Now, with equations (4.32), (4.34), (4.28), (4.17), (4.31) at hand, the Kalman algorithm for recursive state estimation can be summarized as follows:

- **State space model:**

$$\begin{cases} x_{k+1} = F_{k+1,k}x_k + w_k \\ y_k = H_kx_k + v_k \end{cases} \tag{4.35}$$

where \mathbf{w}_k and \mathbf{v}_k are independent, zero-mean, Gaussian noise processes of covariance matrices \mathbf{Q}_k and \mathbf{R}_k , respectively.

- **Initialization:** For $k = 0$, set

$$\begin{cases} \hat{\mathbf{x}}_0 = E[\mathbf{x}_0] \\ \mathbf{P}_0 = E[(\mathbf{x}_0 - E[\mathbf{x}_0])(\mathbf{x}_0 - E[\mathbf{x}_0])^T] \end{cases} \tag{4.36}$$

- **Computation:** For $k = 1, 2, \dots$ compute

– *State estimate propagation:*

$$\hat{\mathbf{x}}_k^- = \mathbf{F}_{k,k-1} \hat{\mathbf{x}}_{k-1}^- \quad (4.37)$$

– *Error covariance propagation:*

$$\mathbf{P}_k^- = \mathbf{F}_{k,k-1} \mathbf{P}_{k-1} \mathbf{F}_{k,k-1}^T + \mathbf{Q}_{k-1} \quad (4.38)$$

– *Kalman gain matrix:*

$$\mathbf{G}_k = \mathbf{P}_k^- \mathbf{H}_k^T [\mathbf{H}_k \mathbf{P}_k^- \mathbf{H}_k^T + \mathbf{R}_k]^{-1} \quad (4.39)$$

– *State estimate update:*

$$\hat{\mathbf{x}}_k = \hat{\mathbf{x}}_k^- + \mathbf{G}_k (\mathbf{y}_k - \mathbf{H}_k \hat{\mathbf{x}}_k^-) \quad (4.40)$$

– *Error covariance update:*

$$\mathbf{P}_k = (\mathbf{I} - \mathbf{G}_k \mathbf{H}_k) \mathbf{P}_k^- \quad (4.41)$$

This summarization, also includes the initialization process. We may select the initial state estimate at time $k = 0$ when no observed data is available as:

$$\hat{\mathbf{x}}_0 = E[\mathbf{x}_0] \quad (4.42)$$

and the initial value of the a posteriori covariance matrix as:

$$\mathbf{P}_0 = E[(\mathbf{x}_0 - E[\mathbf{x}_0])(\mathbf{x}_0 - E[\mathbf{x}_0])^T] \quad (4.43)$$

This choice of initial conditions has the benefit of yielding an unbiased estimate of the state \mathbf{x}_k .

This summarization, also includes the initialization process. We may select the initial state estimate at time $k = 0$ when no observed data is available as:

$$\hat{\mathbf{x}}_0 = E[\mathbf{x}_0] \quad (4.44)$$

and the initial value of the a posteriori covariance matrix as:

$$\mathbf{P}_0 = E[(\mathbf{x}_0 - E[\mathbf{x}_0])(\mathbf{x}_0 - E[\mathbf{x}_0])^T] \quad (4.45)$$

This choice of initial conditions has the benefit of yielding an unbiased estimate of the state \mathbf{x}_k .

4.3.4 Derivation of the Extended Kalman Filter

Up to this point, the proposed Kalman filter is capable of estimating the state vector in a *linear* model of a dynamical system. However, in practice, we usually have to deal with *nonlinear* models. Hence, we extend the usage of Kalman filtering to nonlinear systems by a linearization procedure. The resulting filter is accredited as the *Extended Kalman Filter (EKF)*. This extension is feasible because of the fact that the Kalman filter is described in terms of difference equations in the case of discrete-time systems.

In order to describe the extended Kalman filter, consider a nonlinear dynamical system described by the following state space model:

$$\mathbf{x}_{k+1} = \mathbf{f}(\mathbf{k}, \mathbf{x}_k) + \mathbf{w}_k \quad (4.46)$$

$$\mathbf{y} = \mathbf{h}(\mathbf{k}, \mathbf{x}_k) + \mathbf{v}_k \quad (4.47)$$

where, as before \mathbf{w}_k and \mathbf{v}_k are independent zero mean white Gaussian noise processes with covariance matrices \mathbf{R}_k and \mathbf{Q}_k , respectively; $\mathbf{f}(\mathbf{k}, \mathbf{x}_k)$ denotes a nonlinear transition matrix which can be time-variant and $\mathbf{h}(\mathbf{k}, \mathbf{x}_k)$ denotes a nonlinear measurement matrix that can be time-variant.

The fundamental idea of the extended Kalman filter is to *linearize* the state space model of (4.46) and (4.47) at each time instant around the most recent state estimate, which would be either $\hat{\mathbf{x}}_k$ or $\hat{\mathbf{x}}_k^-$, depending upon which particular function is being considered. Once a linear estimate of the model is attained, the standard Kalman filter equations can be applied. In other words, the following two steps need to be taken:

Step 1 : The following two matrices are constructed:

$$F_{k+1,k} = \left. \frac{\partial \mathbf{f}_{k,\mathbf{x}}}{\partial \mathbf{X}} \right|_{\mathbf{x}=\hat{\mathbf{x}}_k} \quad (4.48)$$

$$\mathbf{H}_k = \left. \frac{\partial \mathbf{h}_{k,\mathbf{x}_k}}{\partial \mathbf{X}} \right|_{\mathbf{x}=\hat{\mathbf{x}}_k^-} \quad (4.49)$$

where the *Jacobian* $\frac{\partial \mathbf{g}}{\partial \mathbf{x}}$ for a vector of functions

$$\mathbf{g}(\mathbf{x}) = \begin{bmatrix} \mathbf{g}_1(x_1, x_2, \dots, x_n) \\ \mathbf{g}_2(x_1, x_2, \dots, x_n) \\ \vdots \\ \mathbf{g}_m(x_1, x_2, \dots, x_n) \end{bmatrix} \quad (4.50)$$

in variables x_1, x_2, \dots, x_n is:

$$\frac{\partial \mathbf{g}}{\partial \mathbf{x}} = \begin{bmatrix} \frac{\partial g_1}{\partial x_1} & \frac{\partial g_1}{\partial x_2} & \cdots & \frac{\partial g_1}{\partial x_n} \\ \frac{\partial g_2}{\partial x_1} & \frac{\partial g_2}{\partial x_2} & \cdots & \frac{\partial g_2}{\partial x_n} \\ \vdots & \vdots & \cdots & \vdots \\ \frac{\partial g_m}{\partial x_1} & \frac{\partial g_m}{\partial x_2} & \cdots & \frac{\partial g_m}{\partial x_n} \end{bmatrix} \quad (4.51)$$

The entries of $F_{k+1,k}$ and \mathbf{H}_k are all computable, by having $\hat{\mathbf{x}}_k$ and $\hat{\mathbf{x}}_k^-$ available at time k .

Step 2 : With $F_{k+1,k}$ and \mathbf{H}_k at hand, calculating a *first-order Taylor approximation* of the nonlinear functions $\mathbf{F}(k, \mathbf{x}_k)$ and $\mathbf{H}(k, \mathbf{x}_k)$ around $\hat{\mathbf{x}}_k$ and $\mathbf{F}(k, \hat{\mathbf{x}}_k^-)$ would

be feasible. Therefore, $\mathbf{F}(k, \mathbf{x}_k)$ and $\mathbf{H}(k, \mathbf{x}_k)$ are approximated as follows:

$$\mathbf{F}(k, \mathbf{x}_k) \simeq \mathbf{F}(\mathbf{x}, \hat{\mathbf{x}}_k) + \mathbf{F}_{k+1,k}(\mathbf{x}, \hat{\mathbf{x}}_k) \quad (4.52)$$

$$\mathbf{H}(k, \mathbf{x}_k) \simeq \mathbf{H}(\mathbf{x}, \hat{\mathbf{x}}_k^-) + \mathbf{H}_{k+1,k}(\mathbf{x}, \hat{\mathbf{x}}_k^-) \quad (4.53)$$

Hence, the nonlinear state equation (4.46) and (4.47) can be approximated as:

$$\mathbf{x}_{k+1} \simeq \mathbf{F}_{k+1,k}\mathbf{x}_k + \mathbf{w}_k + \mathbf{d}_k \quad (4.54)$$

$$\bar{\mathbf{y}}_k \simeq \mathbf{H}_k\mathbf{x}_k + \mathbf{v}_k \quad (4.55)$$

where \mathbf{d}_k and $\bar{\mathbf{y}}_k$ are defined as:

$$\mathbf{d}_k = \mathbf{f}(\mathbf{x}, \hat{\mathbf{x}}_k) - \mathbf{F}_{k+1,k}\hat{\mathbf{x}}_k \quad (4.56)$$

$$\bar{\mathbf{y}}_k = y_k - (h(x, x_k^-) - H_k\hat{x}_k^-) \quad (4.57)$$

The entries of \mathbf{d}_k are all known at time k ; similarly, the entries of $\bar{\mathbf{y}}_k$ are all known at time k ; $\bar{\mathbf{y}}_k$ can be regarded as an observation vector at time k .

As a result, given the state space model of (4.56) and (4.57), we may apply the Kalman filter theory of Section 4.3.3 to derive the extended Kalman filter.

Following is a summary of the extended Kalman filter algorithm:

- State space model:

$$\begin{cases} \mathbf{x}_{k+1} = \mathbf{f}(k, \mathbf{x}_k) + \mathbf{w}_k \\ \mathbf{y} = \mathbf{h}(k, \mathbf{x}_k) + \mathbf{v}_k \end{cases} \quad (4.58)$$

where \mathbf{w}_k and \mathbf{v}_k are independent, zero-mean, Gaussian noise processes of covariance matrices \mathbf{Q}_k and \mathbf{R}_k , respectively.

- Definitions:

$$\begin{cases} \mathbf{F}_{k+1,k} = \left. \frac{\partial \mathbf{f}(k, \mathbf{x})}{\partial \mathbf{x}} \right|_{\mathbf{x}=\hat{\mathbf{x}}_k} \\ \mathbf{H}_k = \left. \frac{\partial \mathbf{h}(k, \mathbf{x})}{\partial \mathbf{x}} \right|_{\mathbf{x}=\hat{\mathbf{x}}_k^-} \end{cases} \quad (4.59)$$

- **Initialization:** For $k = 0$, set

$$\begin{cases} \hat{\mathbf{x}}_0 = E[\mathbf{x}_0] \\ \mathbf{P}_0 = E[(\mathbf{x}_0 - E[\mathbf{x}_0])(\mathbf{x}_0 - E[\mathbf{x}_0])^T] \end{cases} \quad (4.60)$$

- **Computation:** For $k = 1, 2, \dots$ compute

- *State estimate propagation:*

$$\hat{\mathbf{x}}_k^- = \mathbf{f}(k, \hat{\mathbf{x}}_{k-1}) \quad (4.61)$$

- *Error covariance propagation:*

$$\mathbf{P}_k^- = \mathbf{F}_{k,k-1} \mathbf{P}_{k-1} \mathbf{F}_{k,k-1}^T + \mathbf{Q}_{k-1} \quad (4.62)$$

- *Kalman gain matrix:*

$$\mathbf{G}_k = \mathbf{P}_k^- \mathbf{H}_k^T [\mathbf{H}_k \mathbf{P}_k^- \mathbf{H}_k^T + \mathbf{R}_k]^{-1} \quad (4.63)$$

- *State estimate update:*

$$\hat{\mathbf{x}}_k = \hat{\mathbf{x}}_k^- + \mathbf{G}_k (\mathbf{y}_k - \mathbf{h}(k, \hat{\mathbf{x}}_k^-)) \quad (4.64)$$

- *Error covariance update:*

$$\mathbf{P}_k = (\mathbf{I} - \mathbf{G}_k \mathbf{H}_k) \mathbf{P}_k^- \quad (4.65)$$

Based on the same logic the continuous extended Kalman filter equations can be written as follows¹:

- **Nonlinear dynamic model:**

$$\begin{cases} \dot{\mathbf{x}} = \mathbf{f}(\mathbf{t}, \mathbf{x}(\mathbf{t})) + \mathbf{w}(\mathbf{t}) \\ \mathbf{y} = \mathbf{h}(\mathbf{t}, \mathbf{x}(\mathbf{t})) + \mathbf{v}(\mathbf{t}) \end{cases} \quad (4.66)$$

where $\mathbf{w}(\mathbf{t})$ and $\mathbf{v}(\mathbf{t})$ are independent, zero-mean, Gaussian noise processes of covariance matrices $\mathbf{Q}(\mathbf{t})$ and $\mathbf{R}(\mathbf{t})$, respectively.

¹Please note that for implementation purposes the discrete equations have been used.

- Definitions:

$$\begin{cases} \mathbf{F}^{[1]}(\mathbf{t}) = \left. \frac{\partial \mathbf{f}(t, \mathbf{x})}{\partial \mathbf{x}} \right|_{\mathbf{x}=\hat{\mathbf{x}}(t)} \\ \mathbf{H}^{[1]}(\mathbf{t}) = \left. \frac{\partial \mathbf{h}(t, \mathbf{x})}{\partial \mathbf{x}} \right|_{\mathbf{x}=\hat{\mathbf{x}}(t)} \end{cases} \quad (4.67)$$

- Computation: compute

- *Error covariance:*

$$\dot{\mathbf{P}}(\mathbf{t}) = \mathbf{F}^{[1]}(\mathbf{t})\mathbf{P}(\mathbf{t}) + \mathbf{P}(\mathbf{t})\mathbf{F}^{[1]\mathbf{T}}(\mathbf{t}) + \mathbf{Q}(\mathbf{t}) - \bar{\mathbf{K}}(\mathbf{t})\mathbf{R}(\mathbf{t})\bar{\mathbf{K}}^{\mathbf{T}}(\mathbf{t}) \quad (4.68)$$

- *Kalman gain matrix:*

$$\bar{\mathbf{K}}(\mathbf{t}) = \mathbf{P}(\mathbf{t})\mathbf{H}^{[1]\mathbf{T}}\mathbf{R}^{-1} \quad (4.69)$$

- *State estimate:*

$$\dot{\hat{\mathbf{x}}}(\mathbf{t}) = \mathbf{f}(\mathbf{t}, \hat{\mathbf{x}}(\mathbf{t})) + \bar{\mathbf{K}}(\mathbf{t})[\mathbf{y}(\mathbf{t}) - \mathbf{h}(\mathbf{t}, \hat{\mathbf{x}}(\mathbf{t}))] \quad (4.70)$$

4.3.5 Fault Detection

If we define the residual signal $r(t)$ as $r(t) = y(t) - \hat{y}^-(t)$, assuming convergence of the EKF estimator its components will remain in a bounded band when there is no fault present in the system and the real model of the system is close to the model used in the fault detection design process. However, when the actual model is affected by faults, the Kalman filter predictions will have a larger than usual discrepancy from system states. Hence, these proposed nonzero error signals can be interpreted as appropriate fault signatures. Nonetheless, it is required to perform some distillation on these raw residual signals before they can be used for fault detection. For instance, they are very likely to include high frequency oscillations which make fault detection very difficult. In order to tackle this problem, a moving average technique has been used which filters these high frequency oscillations and facilitates the detection of faults. The schematic of this approach is depicted in Figure 4.3.

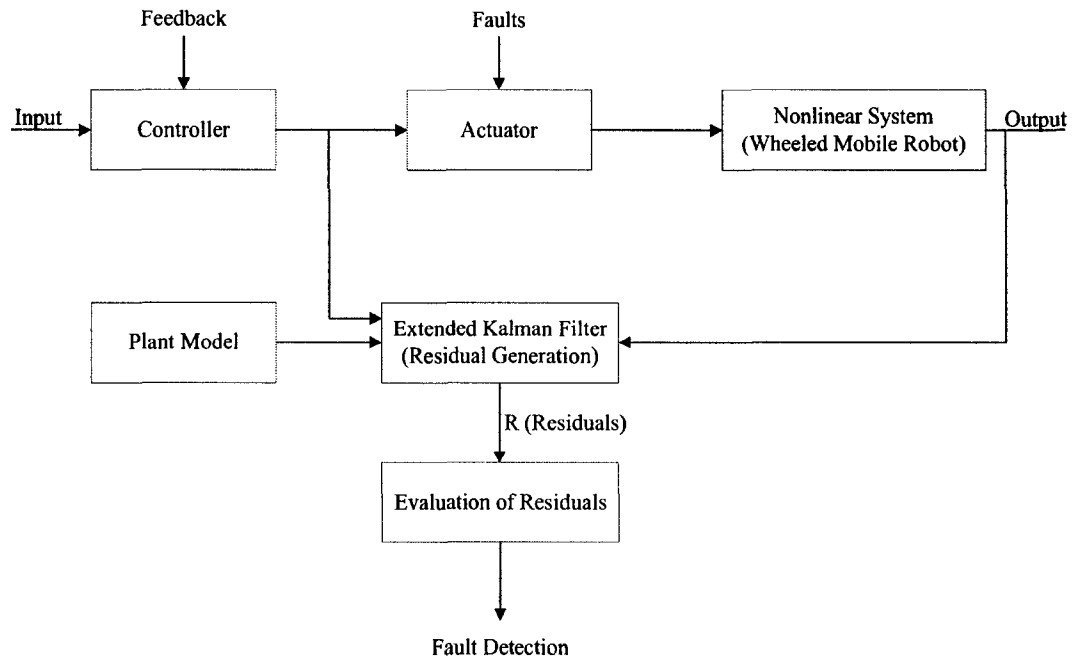


Figure 4.3: Schematic of the Proposed Fault Detection Approach Based on Extended Kalman Filter (EKF)

After generating the distilled residual signal, the performance of the model is simulated for a large number of fault-free circumstances to determine the threshold for each residual signal. Therefore, lower and upper bounds will be obtained which determine the minimum and maximum values that each residual signal can reach under fault-free operating conditions. When the residual signal values are within this region no fault is detected; but whenever a distilled residual signal exceeds its thresholds, the Fault Detection module will recognize the existence of a fault.

4.4 Neural Network Model Based Fault Detection

Approach

In this section, an alternative neural network model based approach for fault diagnosis is proposed. Subsequently in the next chapter the performance of this approach is compared with the performance of the formerly introduced EKF approach.

This approach is applicable to a general class of nonlinear systems. Therefore, the theory would be explained for a general class of nonlinear systems and essentially the mobile robot system which we are concerned about would be covered.

Consider the general multivariable nonlinear dynamic system characterized by the following equation [Zhang 02]:

$$\dot{x} = f(x, u) + \mathcal{B}(t - T_0)\phi(x, u) \quad (4.71)$$

where $x \in \mathbb{R}^n$ is the state vector of the system, $u \in \mathbb{R}^m$ is the input vector, $f, \phi : \mathbb{R}^n \times \mathbb{R}^m \mapsto \mathbb{R}^n$ are a smooth vector fields, and $\mathcal{B}(t - T_0)$ is a matrix function representing the time profile of the faults. The vector fields f and ϕ represent the dynamics of the nominal model and the change in the system dynamics due to a fault. It is noteworthy to mention that it has been assumed here that the system states and controls remain bounded before and after the occurrence of the fault; in other words, there exist some stability region $\mathcal{S} \subset \mathbb{R}^n \times \mathbb{R}^m$, such that $(x(t), u(t)) \in \mathcal{S}, \forall t \geq 0$.

As a matter of fact, the reason for introducing such a uniform boundedness assumption is just a formal one. Here, we deal with the design of a fault detection scheme based on the measurement of $x(t)$ and $u(t)$. In fact, since no fault accommodation is considered here, the feedback controller must be such that the measurement signals $x(t)$ and $u(t)$ remain bounded for all $t \geq 0$ before and after the occurrence of a fault. Indeed, both of the controllers designed in Chapter 3 satisfy this condition.

Nevertheless, it is crucial to emphasize that both of the discussed fault diagnosis schemes in this chapter are not dependent on the structure of the controller. In fact, it will become more clear later on, that this approach, as well as the EKF approach, will make use of $x(t)$ and $u(t)$ to yield the detection decision, but it will not affect the behavior of the system at all. In other words, these two schemes are both categorized under passive fault detection schemes as described in Section 2.6.

Regarding the faults affecting the system, from a qualitative perspective, the term $\mathcal{B}(t - T_0)\phi(x, u)$ represents the deviation in the system dynamics due to the fault. The matrix $\mathcal{B}(t - T_0)$ describes the time profile of a fault that happens at some unknown time T_0 ; and $\phi(x, u)$ denotes the fault function. This description endorses both additive and multiplicative faults and even more general nonlinear faults.

A neural network state estimator has been used to detect faults. Under normal and healthy (fault-free) operating conditions this estimator monitors the system while under faulty conditions it detects the occurrence of the fault.

Based on the system characterization in (4.71), the fault detection estimator would be as follows:

$$\dot{\hat{x}}^0 = f(x, u) + \hat{\psi}(x, u, \hat{W}^0) \quad (4.72)$$

where \hat{x}^0 is the estimated state vector, $\hat{\psi} : \mathbb{R}^n \times \mathbb{R}^m \times \mathbb{R}^p \mapsto \mathbb{R}^n$ is an online neural network approximation model and \hat{W}^0 represents a vector of adjustable weights of the online neural network approximator.

Artificial neural networks have been broadly used for system identification due to their ability to learn complex mappings from a set of examples. The adaptive feature, the mapping property and the capability of neural networks to cope with uncertainties, make them an appropriate choice for identification and state estimation of nonlinear systems. For the same reasons, they are a suitable option for state estimation in the process of residual generation in fault detection applications.

A number of different types of artificial neural networks have been used for identification of nonlinear systems. Notwithstanding, in most cases no mathematical proof of stability is provided. For instance backpropagation is broadly used in identification and control problems (e.g. see [Narendra 90; Talebi 00]) and is capable of providing propitious results. Nevertheless, the major disadvantage of the previous works on backpropagation is the lack of mathematical proof of stability. The exploited approach here is suitable for identification of general multi-input multi-output nonlinear systems. The weight update mechanism is based on a modified propagation algorithm [Abdollahi 06]. Antithetic to many other methods, the employed approach here neither assumes knowledge of nonlinearities of the system nor that the nonlinear system is linear in its parameters.

4.4.1 The Neural Network Based Identifier

In general, consider the following nonlinear system:

$$\dot{x} = \mathcal{F}(x, u) \quad (4.73)$$

where $u \in \mathbb{R}^m$ is the input vector and $x \in \mathbb{R}^n$ is the state vector of the system and $\mathcal{F}(\cdot)$ is an unknown nonlinear function. It is assumed that the open loop system (4.73) is stable which is the usual assumption in identification procedures. By adding and subtracting Ax to the right hand side of (4.73), where A is an arbitrary Hurwitz matrix, we would have:

$$\dot{x} = Ax + \mathcal{G}(x, u) \quad (4.74)$$

where $\mathcal{G}(x, u) = \mathcal{F}(x, u) - Ax$. Based on (4.74), a recurrent network model denoted by N can be built by parameterizing the mapping \mathcal{G} by static feedforward neural network architectures. Consequently, the following model would be considered for

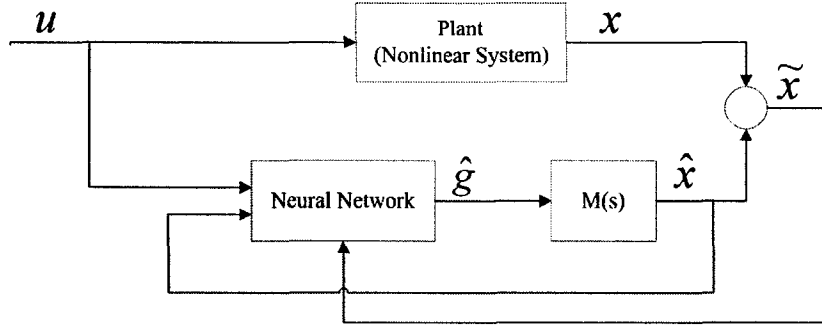


Figure 4.4: Schematic of the Neural Network Identifier

identification:

$$\dot{\hat{x}} = A\hat{x} + \hat{\mathcal{G}}(\hat{x}, u) \quad (4.75)$$

where \hat{x} denotes the estimated states.

The schematic of this identifier is illustrated in Figure 4.4. With respect to the Hurwitz matrix A , the matrix $M(s) = (sI - A)^{-1}$ is defined as an $n \times n$ matrix whose elements are stable transfer functions. It has been shown [Abdollahi 06] that for any x restricted to the compact set S of $x \in \mathbb{R}^n$ and for some sufficiently large number of hidden layer neurons, there exist weights and thresholds such that any continuous function in the compact set S can be represented as:

$$\mathcal{G}(x, u) = W\sigma(V\bar{x}) + \varepsilon(x) \quad (4.76)$$

where W and V are ideal unknown weight matrices, $\bar{x} = [x \ u]^T$, $\varepsilon(x) \leq \varepsilon_N$ is the bounded approximation error of the neural network and $\sigma(\cdot)$ is the transfer function of the hidden neurons that is commonly considered as a sigmoidal function:

$$\sigma_i(V_i\bar{x}) = \frac{2}{1 + e^{-2V_i\bar{x}}} - 1 \quad (4.77)$$

where V_i is the i th row of V and $\sigma_i(V_i\bar{x})$ is the i th element of $\sigma(V\bar{x})$. Therefore, the function \mathcal{G} can be expressed as follows:

$$\hat{\mathcal{G}}(\hat{x}, u) = \hat{W}\sigma(\hat{V}\hat{x}) \quad (4.78)$$

The identifier can then be articulated as follows:

$$\dot{\hat{x}} = A\hat{x} + \hat{W}\sigma(\hat{V}\hat{x}) \quad (4.79)$$

By defining the identifier error as $\tilde{x} = x - \hat{x}$ and using (4.74),(4.78) and (4.79) the error dynamics can be stated as:

$$\dot{\tilde{x}} = A\tilde{x} + \tilde{W}\sigma(\hat{V}\hat{x}) + w(t) \quad (4.80)$$

where $\tilde{W} = W - \hat{W}$ and $w(t) = W[\sigma(V\bar{x}) - \sigma(\hat{V}\hat{x})] + \varepsilon(x)$ is a bounded disturbance term. In other words, $\|w(t)\| \leq \bar{w}$ for some positive constant \bar{w} , because of the sigmoidal function. According to the proof in [Abdollahi 06], considering the plant model (4.71) and identifier model (4.79), if the weights of the artificial neural network are updated according to the following equations:

$$\dot{\hat{W}} = -\eta_1 \left(\frac{\partial J}{\partial \hat{W}} \right) - \rho_1 \|\tilde{x}\| \hat{W} \quad (4.81)$$

$$\dot{\hat{V}} = -\eta_2 \left(\frac{\partial J}{\partial \hat{V}} \right) - \rho_2 \|\tilde{x}\| \hat{V} \quad (4.82)$$

then $\tilde{x}, \tilde{W}, \tilde{V} \in L_\infty$, i.e., the estimation error and weights errors are bounded. Here, $\eta_1, \eta_2 > 0$ are learning rates; ρ_1 and ρ_2 are small positive numbers and $J = \frac{1}{2}(\tilde{x}^T \tilde{x})$ is the neural network objective function. It is noteworthy that the first terms in (4.81) and (4.82) are the common backpropagation algorithm terms while the last ones are modification terms which add extra damping for robustness.

The exact calculation of the partial derivatives in (4.81) and (4.82) will lead to the following weight matrix update formulae:

$$\dot{\hat{W}} = -\eta_1 (\tilde{x}^T A^{-1})^T (\sigma(\hat{V}\hat{x}))^T - \rho_1 \|\tilde{x}\| \hat{W} \quad (4.83)$$

$$\dot{\hat{V}} = -\eta_2 (\tilde{x}^T A^{-1} \hat{W} (I - \Lambda(\hat{V}\hat{x})))^T (\hat{x})^T - \rho_2 \|\tilde{x}\| \hat{V} \quad (4.84)$$

where $\Lambda(\hat{V}\hat{x}) = \text{diag}\{\sigma_i^2(\hat{V}_i\hat{x})\}$, $i = 1, 2, \dots, m$.

Now, by applying this identifier to the system defined in (4.71) one can easily calculate \hat{y}^0 which is the estimation of the states.

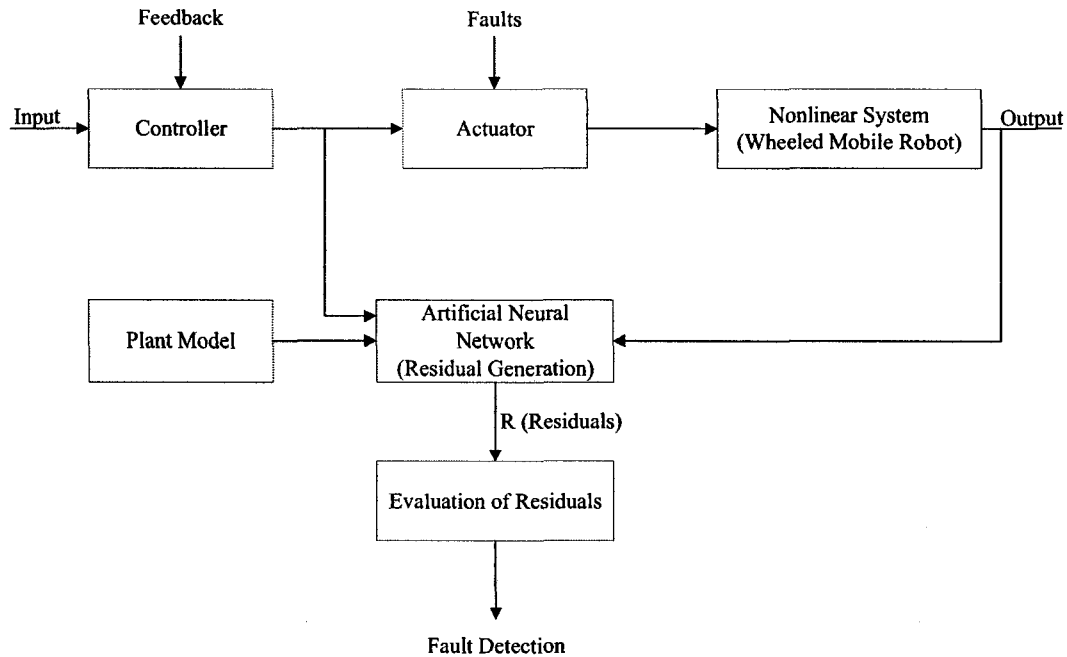


Figure 4.5: Schematic of the Proposed Fault Detection Approach Based on Neural Networks

4.4.2 Fault Detection

Following a similar path as in Section 4.3.5, if we define the residual signal $r(t) = y(t) - \hat{y}^0(t)$, due to convergence of the neural network estimator its components will remain in a bounded band when there is no fault present in the system and the real model of the system is close to the model used in the fault detection design process. However, when the actual model is affected by faults, the neural network estimations will have a larger than usual discrepancy from system states. Hence, these proposed nonzero error signals can be interpreted as appropriate fault signatures. Nonetheless, it is required to perform some distillation on these raw residual signals before they can be used for fault detection. For instance, they are very likely to include high frequency oscillations which make fault detection very difficult. In order to tackle this problem, a moving average technique has been used which filters the high frequency oscillations

and facilitates the detection of faults. The schematic of this approach is depicted in Figure 4.5.

Again as described in Section 4.3.5, after generating the distilled residual signal, the performance of the model is simulated for a large number of fault-free circumstances to determine the threshold for each residual signal. So, we would also be able to differentiate between normal learning error in the training and faults. Therefore, lower and upper bounds are constructed which determine the minimum and maximum values that each residual signal can reach under fault-free operating conditions. When the residual signal values are within this region no fault is detected; but whenever a distilled residual signal exceeds its thresholds, the Fault Detection module will recognize the existence of a fault.

4.5 Summary and Conclusions

In this chapter, two model consistency based approaches have been proposed to tackle the problem of fault detection in wheeled mobile robots as a subclass of nonlinear systems. The first approach is based on identification of the system via Extended Kalman Filtering (EKF). In this approach, a novel residual generation method has been introduced which is based on defining the residual as the difference between the measured state values and the *a priori estimate*² of the state \hat{x}_k^- instead of the usual estimate of the state. In general, this approach is suitable for all nonlinear systems for which the Jacobian is defined. Nonetheless, this approach requires the computation of the Jacobian and an inverse matrix at each iteration which might cause some numerical instabilities³ In the second approach, an artificial neural network has been

²This concept has been introduced in Section 4.3.3.

³A large number of these kind of problems alongside with their solutions have been addressed in [Grewal 01].

used as the state estimator. A modified stable back propagation algorithm has been used in this part. The benefit of this algorithm is that it neither assumes knowledge of nonlinearities of the system nor that the nonlinear system is linear in its parameters. This approach is applicable to the general class of nonlinear systems as well.

Chapter 5

Comparative Study and Simulation Results

5.1 Introduction

In this chapter the performance of the proposed EKF fault diagnosis approach is evaluated in different scenarios and under different types of faults. In each case, the results are compared with the results of the alternative neural network model based approach which is discussed in Section 4.4. The advantages and disadvantages of each approach will be discussed in each case.

In all the simulation results shown in this chapter, a random signal of the magnitude less than 10^{-3} *N.m.* is considered as the representative of external disturbance. Moreover, the measurement noise is considered to be random signal in the range of $\pm 10^{-2}$ *m* for *x*, *y* and $\pm 10^{-2}$ *rad* for θ .

5.2 Controller Performance Under Faulty Conditions

As the first step towards fault diagnosis design we should analyze the impact of different categories of faults on the controlled WMR. Two different types of faults are considered here. Firstly, the effects of a locked in place fault¹ in the actuator² of the driving subsystem of a WMR in the presence of dynamic linear control and feedback linearization control are investigated. The same procedure is then followed for a loss of effectiveness fault³ in the actuator of the driving subsystem.

In the considered scenario here the objective of the wheeled mobile robot is to track a trajectory which is described by Equation (5.1), namely

$$x_d(t) = A_1 \sin(f_1 t) \quad y_d(t) = A_2 \sin(f_2 t) \quad t \in [0, T] \quad (5.1)$$

Numerical simulation results are provided for the eight-shaped reference trajectory where $A_1 = 3$, $A_2 = 4$, $f_1 = 1$ and $f_2 = 0.5$.

5.2.1 Locked In Place Fault

Under this scenario the actuator signal of the driving subsystem would remain at a fixed value from a certain point of time (here $t_f = 15s$) onward. In other words, the actuator response which sets the speed (v) of the WMR would not change after the occurrence of such a fault. We would like to see how this fault might affect the trajectory tracking of the WMR.

¹This is a common type of fault which is usually considered for case studies. For more details see p. 25 of [Simani 03]

²The reason for considering *actuator faults* is addressed in Section 1.1 and Table 1.1

³This is another common type of fault which is usually considered for case studies. For more details see p. 25 of [Simani 03]

In order to see how different controllers react to this type of fault, simulation results are given for a wheeled mobile robot under both dynamic linear control and feedback linearization based control.

Dynamic Linear Controller Performance

In this case the wheeled mobile robot is controlled by the dynamic controller described in Section 3.4.2 and is tracking its desired trajectory when a fault occurs at $t_f = 15s$.

As described before, here the fault has occurred only in the driving subsystem. As a result, only v in the governing equations (3.4) has been affected directly. But, due to the existence of feedback signals in the control loops, the effect of this driving signal fault can be slightly observed in the steering signal as well. This phenomenon is observable in Fig. 5.1(a) and Fig. 5.1(b).

In Fig. 5.1(c) it can be seen that this fault causes wheeled mobile robot to leave its desired track completely. As a result, the norm of its tracking error starts to increase without a bound (Fig. 5.1(d)).

Feedback Linearization Based Controller Performance

In this case the wheeled mobile robot is controlled by the dynamic feedback linearization based controller described in Section 3.4.3 and is tracking its desired trajectory when a fault occurs at $t_f = 15s$.

As can be seen in Fig. 5.2(a) and Fig. 5.2(b), similar to the previous case, the occurrence of fault in the driving subsystem affects the steering subsystem. By comparing Fig. 5.2(b) and Fig. 5.1(b), one can note that the effect of this impact is stronger in this case than the previous case.

With reference to Fig. 5.2(c) one can observe that although the occurrence of the fault causes the mobile robot to divert from its desired trajectory, the norm of

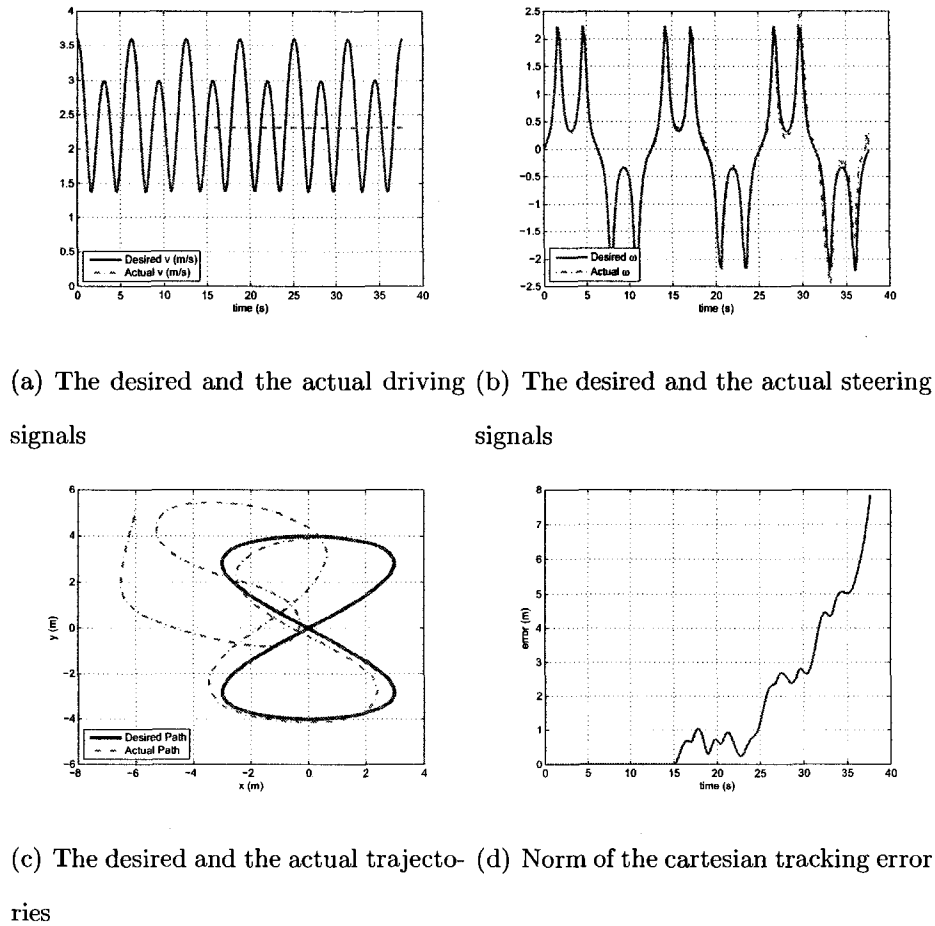
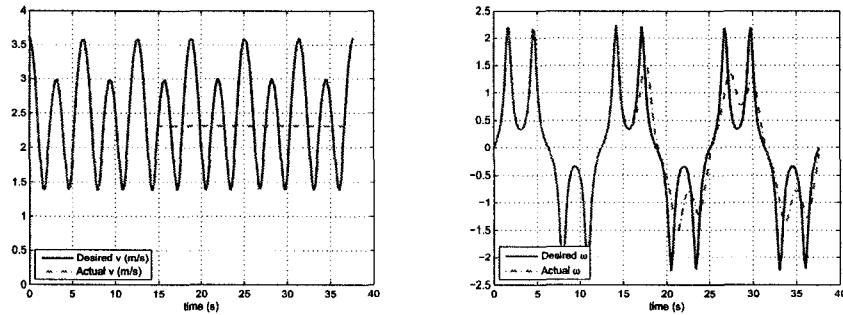


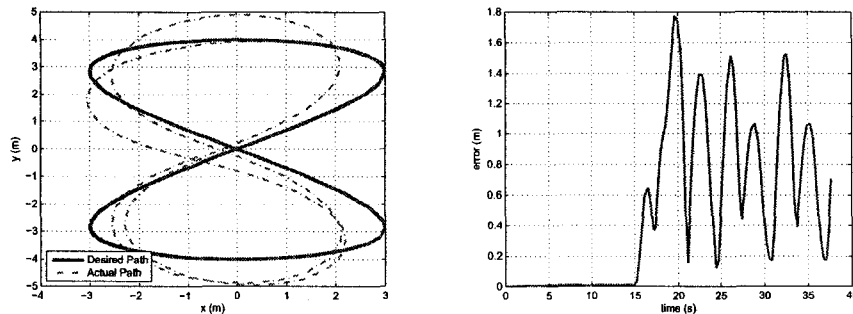
Figure 5.1: Dynamic Linear controller performance in the presence of a locked in place fault which has occurred at $t = 15s$

the trajectory tracking error is much less than the previous case (by comparing Fig. 5.1(d) with Fig. 5.2(d)).

In summary, the impact of the locked in place fault on the trajectory tracking performance of the wheeled mobile robot is more observable when the robot is controlled by the dynamic linear controller rather than the dynamic feedback linearization based controller. This fact, makes fault detection easier in the former case while harder in the latter. According to the aircraft incident that was described in Section 2.6, this robustness might be able to mask the occurrence of a fault.



(a) The desired and the actual driving signals (b) The desired and the actual steering signals



(c) The desired and the actual trajectories (d) Norm of the cartesian tracking error

Figure 5.2: Dynamic feedback linearization controller performance in the presence of a locked in place fault which has occurred at $t = 15$ s

5.2.2 Loss of Effectiveness Fault

In this scenario due to the loss of actuator effectiveness fault from a certain given time onwards the system would receive only a certain percentage of the actuator signal which it should have. Consequently, the actuator response which sets the speed (v) of the WMR would be weaker than the required amount for the desired control. Hence, we would like to see how this fault might affect the trajectory tracking of the wheeled mobile robot. In the given numerical simulation results the loss of actuator effectiveness is assumed to be 50%.

Dynamic Linear Controller Performance

In this case the wheeled mobile robot is controlled by the dynamic controller described in Section 3.4.2 and is tracking its desired trajectory when a fault occurs at $t_f = 15s$.

As shown in Fig. 5.3(a) and Fig. 5.3(b), due to the feedback mechanism and design of this type of controller, the loss is recognized and to some extent compensated by the controller itself. Although the wheeled mobile robot deviates from its desired trajectory, it follows a trajectory with a very similar shape and close distance to the desired trajectory (See Fig. 5.3(c)). As a result, the norm of the tracking error -as illustrated in Fig. 5.3(d)- will remain rather small.

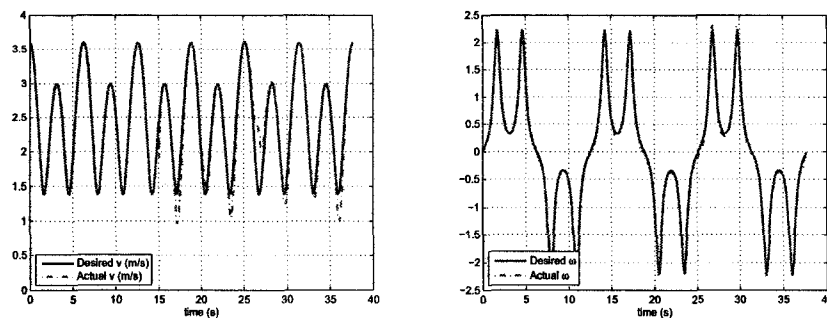
Feedback Linearization Based Controller Performance

In this case the wheeled mobile robot is controlled by the dynamic feedback linearization based controller described in Section 3.4.3 and is tracking its desired trajectory when a fault occurs at $t_f = 15s$.

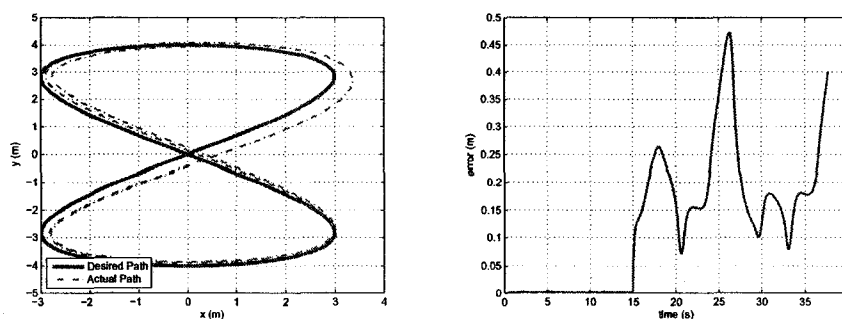
As shown in Fig. 5.4(a), the dynamic feedback linearization based controller tries to compensate the loss of control. Moreover, the impact of the fault in the driving subsystem on the steering subsystem is rather small (See Fig. 5.4(b)). Overall, as shown in Fig. 5.4(d) the deviation of the mobile robot from its desired trajectory would not be very large.

5.3 Convergence Properties of EKF

The performance of the proposed EKF based fault diagnosis technique is very much dependent on the identification performance of the Extended Kalman Filter. Hence, it is reasonable to investigate the identification performance of the Extended Kalman Filter itself before moving on to the next step which is studying the performance of the



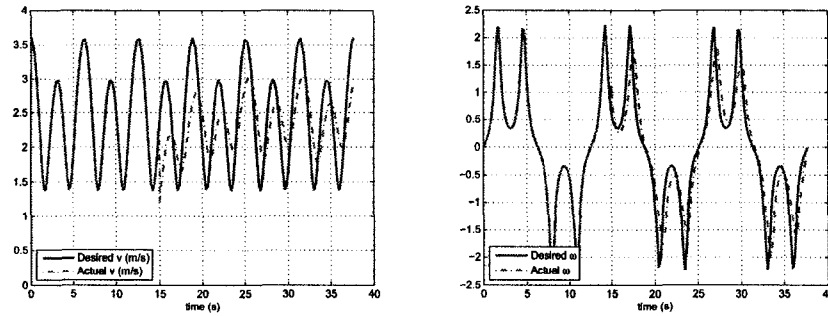
(a) The desired and the actual driving signals (b) The desired and the actual steering signals



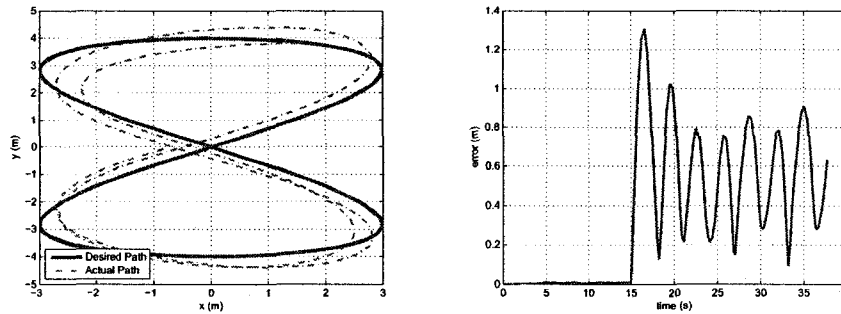
(c) The desired and the actual trajectories (d) Norm of the cartesian tracking error

Figure 5.3: Dynamic linear controller performance in the presence of a 50% loss of effectiveness fault which has occurred at $t = 15$ s

proposed EKF based fault diagnosis technique. In order to do so, estimation under healthy conditions has been numerically simulated. In other words, it is assumed that the Wheeled Mobile Robot (WMR) is tracking the eight-shaped reference trajectory depicted in Figure 3.1 under fault-free conditions and then x , y and θ are estimated by the EKF. As shown in Fig. 5.5(a), Fig. 5.5(b) and 5.5(c) the estimation error norms for x , y and θ would be 0.015, 0.01 and 0.01, respectively. For this simulation it is assumed that $\mathbf{w}_k \sim N(0, 10^{-3})$, $\mathbf{v}_k \sim N(0, 10^{-2})$ and $\mathbf{P}_0 = 10^{-3}\mathbf{I}$ (with respect to the formulation described in Section 4.3.4).



(a) The desired and the actual driving signals (b) The desired and the actual steering signals



(c) The desired and the actual trajectories (d) Norm of the cartesian tracking error

Figure 5.4: Dynamic feedback linearization controller performance in the presence of a 50% loss of effectiveness fault which has occurred at $t = 15$ s

It is noteworthy that the convergence of the EKF -from a theoretical point of view- has been investigated by many researchers (e.g. see [Krener 02; Boutayeb 97]).

5.4 Permanent-Fault Detection Through EKF Approach

In this section the performance of the proposed EKF fault detection technique in the presence of permanent faults is investigated. Permanent faults are the group of faults

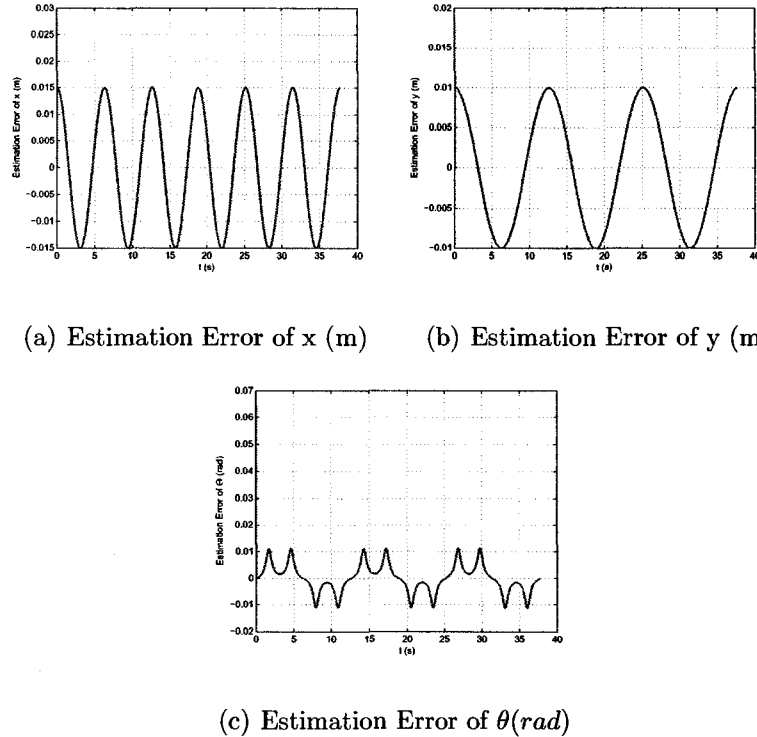


Figure 5.5: Performance of the EKF State Estimator

which do not disappear after their occurrence. As before, both locked-in-place and loss-of-effectiveness faults are considered and in each of these two cases the EKF fault detection technique is applied to two different scenarios. In one scenario, the wheeled mobile robot is controlled by the dynamic linear controller (see Section 3.4.2) while in the other scenario the wheeled mobile robot is controlled by the dynamic feedback linearization controller (see Section 3.4.3). In this section, we assume that only the driving subsystem of the wheeled mobile robot is subject to fault.

5.4.1 Locked In Place Fault in the Driving Subsystem (v)

Under this scenario, the actuator signal of the driving subsystem would freeze at a certain point of time ($t_f = 15s$); in other words, the actuator response which sets the speed (v) of the WMR would not change after the occurrence of such a fault. We

would like to see how this fault might affect the trajectory tracking of the WMR.

In order to see how different controllers react to this type of fault, simulation results are given for a wheeled mobile robot under both dynamic linear control and feedback linearization based control.

- **Dynamic Linear Controller**

Here, it is assumed that the wheeled mobile robot is controlled by the dynamic linear approach described in Section 3.4.2. The fault has occurred at $t_{fault} = 15s$.

According to Fig. 5.6(a), the residual signal for x exceeds its fault detection threshold sustainedly at $t = 25s$; in addition, Fig. 5.6(b) shows that the residual signal for y exceeds its fault detection threshold sustainedly at $t = 30s$. The residual signal for θ never exceeds its threshold value. Therefore, we can definitely conclude the existence of a fault after $t = 30s$.

- **Feedback Linearization Based Controller**

In the numerical simulation results shown, it is assumed that the wheeled mobile robot is controlled by the dynamic feedback linearization based approach as described in Section 3.4.3. The fault has occurred at $t_{fault} = 15s$.

With reference to Fig. 5.15(a), the residual signal for x exceeds its fault detection threshold sustainedly at $t = 30s$; in addition Fig. 5.7(b) shows that the residual signal for y exceeds its fault detection threshold sustainedly at $t = 23s$. The residual signal for θ in 5.7(c) never exceeds its threshold value. Therefore, we can definitely conclude the existence of a fault after $t = 30s$.

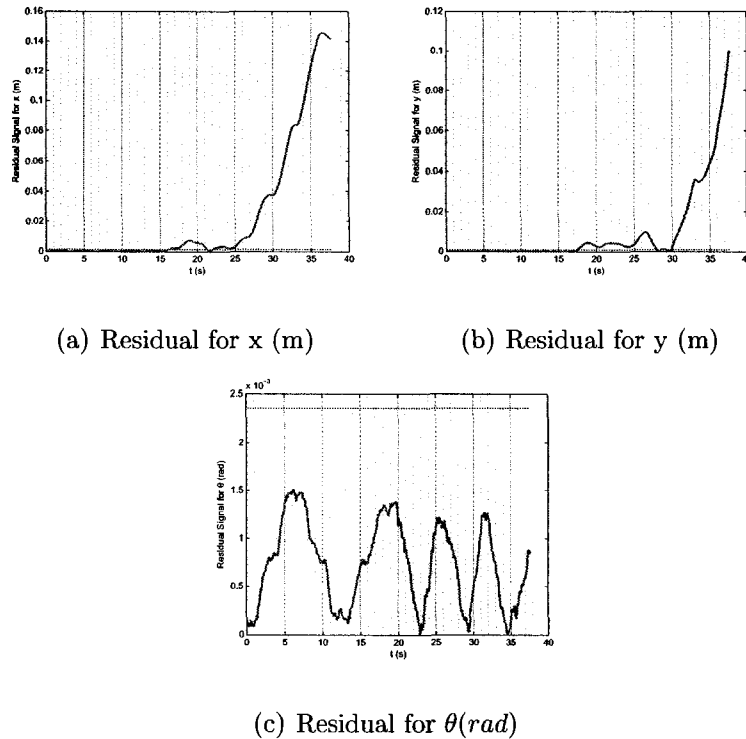


Figure 5.6: EKF Fault Detection Approach for System Subject to Locked In Place Fault under Dynamic Linear Control

5.4.2 Loss of Effectiveness Fault in the Driving Subsystem

(v)

In this scenario, due to the loss of actuator effectiveness, from a certain time onwards the system would receive only a certain percentage of the actuator signal. As a result the actuator response which sets the speed (v) of the WMR would be weaker than the required amount for the desired control. Hence, we would like to see how this fault might affect the trajectory tracking of the wheeled mobile robot.

- **Dynamic Linear Controller**

The dynamic linear controller designed in Section 3.4.2 is exploited here. The fault has occurred at $t_{fault} = 15s$.

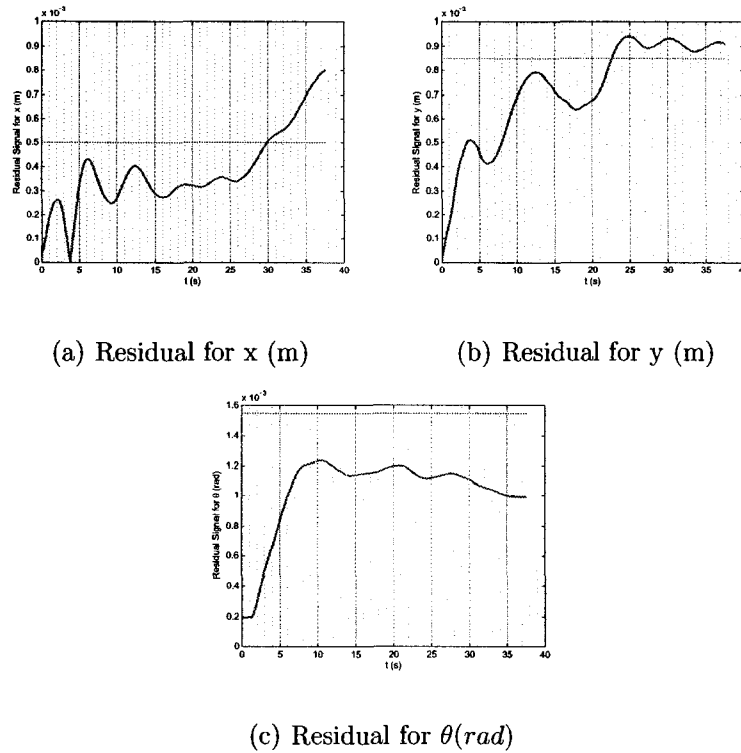


Figure 5.7: EKF Fault Detection Approach for System Subject to Locked In Place Fault under Feedback Linearization Based Control

– 80% Loss of Effectiveness

With reference to Fig. 5.8(a), the residual signal for x exceeds its fault detection threshold sustainedly at $t = 19s$; in addition Fig. 5.8(b) shows that the residual signal for y exceeds its fault detection threshold sustainedly at $t = 19s$. The residual signal for θ in 5.8(c) never exceeds its threshold value. Hence, we can definitely conclude the existence of a fault after $t = 19s$.

– 50% Loss of Effectiveness

As shown in Fig. 5.9(a), the residual signal for x exceeds its fault detection threshold sustainedly at $t = 23s$; in addition Fig. 5.9(b) shows that the residual signal for y exceeds its fault detection threshold sustainedly at

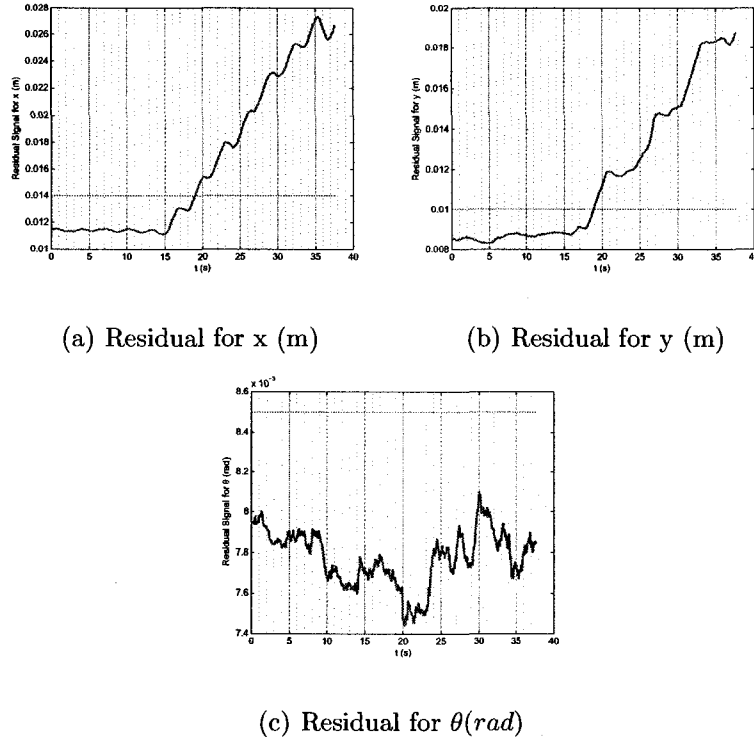


Figure 5.8: EKF Fault Detection Approach for System Subject to 80% Loss of Effectiveness Fault under Dynamic Linear Control

$t = 26$ s. The residual signal for θ in 5.9(c) never exceeds its threshold value. Therefore, we can definitely conclude the existence of a fault after $t = 26$ s.

– 20% Loss of Effectiveness

As shown in Fig. 5.8(a), Fig. 5.8(b) and Fig.5.8(c) the residuals never exceed their threshold values. Hence, we cannot conclude the existence of a fault.

• **Dynamic Feedback Linearization Controller**

The dynamic feedback linearization controller designed in Section 3.4.3 is exploited now. The fault has occurred at $t_{fault} = 15$ s.

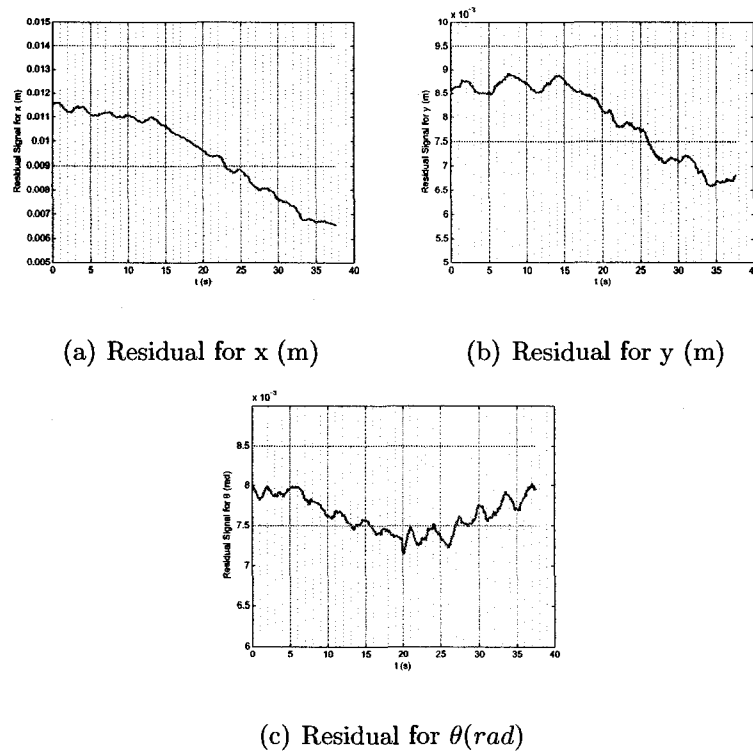


Figure 5.9: EKF Fault Detection Approach for System Subject to 50% Loss Of Effectiveness Fault under Dynamic Linear Control

– 80% Loss of Effectiveness

As illustrated in Fig. 5.11(a), the residual signal for x exceeds its fault detection threshold sustainedly at $t = 26s$; in addition Fig. 5.11(b) shows that the residual signal for y exceeds its fault detection threshold sustainedly at $t = 19s$. The residual signal for θ in 5.11(c) never exceeds its threshold value. Hence, we can definitely conclude the existence of a fault after $t = 26s$.

– 50% Loss of Effectiveness

As shown in Fig. 5.12(a), the residual signal for x exceeds its fault detection threshold sustainedly at $t = 24s$; in addition, Fig. 5.12(b) shows that the residual signal for y exceeds its fault detection threshold sustainedly

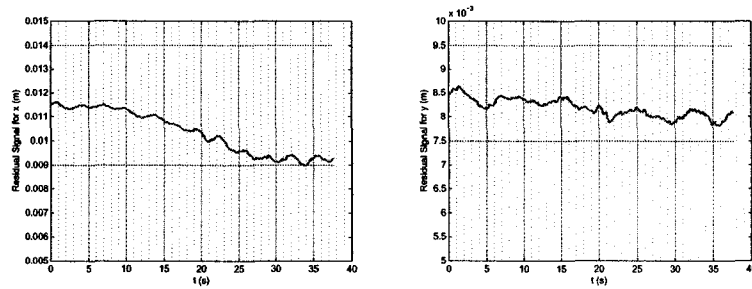
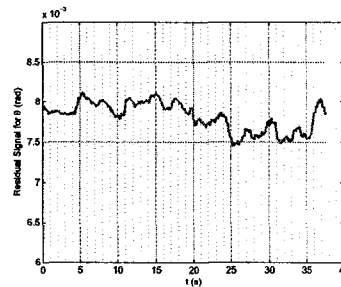
(a) Residual for x (m)(b) Residual for y (m)(c) Residual for θ (rad)

Figure 5.10: EKF Fault Detection Approach for System Subject to 20% Loss Of Effectiveness Fault under Dynamic Linear Control

at $t = 27s$. The residual signal for θ in 5.12(c) never exceeds its threshold value. Therefore, we can definitely conclude the existence of a fault after $t = 27s$.

– 20% Loss of Effectiveness

With reference to Fig.5.13(a), Fig. 5.13(b) and Fig. 5.13(c) the residuals never exceed their threshold values. Hence, we cannot conclude the existence of a fault.

Table 5.1: Permanent-Fault detection time & delay for the EKF approach

Type of Fault	Type of Controller	Fault Injection Time (s)	Fault Detection Time (s)	Fault Detection Delay (s)
Locked in place	Dynamic Linear	15	30	15
	Dynamic Feedback Linearization	15	30	15
Loss of effectiveness (80%)	Dynamic Linear	15	19	4
	Dynamic Feedback Linearization	15	26	4
Loss of effectiveness (50%)	Dynamic Linear	15	26	11
	Dynamic Feedback Linearization	15	27	12
Loss of effectiveness (20%)	Dynamic Linear	15	Not Detected	Not Detected
	Dynamic Feedback Linearization	15	Not Detected	Not Detected

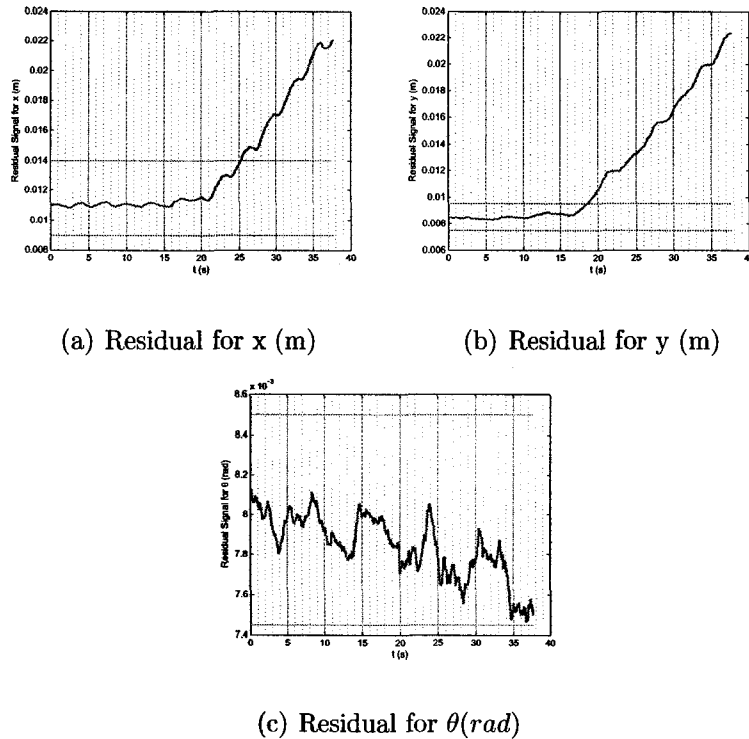


Figure 5.11: EKF Fault Detection Approach for System Subject to 80% Loss Of Effectiveness Fault under Feedback Linearization Based Control

5.5 Permanent-Fault Detection Through Neural Network Approach

In this section, the performance of our proposed neural network model consistency fault detection technique in the presence of permanent faults is investigated. Permanent faults are the group of faults which do not disappear after their occurrence. As before, both locked-in-place and loss-of-effectiveness faults are considered; and in each case the EKF fault detection technique is applied to two different scenarios. In the first scenario, the wheeled mobile robot is controlled by the dynamic linear controller (see Section 3.4.2) while in the second scenario the wheeled mobile robot is controlled by the dynamic feedback linearization controller (see Section 3.4.3). In this section,

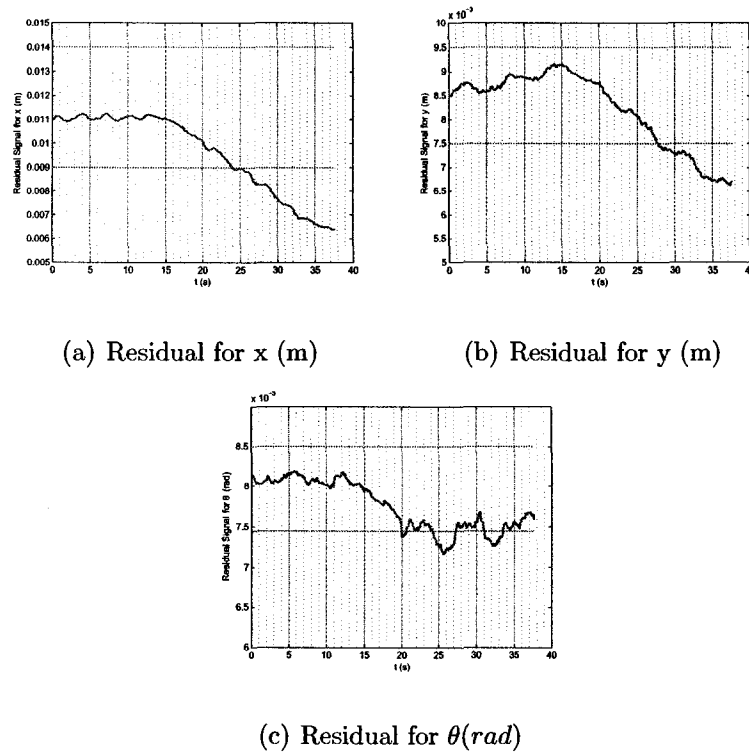


Figure 5.12: EKF Fault Detection Approach for System Subject to 50% Loss of Effectiveness Fault under Feedback Linearization Based Control

we assume that only the driving subsystem of the wheeled mobile robot is subject to fault.

5.5.1 Locked In Place Fault in the Driving Subsystem (v)

Under this scenario, the actuator signal of the driving subsystem would freeze at a certain point of time (say $t_f = 15s$). In other words, the actuator response which sets the speed (v) of the WMR would not change after the occurrence of such a fault. We would like to determine how this fault might affect the trajectory tracking of the WMR.

In order to determine how different controllers react to this type of fault, simulation results are given for a wheeled mobile robot under both dynamic linear control

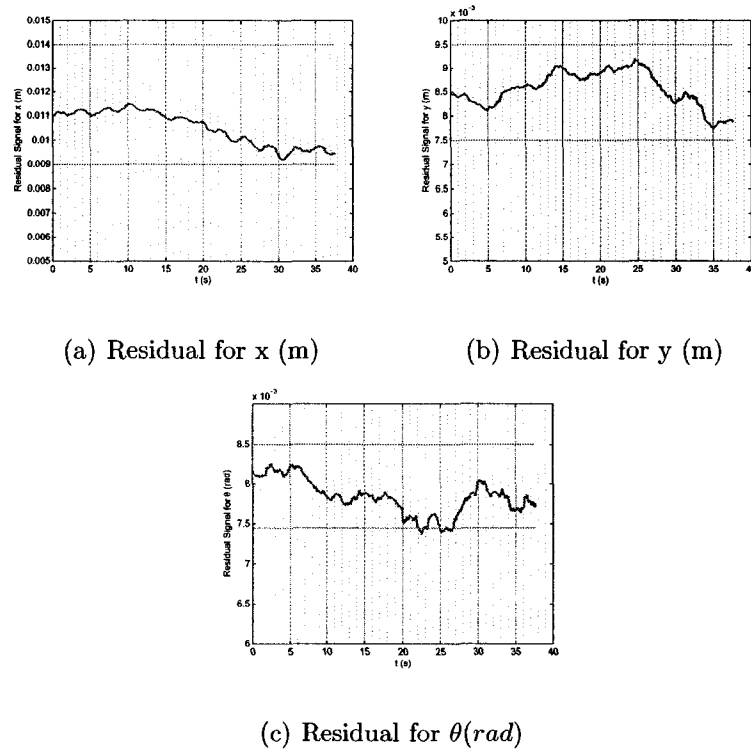


Figure 5.13: EKF Fault Detection Approach for System Subject to 20% Loss of Effectiveness Fault under Feedback Linearization Based Control

and feedback linearization based control.

- **Dynamic Linear Controller**

It is assumed that the wheeled mobile robot is controlled by the dynamic linear approach described in Section 3.4.2. The fault has occurred at $t_{fault} = 15s$.

According to Fig. 5.14(a), the residual signal for x exceeds its fault detection threshold sustainedly at $t = 17s$; in addition, Fig. 5.14(b) shows that the residual signal for y exceeds its fault detection threshold sustainedly at $t = 18s$. The residual signal for θ , depicted in Fig. 5.14(c) exceeds its threshold value at $t = 21s$. Hence, we can definitely conclude the existence of a fault after $t = 18s$.

- **Feedback Linearization Based Controller**

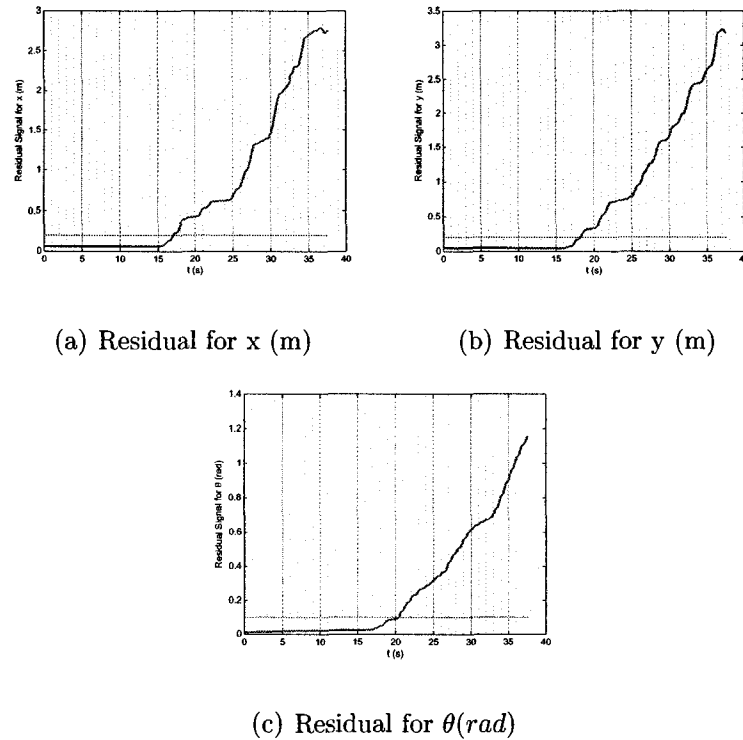


Figure 5.14: Neural Network-based Fault Detection Approach Subject to Permanent Locked In Place Fault under Dynamic Linear Control

In the simulation results shown here it is assumed that the wheeled mobile robot is controlled by the dynamic feedback linearization based approach described in Section 3.4.3.

According to Fig. 5.15(a), the residual signal for x exceeds its fault detection threshold sustainedly at $t = 18s$; in addition, Fig. 5.15(b) shows that the residual signal for y exceeds its fault detection threshold sustainedly at $t = 21s$. The residual signal for θ , depicted in 5.15(c), exceeds its threshold value at $t = 20s$. Hence, we can definitely conclude the existence of a fault after $t = 20s$.

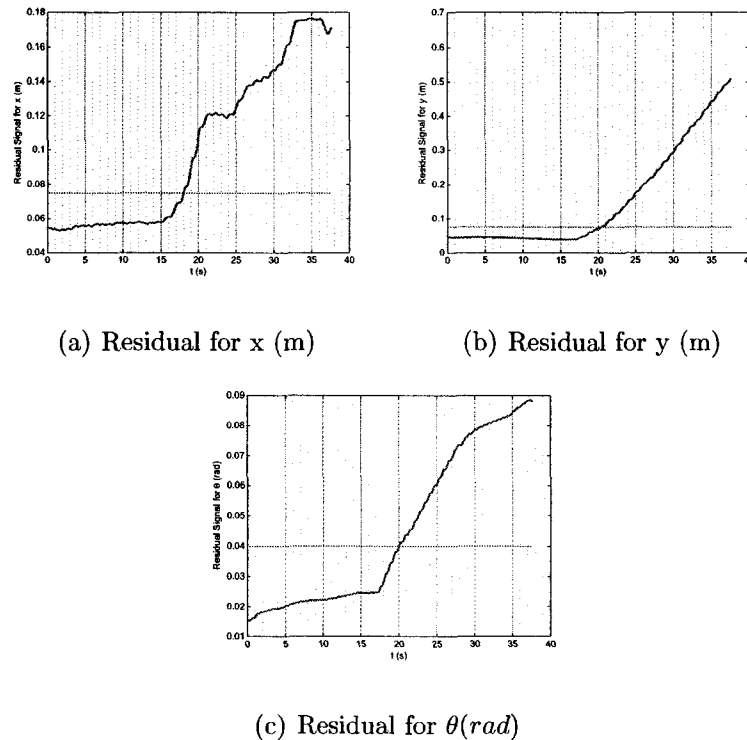


Figure 5.15: Neural Network-based Fault Detection Approach Subject to Permanent Locked In Place Fault under Feedback Linearization Based Control

5.5.2 Loss of Effectiveness Fault in the Driving Subsystem (v)

In this scenario, due to the loss of actuator effectiveness, from a certain time onward the system would receive only a certain percentage of the actuator signal. As a result the actuator response which sets the speed (v) of the WMR would be weaker than the required amount for the desired control. Hence, we would like to see how this fault might affect the trajectory tracking of the wheeled mobile robot.

- **Dynamic Linear Controller**

The dynamic linear controller designed in Section 3.4.2 is exploited here.

– 80% Loss of Effectiveness

According to Fig. 5.16(a), the residual signal for x exceeds its fault detection threshold sustainedly at $t = 15.5s$; in addition Fig. 5.16(b) shows that the residual signal for y exceeds its fault detection threshold sustainedly at $t = 17s$. The residual signal for θ , depicted in 5.16(c), exceeds its threshold value at $t = 17s$. Hence, we can definitely conclude the existence of a fault after $t = 17s$.

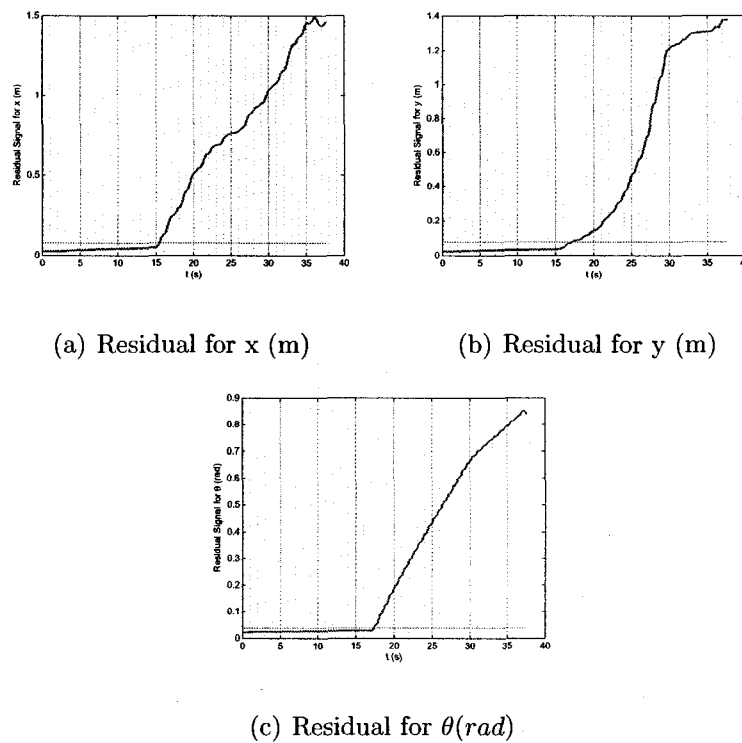


Figure 5.16: Neural Network-based Fault Detection Approach Subject to 80% Permanent Loss Of Effectiveness Fault under Dynamic Linear Control

– 50% Loss of Effectiveness

According to Fig. 5.17(a), the residual signal for x exceeds its fault detection threshold sustainedly at $t = 16.5s$; in addition Fig. 5.17(b) shows that the residual signal for y exceeds its fault detection threshold sustainedly at $t = 20s$. The residual signal for θ , depicted in 5.17(c), exceeds its threshold

value at $t = 35s$. Hence, we can definitely conclude the existence of a fault after $t = 20s$.

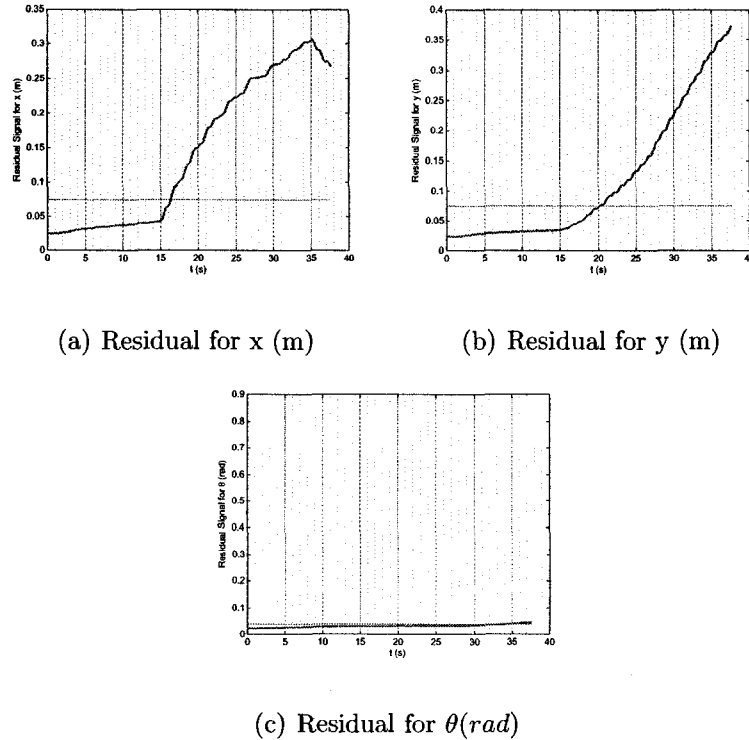


Figure 5.17: Neural Network-based Fault Detection Approach Subject to 50% Permanent Loss Of Effectiveness Fault under Dynamic Linear Control

– 20% Loss of Effectiveness

According to Fig. 5.18(a), the residual signal for x exceeds its fault detection threshold sustainedly at $t = 25s$; in addition Fig. 5.18(a) shows that the residual signal for y exceeds its fault detection threshold sustainedly at $t = 30s$. The residual signal for θ , depicted in 5.18(c), never exceeds its threshold value. Hence, we can definitely conclude the existence of a fault after $t = 30s$.

• Dynamic Feedback Linearization Based Controller

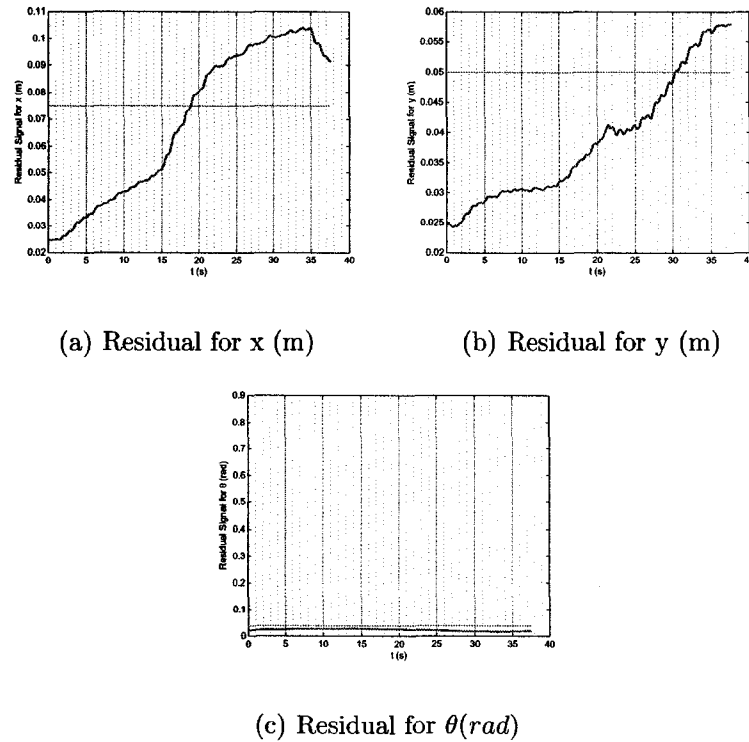


Figure 5.18: Neural Network-based Fault Detection Approach Subject to 20% Permanent Loss Of Effectiveness Fault under Dynamic Linear Control

The dynamic feedback linearization controller designed in 3.4.3 has been exploited here.

– 80% Loss of Effectiveness

According to Fig. 5.19(a), the residual signal for x exceeds its fault detection threshold sustainedly at $t = 18s$; in addition Fig. 5.19(b) shows that the residual signal for y exceeds its fault detection threshold sustainedly at $t = 22s$. The residual signal for θ , depicted in 5.19(c) never exceeds its threshold value. Hence, we can definitely conclude the existence of a fault after $t = 22s$.

– 50% Loss of Effectiveness

According to Fig. 5.20(a), the residual signal for x exceeds its fault detec-

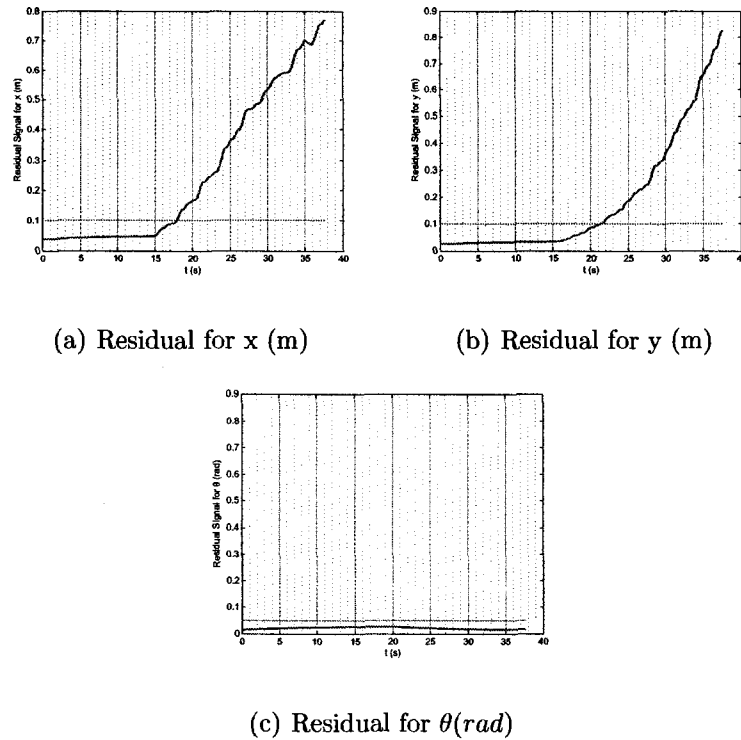


Figure 5.19: Neural Network-based Fault Detection Approach Subject to 80% Permanent Loss Of Effectiveness Fault under Feedback Linearization Based Control

tion threshold sustainedly at $t = 19s$; in addition Fig. 5.20(b) shows that the residual signal for y exceeds its fault detection threshold sustainedly at $t = 31s$. The residual signal for θ never exceeds its threshold value. Therefore, we can definitely conclude the existence of a fault after $t = 31s$.

– 20% Loss of Effectiveness

According to Fig. 5.6(a), the residual signal for x exceeds its fault detection threshold sustainedly at $t = 19s$. The residual signals for θ and y never exceed their threshold value. Hence, we cannot conclude the existence of a fault surely.

Table 5.2: Permanent-Fault detection time & delay for the neural network model consistency based approach

Type of Fault	Type of Controller	Fault Injection Time (s)	Fault Detection Time (s)	Fault Detection Delay (s)
Locked in place	Dynamic Linear	15	18	3
	Dynamic Feedback Linearization	15	20	5
Loss of effectiveness (80%)	Dynamic Linear	15	17	2
	Dynamic Feedback Linearization	15	22	7
Loss of effectiveness (50%)	Dynamic Linear	15	20	5
	Dynamic Feedback Linearization	15	31	16
Loss of effectiveness (20%)	Dynamic Linear	15	30	15
	Dynamic Feedback Linearization	15	Not Detected	Not Detected

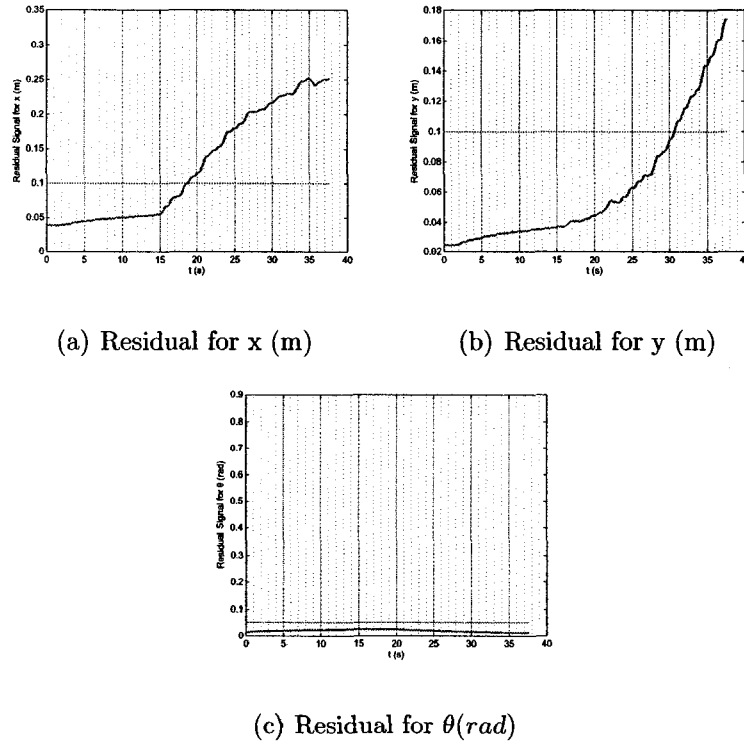


Figure 5.20: Neural Network-based Fault Detection Approach Subject to 50% Permanent Loss Of Effectiveness Fault under Feedback Linearization Based Control

5.6 Intermittent-Fault Detection Through EKF Approach

In this section, the performance of our proposed EKF fault detection technique in the presence of intermittent faults is investigated. Intermittent faults are the group of faults which disappear after a specific period of time. As before, both locked-in-place and loss-of-effectiveness faults are considered; and in each case, the EKF fault detection technique is applied to two different scenarios. In the first scenario, the wheeled mobile robot is controlled by the dynamic linear controller (see Section 3.4.2) while in the second scenario the wheeled mobile robot is controlled by the dynamic feedback linearization controller (see Section 3.4.3). In this section, we assume that

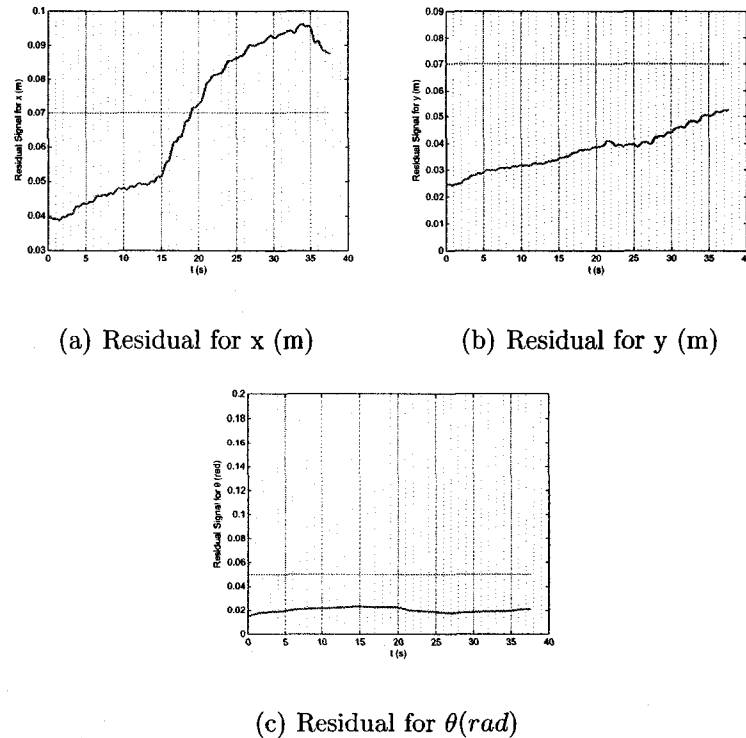


Figure 5.21: Neural Network-based Fault Detection Approach Subject to 20% Permanent Loss Of Effectiveness Fault under Feedback Linearization Based Control

only the driving subsystem of the wheeled mobile robot is subject to fault.

5.6.1 Locked In Place Fault in the Driving Subsystem (v)

Under this scenario, the actuator signal of the driving subsystem would freeze at a given point of time ; in other words, the actuator response which sets the speed (v) of the WMR would not change after the occurrence of such a fault. We would like to determine how this fault might affect the trajectory tracking of the WMR.

In order to see how different controllers react to this type of fault, simulation results are given for a wheeled mobile robot under both dynamic linear control and feedback linearization based control.

- **Dynamic Linear Controller** It is assumed that the wheeled mobile robot is

controlled by the dynamic linear approach described in Section 3.4.2. The fault has occurred at $t_{fault} = 15s$ and has disappeared at $t_{fault_end} = 25s$. With reference to Fig. 5.22(a) and Fig. 5.22(b), we can confirm the existence of a fault in the driving subsystem between $t = 22s$ and $t = 38s$.

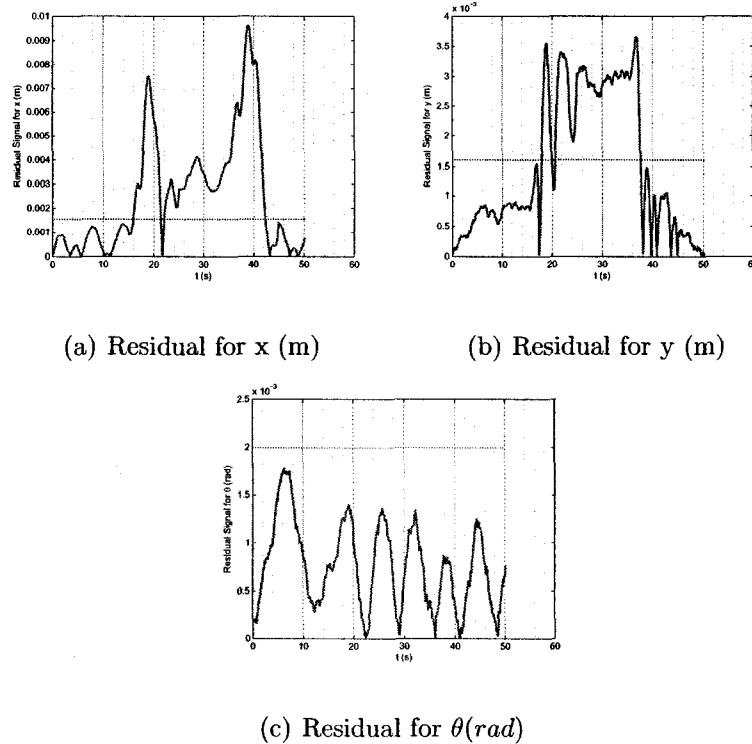


Figure 5.22: EKF Fault Detection Approach Subject to Intermittent Locked In Place Fault under Dynamic Linear Control

- Feedback Linearization Based Controller** In the simulation results shown here, it is assumed that the wheeled mobile robot is controlled by the dynamic feedback linearization based approach described in Section 3.4.3. The fault has occurred at $t_{fault} = 15s$ and has disappeared at $t_{fault_end} = 25s$. With reference to Fig. 5.23(a), Fig. 5.23(b) and Fig. 5.23(c) we cannot confirm the existence of a fault during this period.

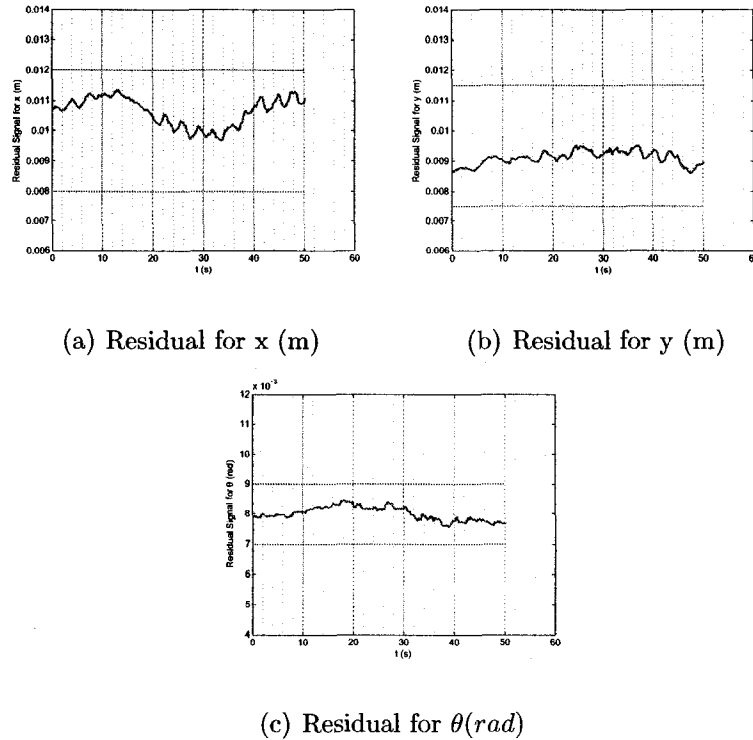


Figure 5.23: EKF Fault Detection Approach Subject to Intermittent Locked In Place Fault under Feedback Linearization Based Controller

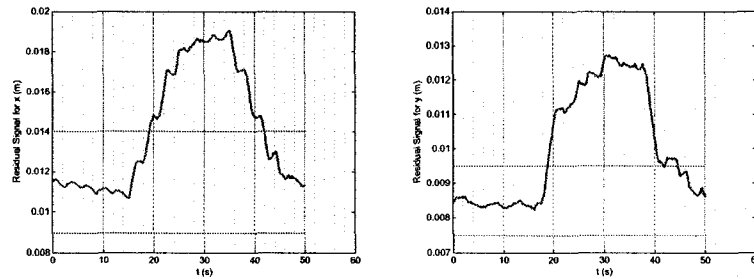
5.6.2 Loss Of Effectiveness Fault in the Driving Subsystem

(v)

In this scenario, due to the loss of actuator effectiveness, from a certain time onward the system would receive only a certain percentage of the actuator signal which it should have. As a result, the actuator response which sets the speed (v) of the WMR would be weaker than the required amount for the desired control. Hence, we would like to see how this fault might affect the trajectory tracking of the wheeled mobile robot.

- **Dynamic Linear Controller** Here, it is assumed that the wheeled mobile robot is controlled by the dynamic linear approach described in Section 3.4.2. The

fault has occurred at $t_{fault} = 15s$ and has disappeared at $t_{fault_end} = 25s$. With reference to Fig. 5.24(a) and Fig. 5.24(b), we can confirm the existence of a fault in the driving subsystem between $t = 19s$ and $t = 42s$.



(a) Residual for x (m)

(b) Residual for y (m)

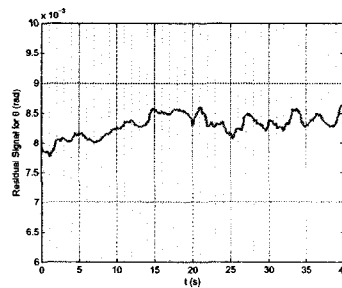
(c) Residual for θ (rad)

Figure 5.24: EKF Fault Detection Approach Subject to 80% Intermittent(between 15s and 25s) Loss Of Effectiveness Fault under Dynamic Linear Control

- Feedback Linearization Based Controller** In the numerical simulation results here, it is assumed that the wheeled mobile robot is controlled by the dynamic feedback linearization based approach described in Section 3.4.3. According to Fig. 5.24(a) and Fig. 5.24(b), we can confirm the existence of a fault in the driving subsystem between $t = 25s$ and $t = 45s$.

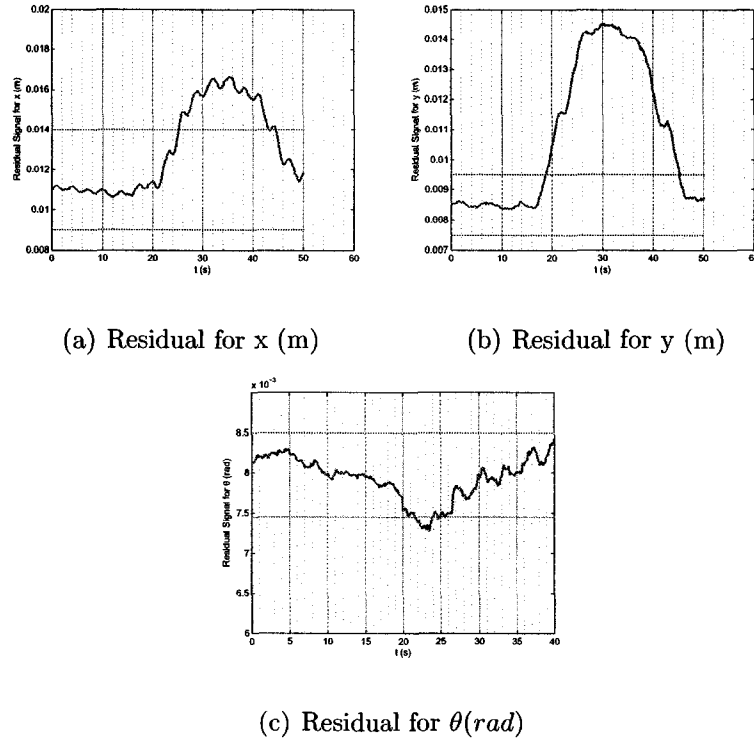


Figure 5.25: EKF Fault Detection Approach Subject to 80% Intermittent (between 15s and 25s) Loss Of Effectiveness Fault under Feedback Linearization Based Controller

5.7 Intermittent-Fault Detection Through Neural Network Approach

In this section, the performance of the proposed neural network model consistency fault detection technique in the presence of intermittent faults is investigated. Intermittent faults are the group of faults which disappear after a specific period of time. As usual, both locked-in-place and loss-of-effectiveness faults have been considered; and in each of these two cases, the EKF fault detection technique has been applied to two different scenarios. In one scenario, the wheeled mobile robot is controlled by the dynamic linear controller (see Section 3.4.2) while in the other scenario the wheeled mobile robot is controlled by the dynamic feedback linearization controller

Table 5.3: Intermittent-Fault detection time & delay for the EKF approach

Type of Fault	Type of Controller	Fault Appearance (s)	Fault Appearance Detection (s)	Fault Disappearance (s)	Fault Disappearance Detection (s)
Locked in place	Dynamic Linear	15	22	25	38
	Dynamic Feedback Linearization	15	-	25	-
Loss of effectiveness (80%)	Dynamic Linear	15	19	25	42
	Dynamic Feedback Linearization	15	25	25	45

(see Section 3.4.3). In this section, we assume that only the driving subsystem of the wheeled mobile robot has been subject to fault.

5.7.1 Locked In Place Fault in Driving Subsystem (v)

Under this scenario, the actuator signal of the driving subsystem would freeze at a certain point of time (here $t_f = 15s$); In other words, the actuator response which sets the speed (v) of the WMR would not change after the occurrence of such a fault. We would like to see how this fault might affect the trajectory tracking of the WMR.

In order to see how different controllers react to this type of fault, simulation results are given for a wheeled mobile robot under both dynamic linear control and feedback linearization based control.

- **Dynamic Linear Controller** Here, it is assumed that the wheeled mobile robot is controlled by the dynamic linear approach described in 3.4.2. The fault

has occurred at $t_{fault} = 15s$ and has disappeared at $t_{fault_end} = 25s$. With reference to 5.26(a) and 5.26(b), we can confirm the existence of a fault in the driving subsystem between $t = 20s$ and $t = 38s$.

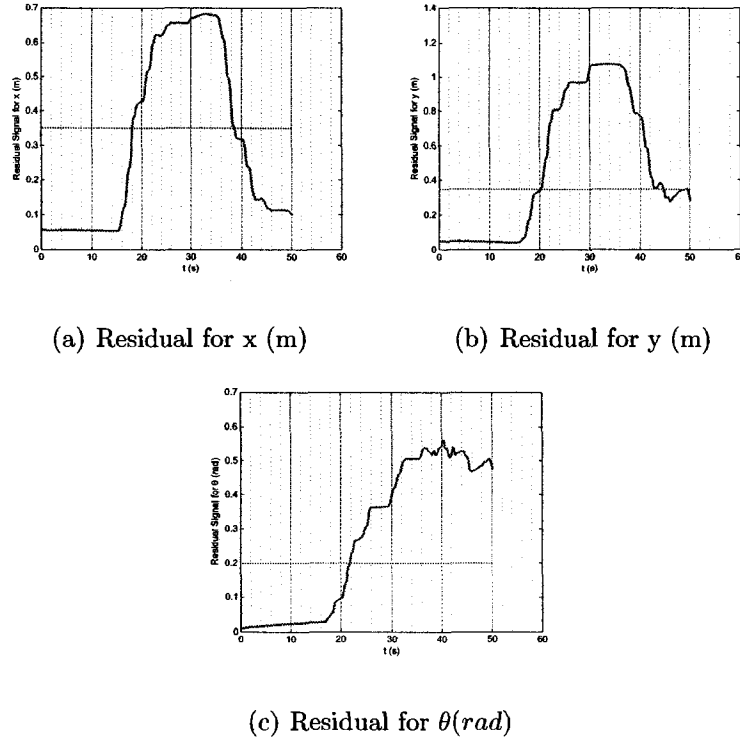


Figure 5.26: NN Fault Detection Approach Subject to Intermittent Locked In Place Fault under Dynamic Linear Control

- Feedback Linearization Based Controller** In the numerical simulation results here, it is assumed that the wheeled mobile robot is controlled by the dynamic feedback linearization based approach described in Section 3.4.3. The fault has occurred at $t_{fault} = 15s$ and has disappeared at $t_{fault_end} = 25s$. According to 5.27(a) and 5.27(b), we can confirm the existence of a fault in the driving subsystem between $t = 22s$ and $t = 78s$

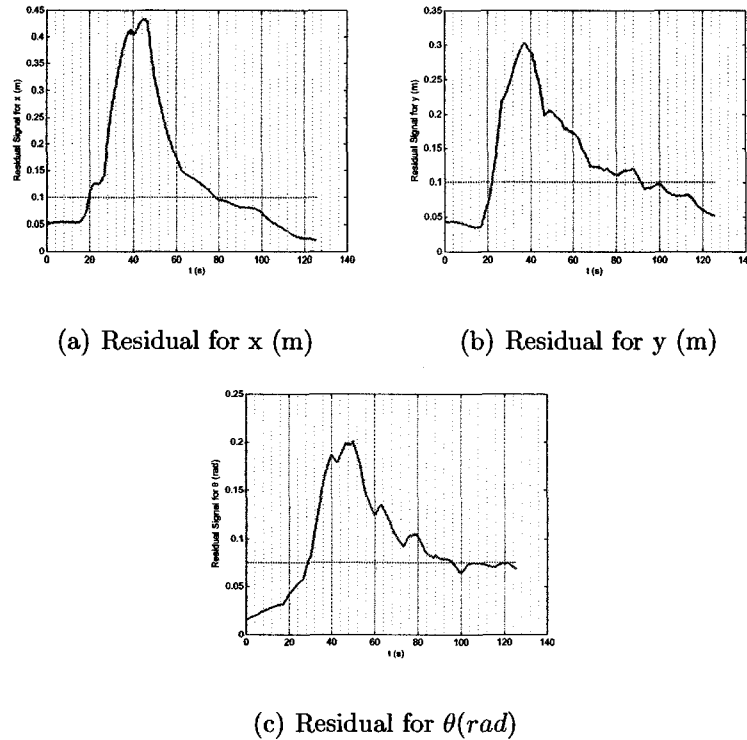


Figure 5.27: NN Fault Detection Approach Subject to Intermittent Locked In Place Fault under Feedback Linearization Based Control

5.7.2 Loss Of Effectiveness Fault in Driving Subsystem (v)

In this scenario, due to the loss of actuator effectiveness, from a certain time onward the system would receive only a certain percentage of the actuator signal which it should have. As a result, the actuator response which sets the speed (v) of the WMR would be weaker than the required amount for the desired control. Hence, we would like to see how this fault might affect the trajectory tracking of the wheeled mobile robot.

- **Dynamic Linear Controller** Here, it is assumed that the wheeled mobile robot is controlled by the dynamic linear approach described in 3.4.2. The fault has occurred at $t_{fault} = 15s$ and has disappeared at $t_{fault_end} = 25s$. According

to 5.28(a) and 5.28(b), we can confirm the existence of a fault in the driving subsystem between $t = 23s$ and $t = 92s$

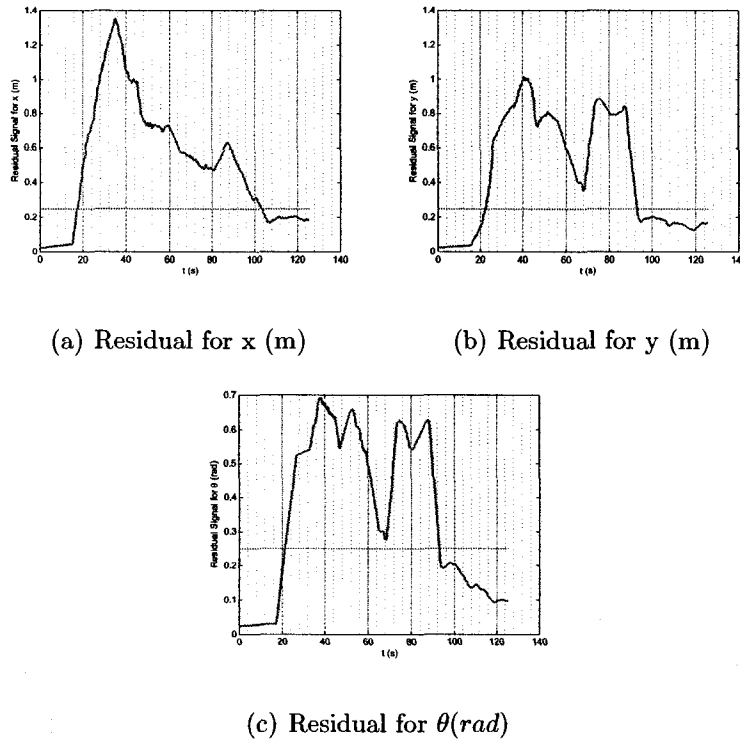
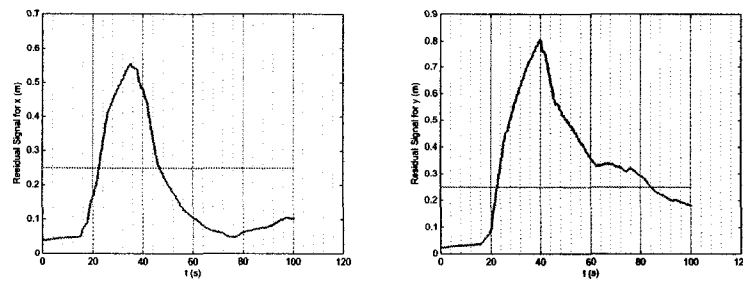


Figure 5.28: NN Fault Detection Approach Subject to 80% Intermittent(between 15s and 25s) Loss Of Effectiveness Fault under Dynamic Linear Control

- Feedback Linearization Based Controller** In the numerical simulation results here, it is assumed that the wheeled mobile robot is controlled by the dynamic feedback linearization based approach described in Section 3.4.3. The fault has occurred at $t_{fault} = 15s$ and has disappeared at $t_{fault_end} = 25s$. With reference to 5.29(a) and 5.29(a), we can confirm the existence of a fault in the driving subsystem between $t = 23s$ and $t = 46s$.



(a) Residual for x (m)

(b) Residual for y (m)

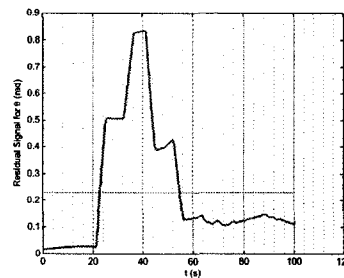
(c) Residual for $\theta(rad)$

Figure 5.29: NN Fault Detection Approach Subject to 80% Intermittent (between 15s and 25s) Loss Of Effectiveness Fault under Feedback Linearization Based Controller

5.8 Summary and Conclusions

In Section 5.2.1, the impact of the locked in place fault on the trajectory tracking performance of a wheeled mobile robot under both dynamic linear controller and dynamic feedback linearization controller has been studied. With regard to Figure 5.1(d) and 5.2(d), it is evident that the wheeled mobile robot under dynamic linear controller is much more affected in comparison to the wheeled mobile robot under dynamic feedback linearization controller. In other words, the dynamic feedback linearization controller shows a more robust reaction to this kind of fault.

In Section 5.2.2, the impact of the loss of effectiveness fault on the trajectory tracking performance of a wheeled mobile robot under both dynamic linear controller

Table 5.4: Intermittent-Fault detection time & delay for the neural network model consistency based approach

Type of Fault	Type of Controller	Fault Appearance (s)	Fault Appearance Detection(s)	Fault Disappearance (s)	Fault Disappearance Detection(s)
Locked in place	Dynamic Linear	15	20	25	38
	Dynamic Feedback Linearization	15	22	25	78
Loss of effectiveness (80%)	Dynamic Linear	15	23	25	92
	Dynamic Feedback Linearization	15	23	25	46

and dynamic feedback linearization controller has been studied. With regard to Figure 5.3(d) and 5.4(d), it is observed that the impact of the fault on the performance of both these controllers is rather similar and the overall level of impact is much less than the impact of locked in place fault. Comparing Table 5.4.2 and Table 5.5.2 shows that, with regard to Permanent-Faults, for large loss of effectiveness faults the extended Kalman filter approach has a better performance than the neural network approach. But for detecting locked in place faults and small loss of effectiveness faults the performance of the neural network approach is better. These two table imply that small loss of effectiveness faults under a robust controller like the dynamic feedback linearization controller are not detectable⁴. With regard to Intermittent-Fault detection, comparing Table 5.6.2 and Table 5.7.2 shows that the extended

⁴This is related to the phenomenon addressed in the aircraft incident story in Section 2.6.

Kalman filter approach has a much better capability in detecting the disappearance of the fault than neural network approach.

Chapter 6

Concluding Remarks

6.1 Conclusions

This thesis has investigated two model consistency based approaches for fault diagnosis in wheeled mobile robots (WMR). In the considered application, a nonholonomic wheeled mobile robot was required to track a predefined trajectory in an obstacle free environment.

As the first step, two different types of controllers are designed to guarantee that the mobile robot is capable of tracking the desired trajectory. However, the actuators, of the different mobile robot subsystems, which perform the control commands are vulnerable to a number of faults. The major two subsystems whose actuators might affect the vital mobility feature of the wheeled mobile robot and cause unwanted deviations from the desired path include the driving subsystem and the steering subsystem. The driving subsystem is responsible for linear velocity (v) of the mobile robot, while the steering subsystem is in charge of the angular velocity (ω) of the wheeled mobile robot. In particular, loss of effectiveness and locked in place signals have been considered as two principal faults which might impact those two

subsystems.

In search for the goal of detecting the occurrence of faults in WMR subsystems, two different model consistency based fault detection approaches have been proposed.

The first approach, is based on identification of the system through an Extended Kalman Filter (EKF). A novel technique for residual generation has been proposed. The performance of the proposed fault detection approach has been studied in trajectory tracking of wheeled mobile robots which is a common application of these mobile apparatus. It has been shown that the robustness of the controller has a very slight impact on this detection scheme and will not be able to mask the occurrence of faults.

The second approach, is based on identification of the system through a stable neural network. A novel model consistency based approach has been proposed which does not suffer from lack of proof for stability as a large number of other neural network based approaches do. The application of the proposed approach in fault detection amid a trajectory tracking mission of a mobile robot has been studied. It has been shown that the robustness of the controller slightly impacts the fault detection procedure and the amount of fault detection delay time.

As described in Section 5.8, the overall performance of the extended Kalman filter approach can be considered slightly better than the neural network approach because it is not only capable of detecting the occurrence of faults but also capable of rather quick detection of disappearance of the fault in case of intermittent faults. Nevertheless, it should be noted that the neural network approach sometime performs better in case of existence of permanent faults and in case of existence of small faults under rather robust controllers like the feedback linearization controller.

In summary, the main contributions of this thesis can be outlined as follows:

- Design of a fault detection approach based on Extended Kalman Filters (EKF) for a wheeled mobile robot (WMR) which is tracking a predefined trajectory in an obstacle free environment.
- Introduction of a new way of residual generation with Extended Kalman Filters (EKF) based state prediction. The residual generation approach is novel because it is based on defining the residual as the difference between the measured state values and the *a priori estimate*¹ of the state \hat{x}_k^- instead of the usual estimate of the state.
- Design of a fault detection approach based on Artificial Neural Networks for a wheeled mobile robot (WMR) which is tracking a predefined trajectory in an obstacle free environment.

6.2 Future Research Directions

Although fault diagnosis techniques have been rather well developed for linear systems in the recent decades, they are far from maturity in field of nonlinear systems and their applications. The following are some of the many different subjects which could be considered as the future research directions in this field:

Fault isolation and recovery, are two crucial steps after fault detection. As observed in this thesis, the proposed approaches were not capable of isolating all faults. Whereas, in a real world situation, the fault detection step should lead to further steps of handling a fault which are isolation and recovery phases.

Fault prognosis, is another issue of interest. This step which can be added in the overall strategy for handling faults would lead to condition based maintenance; as a

¹This concept has been introduced in Section 4.3.3.

result, it would be of great practical and economic interest to develop such schemes.

Active fault diagnosis for nonlinear systems and mobile robots is still an open problem. Although this issue has been studied for linear systems, it has remained almost untouched for nonlinear systems like mobile robots.

As a matter of fact, there are a large number of open problems in the area of fault diagnosis for nonlinear systems in general and for mobile robots in particular. Here, we have tried to discuss the most undeveloped issues.

Bibliography

- [Abdollahi 06] F. Abdollahi, H.A. Talebi & R.V. Patel. *Stable Identification Of Nonlinear Systems Using Neural Networks: Theory And Experiments*. IEEE/ASME Transactions on Mechatronics, vol. 11, no. 4, pages 488–495, August 2006.
- [Aicardi 95] M. Aicardi, G. Casalino, A. Bicchi & A. Balestrino. *Closed Loop Steering Of Unicycle-Like Vehicles Via Lyapunov Techniques*. IEEE Robotics & Automation Magazine, vol. 2, no. 1, pages 27–35, 1995.
- [Alexander 89] J.C. Alexander & J.H. Maddocks. *On Kinematics Of Wheeled Mobile Robots*. International Journal Of Robotics Research, vol. 8, no. 5, pages 15–27, 1989.
- [Anderson 83] J.L. Anderson. *Space station autonomy requirements*. In Computers in Aerospace Conference, 4th, pages 164–170, Hartford, CT, October 24-26 1983. American Institute of Aeronautics and Astronautics.
- [Babuska 02] R. Babuska. Recent advances in intelligent paradigms and applications, chapitre Neuro-Fuzzy Methods For Modeling and Identification, pages 161–186. Springer-Verlag, Heidelberg, 2002.
- [Bakiotis 79] C. Bakiotis, J. Raymond & A. Rault. *Parameter Indentification and Discriminant Analysis For Jet Engine Mechanical State Diagnosis*. In IEEE Conference on Decision and Control, Fort Lauderdale, 1979.

- [Basseville 93] M. Basseville & I.V. Nikiforov. *Detection of abrupt changes: Theory and application*. Information and System Sciences Series. Prentice Hall, April 1993.
- [Beard 71] R.V. Beard. *Failure accomodation in linear systems through self-reorganization*. PhD thesis, Massachusetts Institute of Technology. Dept. of Aeronautics and Astronautics, 1971.
- [Blanke 06] M. Blanke, M. Kinnaert, Lunze J. & Staroswiecki M. *Diagnosis and fault-tolerant control*. Springer, second edition, September 2006.
- [Bocaniala 04] C.D. Bocaniala, J. Sa da Costa & V. Palade. *A Novel Fuzzy Classification Solution For Fault Diagnosis*. International Journal of Fuzzy and Intelligent Systems, vol. 15, no. 3-4, pages 195–206, 2004.
- [Bocaniala 05] C.D. Bocaniala, J. Sa da Costa & V. Palade. *Fuzzy-based Refinement Of The Fault Diagnosis Task In Industrial Devices*. International Journal of Fuzzy and Intelligent Systems, vol. 16, no. 6, pages 599–614, 2005.
- [Boutayeb 97] M. Boutayeb, H. Rafaralahy & M. Darouach. *Convergence Analysis of the Extended Kalman Filter Used as an Observer for Nonlinear Deterministic Discrete-Time Systems*. IEEE Transactions on Automatic Control, vol. 42, no. 4, pages 581–586, April 1997.
- [Calado 01] J.M.G Calado, J. Korbicz, K. Patan, R.J. Patton & J.M.G Sa da Cost. *Soft Computing Approaches to Fault Diagnosis For Dynamic systems*. European Journal Of Control, vol. 7, pages 248–286, 2001.
- [Campbell 04] S.L. Campbell & R. Nikoukhah. *Auxiliary signal design for failure detection*. Princeton Series in Applied Mathematics. Princeton University Press, January 2004.

- [Campion 91] G. Campion, B. d'Andrea Novel & G. Bastin. *Modeling and State Feedback Control Of Nonholonomic Mechanical Systems*. In Proceedings Of The 30Th IEEE Conference On Decision And Control, pages 1184–1189, Brighton, UK, 1991.
- [Canudas de Wit 92] C. Canudas de Wit & O.J. Sørдалen. *Exponential Stabilization Of Mobile Robots With Nonholonomic Constraints*. IEEE Transactions On Automatic Control, vol. 37, no. 11, pages 1791–1797, 1992.
- [Canudas de Wit 93] C. Canudas de Wit, H. Khenouf, C. Samson & O.J. Sørдалen. Recent trends in mobile robots, chapitre Nonlinear Control Design For Mobile Robots, pages 121–156. World Scientific Publisher, 1993.
- [Carlson 03] J. Carlson & R.R. Murphy. *Reliability Analysis Of Mobile Robots*. In Proceedings of the 2003 IEEE International Conference on Robotics and Automation, volume 1, pages 274 – 281, Taipei, Taiwan, September 2003.
- [Carlson 04] J. Carlson & R.R. Murphy. *An Investigation Of Mml Methods For Fault Diagnosis In Mobile Robots*. In Proceedings of The 2004 IEEE/RSJ International Conference on Intelligent Robots and Systems, Sendai, Japan, September 28 - October 2 2004.
- [Chen 99] J. Chen & R.J. Patton. Robust model-based fault diagnosis for dynamic systems. International Series on Asian Studies in Computer and Information Science. Kluwer Academic Publishers, 1999.
- [Chow 84] E.Y. Chow & A.S. Willsky. *Analytical Redundancy and The Design of Robust Detection Systems*. IEEE Transactions on Automatic Control, vol. 29, no. 7, pages 603–614, 1984.

- [Clark 78] R.N. Clark. *Instrument Fault Detection*. IEEE Transaction Aero. & Electronic Systems, vol. 14, no. 3, 1978.
- [d'Andrea-Novel 95] B. d'Andrea-Novel, G. Bastin & G. Campion. *Control Of Nonholonomic Wheeled Mobile Robots By State Feedback Linearization*. International Journal Of Robotics Research, vol. 14, no. 6, pages 543–559, 1995.
- [De Luca 93] A. De Luca & M.D. Di Benedetto. *Control Of Nonholonomic Systems Via Dynamic Compensation*. Kybernetika, vol. 29, no. 6, pages 593–559, 1993.
- [De Luca 98] A. De Luca, G. Oriolo & C. Samson. Robot motion planning and control, volume 229 of *Notes In Control And Information Sciences*, chapitre Feedback Control Of A Nonholonomic Car-like Robot, pages 171–253. Springer, London, UK, 1998.
- [De Luca 03] A. De Luca, G. Oriolo & M. Vendittelli. *Control of Wheeled Mobile Robots: An Experimental Overview*. Rapport technique, Dipartimento di Informatica e Sistemistica, Universit'a degli Studi di Roma La Sapienza, Italy, 2003.
- [Ding 00] S.X. Ding, T. Jeinisch, P.M. Frank & E.L Dind. *A Unified Approach To The Optimization Of Fault Detection Systems*. International Journal of Adaptive Control and Signal Processing, vol. 14, no. 7, pages 725–745, 2000.
- [Fernndez 04] J. Fernndez, R. Sanz & A. Diguez. *Probabilistic Models For Monitoring And Fault Diagnosis: Application And Evaluation In A Mobile Robot*. Applied Artificial Intelligence, vol. 18, no. 1, pages 43–67, January 2004.

- [Fierro 97] R. Fierro & F.L. Lewis. *Control Of A Nonholomic Mobile Robot: Backstepping Kinematics Into Dynamics*. Journal of Robotic Systems, vol. 14, no. 3, pages 149–163, March 1997.
- [Filbert 82] D. Filbert & K. Metzger. *Quality Test of systems by Parameter Estimation*. In 9th IMEKO Congress, 1982.
- [Fourquet 96] J.Y. Fourquet & M. Renaud. *Time-Optimal Motions For Torque Controlled Wheeled Mobile Robot Along Specified Paths*. In Proceeding of the 35th Conference on Decision and Control, Kobe, Japan, December 1996.
- [Frank 00] P.M. Frank, S.X. Ding & B. Köpper-Selinger. *Current Developments in Theory of FDI*. In IFAC Symposium on Fault Detection, Supervision and Safety For Technical Processes, volume 1, pages 16–27, Budapest, Hungary, 2000.
- [Geiger 82] G. Geiger. *Monitoring of an Electrical Driven Pump Using Continuous-Time Parameter Estimation Models*. In 6th IFAC Symposium on Identification and Parameter Estimation, Washington, 1982. Pergamon Press.
- [Gertler 88] J.J. Gertler. *Survey Of Model-Based Failure Detection And Isolation In Complex Plants*. IEEE Control Systems Magazine, vol. 8, no. 6, pages 3–11, December 1988.
- [Gertler 91] J. Gertler. *Generating Directional Residuals with Dynamic Parity Equations*. In IFAC/IMACS Symposium SAFEPROCESS'91, Baden Baden, Germany, 1991.
- [Gertler 98] J.J. Gertler. *Fault detection and diagnosis in engineering systems*. Marcel Dekker INC., first edition, May 1998.

- [Grewal 01] M.S. Grewal & A.P. Andrews. Kalman filtering : Theory and practice using matlab. Wiley-Interscience Publication, second edition, January 2001.
- [Guide 89] STARTS Guide. *The STARTS purchases Handbook: Software Tools For Application To Large Real-time Systems*. National Computing Centre Publications, Manchester, UK, second edition, 1989.
- [Gustafsson 00] F. Gustafsson. Adaptive filtering and change detection. John Wiley & Sons LTD, first edition, September 2000.
- [Halder 06] B. Halder & N. Sarkar. *Robust Fault Detection And Isolation In Mobile Robot*. Rapport technique, Department of Mechanical Engineering, Vanderbilt University, Nashville, TN, 2006.
- [Hashimoto 03] M. Hashimoto, H. Kawashima & F. Oba. *A Multi-Model Based Fault Detection And Diagnosis Of Internal Sensors For Mobile Robot*. In Proceedings of The 2003 IEEE/RSJ International Conference on Intelligent Robots and Systems, Los Vegas, Nevada, USA, October 2003.
- [Haykin 01] S. Haykin, editeur. Kalman filtering and neural networks. Wiley-Interscience Publication, first edition, October 2001.
- [Himmelblau 78] D.M. Himmelblau. Fault diagnosis in chemical and petrochemical processes. Elsevier, Amsterdam, 1978.
- [Höfling 94] T. Höfling & T. Pfeufer. *Detection of Additive and Multiplicative Faults-Parity Space vs. Parameter Estimation*. In Proceedings of IFAC SAFEPROCESS Symposium'94, Espoo, Finland, 1994.
- [Hohmann 77] H. Hohmann. Automatic monitoring and failure diagnosis for machine tools. Master's thesis, T.H. Darmstadt, Germany, 1977.

- [Isermann 84] R. Isermann. *Process Fault Detction Based on Modeling and Estimation: A Survey*. Automatica, vol. 20, no. 4, pages 387–404, 1984.
- [Isermann 97a] R. Isermann. *Supervision, Fault Detection and Fault Diagnosis Methods: An Introduction*. Control Engineering Practice, vol. 5, no. 5, pages 639–652, 1997.
- [Isermann 97b] R. Isermann & P. Ballè. *Trends in The Application of Model-Based Fault Detection And Diagnosis in Technical Processes*. Control Engineering Practice (CEP), vol. 5, no. 5, pages 638–652, 1997.
- [Isermann 05] R. Isermann. *Fault-diagnosis systems: An introduction from fault detection to fault tolerance*. Springer, first edition, November 2005.
- [Isidori 95] A. Isidori. *Nonlinear control systems*. Springer, London, UK, 3rd edition, August 1995.
- [Jiang 99] Z-P Jiang & H. Nijmeijer. *A Recursive Technique For Tracking Control Of Nonholonomic Systems In Chained Form*. IEEE Transaction On Automatic Control, vol. 44, no. 2, pages 265–279, 1999.
- [Jones 73] H.L. Jones. *Failure detection in linear systems*. PhD thesis, Massachusetts Institute of Technology, Dept. of Aeronautics and Astronautics, 1973.
- [Kalman 60] R.E. Kalman. *A New Approach To Linear Filtering and Prediction Problems*. Journal Of Basic Engineering, vol. 82, pages 34–45, 1960.
- [Kawabata 01] K. Kawabata, S. Okina, T. Fujii & H.; Asama. *A Study Of Self-Diagnosis System For An Autonomous Mobile Robot: Coping With Self-Condition Using Internal Sensory Information*. In IECON '01: The 27th Annual Conference of the IEEE Industrial Electronics Society, volume 1, pages 381 – 386, 29 Nov.- 2 Dec. 2001.

- [Kawabata 02] K. Kawabata, T. Akamatsu & H. Asama. *A Study Of Self-Diagnosis System Of An Autonomous Mobile Robot: Expansion Of State Sensory Systems*. In Proceedings of The 2002 IEEE/RSJ International Conference on Intelligent Robots and Systems, EPFL, Lausanne, Switzerland, October 2002.
- [Korbicz 04] J. Korbicz, Koscielny J.M., Kowalczyk Z. & Cholewa W., editeurs. *Fault diagnosis: Models, artificial intelligence, applications*. Springer, first edition, February 2004.
- [Krener 02] A.J. Krener. Directions in mathematical systems theory and optimization, chapitre The Convergence of the Extended Kalman Filter, pages 173–182. Springer Verlag, Berlin, 2002.
- [Li 07] Z.Q. Li, L. Ma & K. Khorasani. *Fault Diagnosis of an Actuator in the Attitude Control Subsystem of a Satellite using Neural Networks*. In International Joint Conference on Neural Networks 2007(IJCNN 2007), pages 2658 – 2663, Orlando, FL, USA, 12-17 Aug 2007.
- [Luo 05] M. Luo, D. Wang, M. Pham, C.B. Low, J.B. Zhang, D.H. Zhang & Y.Z. Zhao. *Model-Based Fault Diagnosis/Prognosis For Wheeled Mobile Robots: A Review*. In IECON '05: 32nd Annual Conference of IEEE Industrial Electronics Society, page 6, November 2005.
- [Mamdani 76] E.H. Mamdani. *Advances in Linguistic Synthesis of Fuzzy Controllers*. International Journal Of Man-Machine Studies, vol. 8, pages 669–678, 1976.
- [Marcu 03] T. Marcu, B. Köppen-Seliger, P.M. Frank & S.X. Ding. *Dynamic Functional-link Neural Networks Genetically Evolved Applied To Fault*

- Diagnosis*. In Proceedings of The 7th European Control Conference ECC'03, University of Cambridge, UK, 1-4 September 2003.
- [Marsland 05] S. Marsland, U. Nehmzowb & J. Shapiroc. *On-Line Novelty Detection For Autonomous Mobile Robots*. Robotics and Autonomous Systems, vol. 51, no. 2-3, pages 191–206, May 2005.
- [Masoumnia 89] M. Masoumnia, G.C. Verghese & A.S. Willsky. *Failure Detection and Identification*. IEEE Transaction on Automatic Control, 1989.
- [M'Closkey 97] R.T. M'Closkey & R.M. Murray. *Exponential Stabilization Of Driftless Nonlinear Control Systems Using Homogeneous Feedback*. IEEE Transactions On Automatic Control, vol. 42, no. 5, pages 614–628, 1997.
- [Morin 97] P. Morin & C. Samson. *Application Of Backstepping Techniques To Time-Varying Exponential Stabilization Of Chained Systems*. European Journal Of Control, vol. 3, pages 15–36, 1997.
- [Murphy 99] R.R. Murphy & D. Hershberger. *Handling Sensing Failures in Autonomous Mobile Robots*. The International Journal of Robotics Research, vol. 18, no. 4, pages 382–400, April 1999.
- [Narendra 90] K.S. Narendra & K. Parthasarathy. *Identification and Control of Dynamical Systems Using Neural Networks*. IEEE Transactions on Neural Networks, vol. 1, no. 1, pages 4–27, March 1990.
- [Neimark 72] J.I. Neimark & Fufaev. *Dynamics Of Nonholonomic Systems*. In American Mathematical Society, Providence, RI, 1972.
- [Nicosia 01] S. Nicosia, B. Siciliano, A. Bicchi & P. Valigi, editeurs. *Ramsete: Articulated and mobile robotics for services and technologies*. Lecture

Notes In Control And Information Sciences. Springer, Germany, 1st edition, June 2001.

- [Niemann 97] H.H. Niemann & J. Stoustrup. *Integration Of Control And Fault Detection: Nominal And Robust Design*. In Proceedings Of The Third IFAC Symposium on Fault Detection, Supervision and Safety for Technical Processes (SAFEPROCESS 1997), pages 341–346, Hull, England, 1997.
- [Noreils 90] F.R. Noreils. *Integrating Error Recovery In A Mobile Robot Control System*. In Proceedings Of The 1990 IEEE International Conference On Robotics And Automation, volume 1, pages 396–401, Cincinnati, OH, 13-18 May 1990.
- [Ostergaard 05] K. Ostergaard, D. Vinther, M. Bisgaard, R. Izadi-Zamanabadi & Bendtsen J.D. *Experimental Fault Detection and Accomodation for an Agricultural Mobile Robot*. In Proceedings of the 16th. IFAC World Congress, 3-8 July 2005.
- [Palade 02] V. Palade, R.J. Patton, F.J. Uppal, J. Quevedo & S. Daley. *Fault Diagnosis of An Industrial Gas Turbine Using Neuro-Fuzzy Methods*. In Proceedings of The 15th IFAC World Congress, pages 2477–2482, Barcelona, Spain, 21-26 July 2002.
- [Palade 06] V. Palade, Bocaniala C.D. & L.C. Jain, editeurs. Computational intelligence in fault diagnosis. Advanced Information and Knowledge Processing. Springer, August 2006.
- [Papoulis 02] A. Papoulis & S.U. Pillai. Probability, random variables and stochastic processes. McGraw-Hill Publishing Co., 4th rev edition edition, January 2002.

- [Patton 94] R.J. Patton & J. Chen. *A Review of Parity Space Approached of Fault Diagnosis For Aerospace Systems*. AIAA Journal of Guidance, Control & Dynamics, vol. 17, no. 2, pages 278–285, 1994.
- [Patton 99] R.J. Patton, C.J. Lopez-Toribio & F.J. Uppal. *Artificial Intelligence Approaches To Fault Diagnosis For Dynamic Systems*. International Journal Of Applied Mathematics and Computer Science, vol. 9, no. 3, pages 471–518, 1999.
- [RAC 95] Rome Laboratory RAC. *A Practical Guide For Commercial Products And Military Systems Under Acquisition Reform*. Rome Laboratory & RAC, Rome, New York, USA, commercial practices edition, 1995.
- [Rault 71] A. Rault, A. Richalet, A. Barbot & J.P. Sergenton. *Identification and Modeling of a Jet Engine*. In IFAC Symposium on Digital Simulation of Continuous Processes, 1971.
- [Roumeliotis 98a] S.I. Roumeliotis, G.S. Sukhatme & G.A. Bekey. *Fault Detection And Identification In A Mobile Robot Using Multiple-Model Estimation*. In Proceedings of the 1998 IEEE International Conference on Robotics and Automation, volume 3, pages 2223 – 2228, Leuven, Belgium, May 1998.
- [Roumeliotis 98b] S.I. Roumeliotis, G.S. Sukhatme & G.A. Bekey. *Sensor Fault Detection And Identification In A Mobile Robot*. In Proceedings of The 1998 IEEE/RSJ International Conference on Intelligent Robots and Systems, Victoria, BC, Canada, October 1998.
- [Samson 91] C. Samson & K. Ait-Abderrahim. *Feedback Control Of A Nonholonomic Wheeled Cart In A Cartesian Space*. In Proceedings Of 1991

- IEEE International Conference On Robotics And Automation, pages 1136–1141, Sacramento, CA, 1991.
- [Samson 93] C. Samson. *Time-varying Feedback Stabilization Of Car-Like Wheeled Mobile Robots*. International Journal Of Robotics Research, vol. 12, no. 1, pages 55–64, 1993.
- [Samson 95] C. Samson. *Control Of Chained Systems: Application To Path Following And Time-Varying Point-Stabilization Of Mobile Robots*. IEEE Transactions On Automatic Control, vol. 40, no. 1, pages 64–77, 1995.
- [Siebert 76] H. Siebert & R. Isermann. *Fault Diagnosis via On-line Correlation Analysis*. Rapport technique, VDI/VDE Darmstadt, Germany, 1976.
- [Simani 03] S. Simani, Fantuzzi C. & Patton R.J. Model-based fault diagnosis in dynamic systems using identification techniques. Springer, first edition, 2003.
- [Skoundrianos 04] E.N. Skoundrianos & S.G. Tzafestas. *Finding Fault - Fault Diagnosis On The Wheels Of A Mobile Robot Using Local Model Neural Networks*. IEEE Robotics & Automation Magazine, vol. 11, no. 3, pages 83 – 90, September 2004.
- [Sobhani-Tehrani 07] E. Sobhani-Tehrani, H.A. Talebi & K. Khorasani. *Neural Parameter Estimators for Hybrid Fault Diagnosis and Estimation in Nonlinear Systems*. In IEEE International Conference on Systems, Man and Cybernetics, 2007. ISIC., pages 3171 – 3176, Montreal, QC, Canada, 7-10 October 2007.
- [Soika 97] M. Soika. *Grid Based Fault Detection And Calibration Of Sensors On Mobile Robots*. In Proceedings of the 1997 IEEE International

- Conference on Robotics and Automation, volume 3, pages 2589–2594, Albuquerque, NM, 20-25 April 1997.
- [Sørdalen 95] O.J. Sørdalen & O. Egeland. *Exponential Stabilization Of Nonholonomic Chained Systems*. IEEE Transactions On Automatic Control, vol. 40, no. 1, pages 35–49, 1995.
- [Takagi 85] T. Takagi & M. Sugeno. *Fuzzy Identification Of Systems And Its Applications To Modeling And Control*. IEEE Transactions on Systems, Man and Cybernetics, vol. 15, no. 1, pages 116–132, 1985.
- [Talebi 00] H.A. Talebi, R.V. Patel & H. Asmer. *Neural Network Based Dynamic Modeling of Flexible-Link Manipulators with Application to the SS-RMS*. Journal of Robotic Systems, vol. 17, no. 7, pages 385 – 401, May 2000.
- [Talebi 07] H.A. Talebi, R.V. Patel & K. Khorasani. *Fault Detection and Isolation for Uncertain Nonlinear Systems with Application to a Satellite Reaction Wheel Actuator*. In IEEE International Conference on Systems, Man and Cybernetics, 2007. ISIC., pages 3140 – 3145, Montreal, QC, Canada, 7-10 October 2007.
- [Tudoroiu 06] N. Tudoroiu, E. Sobhani-Tehrani & K. Khorasani. *Interactive Bank of Unscented Kalman Filters for Fault Detection and Isolation in Reaction Wheel Actuators of Satellite Attitude Control System*. In 32nd Annual IEEE Conference on Industrial Electronics, IECON 2006, pages 264 – 269, Paris, France, November 2006.
- [Tyler 94] M. Tyler & M. Morari. *Optimal and Robust Design of Integrated Control And Diagnostic Modules*. In Proceedings Of The American Control Conference, volume 2, pages 2060–2064, Baltimore, MD, 1994.

- [Uppal 02] F.J. Uppal, R.J. Patton & V. Palade. *Neuro-Fuzzy Based Fault Diagnosis Applied to an Electro-Pneumatic Valve*. In Proceedings of The 15th IFAC World Congress, pages 2483–2488, Barcelona, Spain, 21-26 July 2002.
- [VDI2206 03] VDI2206. *Design Methodology For Mechatronic Systems*. Beuth Verlag, Berlin, Germany, 2003.
- [Verma 04] V. Verma, G. Gordon, R. Simmons & S. Thrun. *Real-Time Fault Diagnosis*. IEEE Robotics & Automation Magazine, vol. 11, no. 2, pages 56–66, June 2004.
- [Welch 04] G. Welch & G. Bishop. *An Introduction to the Kalman Filter*. TR 95-041, University of North Carolina at Chapel Hill, Department of Computer Science, Chapel Hill, NC 27599-3175, April 2004.
- [Willsky 76] A.S. Willsky. *A survey of design methods for failure detection in dynamic systems*. Automatica, vol. 12, no. 6, pages 601–611, November 1976.
- [Yamamoto 99] M. Yamamoto, M. Iwamura & A. Mohri. *Quasi-Time-Optimal Motion Planning Of Mobile Platforms In The Presence Of Obstacles*. In Proceedings of The 1999 IEEE International Conference on Robotics and Automation, Detroit, Michigan, May 1999.
- [Yan 00] T. Yan, J. Ota, A. Nakamura, T. Arai & N. Kuwahara. *Concept Design Of Remote Fault Diagnosis System For Autonomous Mobile Robots*. In Proceedings of the 2000 IEEE/RSJ International Conference on Intelligent Robots and Systems, IROS 2000, volume 2, pages 931–936, 2000.

- [Yan 02] T. Yan, J. Ota, A. Nakamura, T. Arai & N. Kuwahara. *Development Of A Remote Fault Diagnosis System Applicable To Autonomous Mobile Robots*. *Advanced Robotics*, vol. 16, no. 7, pages 573–594, 2002.
- [Yangping 00] Z. Yangping, Z. Bingquan & W. DongXin. *Application of Genetic Algorithms To Fault Diagnosis in Power Plants*. *Reliability Engineering and Systems Safety*, vol. 67, pages 153–160, 2000.
- [Zanardelli 05] W.G. Zanardelli, E.G. Strangasa, H.K. Khalil & J.M. Miller. *Wavelet-based methods for the prognosis of mechanical and electrical failures in electric motors*. *Mechanical Systems and Signal Processing*, vol. 19, no. 2, pages 411–426, March 2005.
- [Zhang 02] X. Zhang, M.M. Polycarpou & T. Parisini. *A Robust Detection And Isolation Scheme For Abrupt And Incipient Faults In Nonlinear Systems*. *IEEE Transactions on Automatic Control*, vol. 47, no. 4, pages 576 – 593, April 2002.
- [Zheng 02] H. Zheng, Z. Li & X. Chen. *Gear Fault Diagnosis Based on Continuous Wavelet Transform*. *Mechanical Systems and Signal Processing*, vol. 16, no. 2-3, pages 447–457, March 2002.
- [Zhuo-hua 05] D. Zhuo-hua, C. Zi-xing & Y. Jin-xia. *Fault Diagnosis and Fault Tolerant Control for Wheeled Mobile Robots under Unknown Environments: A Survey*. In *Proceedings of the 2005 IEEE International Conference on Robotics and Automation*, pages 3428–3433, Baarcelona, Spain, April 2005.

Index

- abrupt fault, 12
- additive fault, 12
- analytical redundancy, 11
- availability, 12

- Chained form, 34
- computational intelligence, 18

- diagnosis, 7
- disturbance, 10
- dynamic extension algorithm, 40

- error, 10
- error covariance propagation, 58
- Extended Kalman Filter (EKF), 61

- failure, 9
- fault, 9
- fault detection, 10, 16
- fault diagnosis, 10
- fault identification, 10
- fault isolation, 10
- fault isolation and identification, 16
- Fuzzy Logic, 19

- Genetic algorithms, 21

- incipient fault, 12
- intermittent fault, 12, 101, 106

- Kalman filter, 51, 54
- Kalman gain, 56

- limit checking, 13
- logical reasoning, 14

- Major Subsystems of WMRs, 49
- malfunction, 10
- Measurement equation, 52
- monitoring, 10
- multiplicative fault, 12

- Neural Network, 19
- Neuro-Fuzzy systems, 20
- nonholonomic systems, 32

- optimum estimates, 53

- permanent-fault, 82, 91
- physical redundancy, 13
- point-to-point motion, 31
- Principle Of Orthogonality, 54
- protection, 11

-
- qualitative Model, 11
 - quantitative Model, 11

 - reliability, 11
 - residual, 10
 - rolling without slipping constraint, 32

 - safety, 11
 - special sensors, 13
 - spectrum analysis, 14
 - supervision, 11
 - symptom, 10

 - technical diagnosis, 8
 - trajectory tracking, 31
 - transition matrix, 52

 - WMR Communication, 50
 - WMR Driving Subsystem, 50
 - WMR Power Subsystem, 49
 - WMR Sensors, 50
 - WMR Steering Subsystem, 50
 - WMR Suspension, 50